

New Schwinger-Dyson equations for non-Abelian gauge theories

D. Binosi^{1,*} and J. Papavassiliou^{2,†}

¹*European Centre for Theoretical Studies in Nuclear Physics and Related Areas (ECT*),
Villa Tambosi, Strada delle Tabarelle 286, I-38050 Villazzano (TN) Italy*

²*Departamento de Física Teórica and IFIC, Centro Mixto, Universidad de Valencia-CSIC,
E-46100, Burjassot, Valencia, Spain*

(Dated: May 26, 2008)

Abstract

We show that the application of the pinch technique to the conventional Schwinger-Dyson equations for the gluon propagator, gluon-quark vertex, and three-gluon vertex, gives rise to new equations endowed with special properties. The new series coincides with the one obtained in the Feynman gauge of the background field method, thus capturing the extensive gauge cancellations implemented by the pinch technique at the level of individual Green's functions. Its building blocks are the fully dressed pinch technique Green's functions obeying Abelian all-order Ward identities instead of the Slavnov-Taylor identities satisfied by their conventional counterparts. As a result, and contrary to the standard case, the new equation for the gluon self-energy can be truncated gauge invariantly at any order in the dressed loop expansion. The construction is streamlined by resorting to the Batalin-Vilkovisky formalism which allows for a concise treatment of all the quantities appearing in the intermediate steps. The theoretical and phenomenological implications of this novel non-perturbative framework are discussed in detail.

PACS numbers: 12.38.Aw, 12.38.Lg, 14.70.Dj

*Electronic address: binosi@ect.it

†Electronic address: Joannis.Papavassiliou@uv.es

I. INTRODUCTION

The Schwinger-Dyson equations (SDE) [1, 2] provide a formal framework for tackling physics problems requiring a non-perturbative treatment. The SDE constitute an infinite system of coupled non-linear integral equations for all Green's functions of the theory, and can be used, at least in principle, to address questions related to chiral symmetry breaking, dynamical mass generation, formation of bound states, and other non-perturbative effects [3, 4]. In practice, their usefulness hinges crucially on one's ability to devise a self-consistent truncation scheme that would select a tractable subset of these equations, without compromising the physics one hopes to describe. Inventing such a scheme for the SDE of gauge theories is a highly non-trivial proposition. The problem originates from the fact that the SDEs are built out of unphysical Green's functions; thus, the extraction of reliable physical information depends critically on delicate all-order cancellations, which may be inadvertently distorted in the process of the truncation. Several of the issues related to the truncation of the SDEs of QED have been addressed in a series of articles [5–8].

The situation becomes even more complicated for strongly coupled non-Abelian gauge theories, such as QCD [9], mainly for the following reasons.

- i.* The complications caused by the dependence of the Green's functions on the gauge-fixing parameter are more acute in non-Abelian gauge-theories, as can be seen already at the level of the most fundamental Green's function, namely the two-point function (propagator) of the corresponding gauge bosons. In QED the photon self-energy (vacuum polarization) is independent of the gauge-fixing parameter, both perturbatively (to all orders) and non-perturbatively; when multiplied by e^2 it forms a physical observable, the QED effective charge. In contradistinction, the gluon self-energy is gauge-dependent already at one loop; depending on the gauge-fixing scheme employed, this dependence may be more or less virulent. This difference is of little practical importance when computing S -matrix elements at a fixed order in perturbation theory, given that the gauge-dependence of the gluon self-energy is guaranteed to cancel against similar contributions from other graphs, but has far-reaching consequences when attempting to truncate the corresponding SDEs, written in some gauge. Contrary to what happens in the perturbative calculation, even if one were to put together the non-perturbative expressions from these truncated SDEs to form a phys-

ical observable, the gauge-cancellations may not go through completely, because the process of the truncation might have distorted them. Thus, there is a high probability of ending up with a residual gauge-dependence infesting one's non-perturbative prediction for a physical observable.

- ii.* In Abelian gauge theories the Green's functions satisfy naive Ward Identities (WIs): given the tree-level WI, the all-order generalization is obtained by simply replacing the tree-level expressions by the all-order ones. In general, this is not true for the Green's functions of non-Abelian gauge theories, where the WIs are modified beyond tree-level, and are replaced by more complicated expressions known as Slavnov-Taylor identities (STIs) [10, 11]; in addition to the basic Green's functions of the theory they involve various composite ghost operators. In order to appreciate how the fact that the Green's functions satisfy STIs may complicate the truncation procedure of the SDEs, let us consider the simplest STI (and WI in this case) satisfied by the photon and gluon self-energies alike, namely

$$q^\alpha \Pi_{\alpha\beta}(q) = 0. \tag{1.1}$$

Eq. (1.1) is without a doubt the most fundamental statement at the level of Green's functions that one can obtain from the BRST symmetry [12]; it affirms the transversality of the gauge-boson self-energy, be it a photon or a gluon, and is valid both perturbatively to all orders as well as non-perturbatively. The problem stems from the fact that in the SDE of $\Pi_{\alpha\beta}(q)$ enter higher order Green's functions, namely the fully-dressed fundamental vertices of the theory. It is these latter Green's functions that in the Abelian context satisfy WIs whereas in the non-Abelian context satisfy STIs. Thus, whereas in QED the validity of Eq. (1.1) can be easily seen at the level of the SDE, simply because $q^\mu \Gamma_\mu(p, p+q) = e[S^{-1}(p+q) - S^{-1}(p)]$, in QCD proving Eq. (1.1) is very difficult, and requires the conspiracy of all full vertices appearing in the SDE. Truncating the SDE naively usually amounts to leaving out some of these vertices, and, as a result, Eq. (1.1) is compromised.

The complications stemming from the two points mentioned above are often compounded by additional problems related to the loss of multiplicative renormalizability and the inability to form renormalization-group invariant quantities.

Recently, a truncation scheme for the SDEs of non-Abelian gauge theories has been proposed [13] that is based on the pinch technique (PT) [14, 15] and its connection with the background field method (BFM) [16, 17] (see below). The way the PT resolves the difficulties related with points (i) and (ii) mentioned above is by imposing a drastic modification already at the level of the building blocks of the SD series, namely the off-shell Green’s functions themselves. The PT is a well-defined algorithm that exploits systematically the symmetries built into physical observables, such as S -matrix elements or Wilson loops, in order to construct new, effective Green’s functions, endowed with very special properties. The basic observation, which essentially defines the PT, is that there exists a fundamental cancellation between sets of diagrams with different kinematic properties, such as self-energies, vertices, and boxes. This cancellation is driven by the underlying BRST symmetry [12], and is triggered when a very particular subset of the longitudinal momenta circulating inside vertex and box diagrams generate out of them (by “pinching” internal lines) propagator-like terms. The latter are reassigned to conventional self-energy graphs, in order to give rise to the aforementioned effective Green’s functions. These new Green’s functions are independent of the gauge-fixing parameter [14, 15, 18–20], satisfy ghost-free, QED-like WIs instead of the complicated STIs [15, 18], display only physical thresholds [21, 22], have correct analyticity properties [23], and are well-behaved at high energies [24].

Of central importance for the ensuing analysis is the connection between the PT and the BFM. The latter is a special gauge-fixing procedure that preserves the symmetry of the action under ordinary gauge transformations with respect to the background (classical) gauge field \widehat{A}_μ^a , while the quantum gauge fields, A_μ^a , appearing inside the loops, transform homogeneously under the gauge group [25]. As a result, the background n -point functions (*i.e.*, those involving \widehat{A}_μ^a fields) satisfy QED-like WIs to all orders. The BFM gives rise to special Feynman rules (see Appendix F); most notably (a) the tree-level vertices involving \widehat{A}_μ^a fields depend in general on the quantum gauge-fixing parameter ξ_Q , used to gauge-fix the quantum gauge fields, and (b) the ghost sector is modified, containing symmetric gluon-ghost vertices, as well as two-gluon–two-ghost vertices. Notice an important point: the background n -point functions are gauge-invariant, in the sense that they satisfy (by construction) QED-like WIs, but are *not* gauge-independent, *i.e.*, they depend explicitly on ξ_Q . The connection between PT and BFM [26, 27], demonstrated to be valid to all orders [28], affirms that the (gauge-independent) PT n -point functions *coincide* with the BFM n -point functions when

the latter are computed at the special value $\xi_Q = 1$, also known as the background Feynman gauge (BFG).

Let us now return to points (i) and (ii) and analyze them from the perspective of the PT. In a nutshell, the way point (i) is resolved, for the prototype case of the gluon self-energy, is the following. The BFG is a privileged gauge, in the sense that it is selected *dynamically* when the gluon self-energy is embedded into a physical observable (such as an on-shell test-amplitude). Specifically, the BFG captures the net propagator-like subamplitude emerging after QED-like conditions have been replicated inside the test-amplitude, by means of the PT procedure. Thus, once the PT rearrangements have taken place, the propagator is removed from the amplitude and is studied in isolation: one considers the SDE for the background gluon self-energy, $\widehat{\Pi}_{\alpha\beta}(q)$, at $\xi_Q = 1$. Solving the SDE in the BFG eliminates any gauge-related exchanges between the solutions obtained for $\widehat{\Pi}_{\alpha\beta}(q)$ and other Green's functions, when put together to form observables; thus, the solutions are free of gauge artifacts. Regarding point (ii), the key ingredient is that now all full vertices appearing in the new SDE satisfy *Abelian* WIs; as a result, gluonic and ghost contributions are *separately* transverse, within *each* order in the “dressed-loop” expansion. Thus, it is much easier to devise truncation schemes that manifestly preserve the validity of Eq. (1.1).

The main results presented in this article are the following. We provide a detailed and complete demonstration of how the application of the PT algorithm at the level of the conventional SD series leads to a new, modified SD series, with the special properties mentioned above. A preliminary discussion of this issue has already appeared in brief communication, dedicated to the SDE of the gluon self-energy [13]. From the technical point of view, here we present a significantly more concise and direct proof, by virtue of a crucial STI, that we employ for the first time. In addition, we extend the analysis to include the SDE for the quark-gluon and three-gluon vertices, which are important ingredients for obtaining a self-contained picture. We emphasize that the three-gluon vertex relevant in this analysis is the one that would correspond, in the BFM language, to $\Gamma_{\widehat{A}AA}$, i.e. one background gluon and two quantum ones merging, and *not* the fully Bose-symmetric vertex $\Gamma_{\widehat{A}\widehat{A}\widehat{A}}$ considered in [15, 29]. The reason is that it is the former vertex that appears in the SDE of the gluon self-energy, in complete accordance with both the PT unitarity arguments [30] (see also Appendix A) and the independent diagrammatic rules of the BFM [17].

Furthermore, we address an important conceptual and practical issue, related to the fact

that, qualitatively speaking, the new SD series expresses the BFG Green's functions in terms of integrals involving the conventional ones. This is already evident at the two-loop level: the two-loop BFM gluon self-energy is written in terms of integrals involving the conventional one-loop gluon self-energy. This example might suggest, at first sight, that one cannot arrive at a genuine SDE involving the same unknown quantity on both sides, but there is a way around it. Specifically, the use of a set of crucial identities, relating the conventional and the BFM Green's functions, allow one to convert the new SD series into a dynamical equation involving either the conventional or the BFM gluon self-energy only.

The paper is organized as follows. In Section II we briefly review the most salient features of the PT methodology and explain qualitatively how the new SD series is obtained and what are its main advantages compared to the conventional SD series, focusing on the truncation possibilities it offers. In Section III we introduce the notation and the formal machinery that will be used in the actual derivation of the PT Schwinger-Dyson equations of QCD. We focus particularly on the Batalin-Vilkovisky formalism and the plethora of relations that it furnishes for the various fundamental and auxiliary Green's functions appearing in our construction. In Section IV we present the central result of this work, namely the detailed derivation of the new set of SDEs. There are three main subsection, dedicated to the construction of the new SDEs for the quark-gluon vertex, the three-gluon vertex, and finally the gluon propagator. In Section V we discuss some of the main practical implications of the new SD series, and present our conclusions and outlook.

The paper contains five appendices. In Appendix A we discuss some subtleties of the extension of the PT algorithm beyond one loop, and in particular how to identify unambiguously the subset of three-gluon vertices that must undergo the PT decomposition. In Appendix B we describe the general strategy for carrying out the renormalization procedure to the new SD series obtained within the PT. Finally, the last four appendices furnish the derivation of several instrumental formulas employed in Section IV, together with a complete set of Feynman rules.

II. THE NEW SDE SERIES: GENERAL PHILOSOPHY AND MAIN RESULTS

In this section we present the general ideas and outline the basic philosophy of our approach, before diving into the complexities of the full SDE construction. The style of this

section is rather qualitative; thus the reader who would like to skip the technicalities can get an overview of the theoretical and practical advantages offered by the new SD series, compared to the conventional formalism.

A. The difficulties with the conventional formulation

Let us first focus on the conventional SD series for the gluon self-energy. Defining the transverse projector

$$P_{\alpha\beta}(q) = g_{\alpha\beta} - \frac{q_\alpha q_\beta}{q^2}, \quad (2.1)$$

we have for the full gluon propagator in the Feynman gauge ($\xi = 1$)

$$i\Delta_{\alpha\beta}(q) = -i \left[P_{\alpha\beta}(q)\Delta(q^2) + \frac{q_\alpha q_\beta}{q^4} \right], \quad (2.2)$$

with $\Delta_{\alpha\beta}^{ab}(q) = \delta^{ab}\Delta_{\alpha\beta}(q)$ (in what follows color factors will be omitted whenever possible).

The scalar function $\Delta(q^2)$ is related to the all-order gluon self-energy

$$\Pi_{\alpha\beta}(q) = P_{\alpha\beta}(q)\Pi(q^2), \quad (2.3)$$

through

$$\Delta(q^2) = \frac{1}{q^2 + i\Pi(q^2)}. \quad (2.4)$$

Since $\Pi_{\alpha\beta}(q)$ has been defined in (2.4) with the imaginary factor i factored out in front, it is simply given by the corresponding Feynman diagrams in Minkowski space. The inverse of $\Delta_{\alpha\beta}(q)$ can be found by requiring that

$$i\Delta_{\alpha\mu}^{am}(q)(\Delta^{-1})_{mb}^{\mu\beta}(q) = \delta^{ab}g_\alpha^\beta, \quad (2.5)$$

and is given by

$$\Delta_{\alpha\beta}^{-1}(q) = iP_{\alpha\beta}(q)\Delta^{-1}(q^2) + iq_\alpha q_\beta, \quad (2.6)$$

or, equivalently,

$$\Delta_{\alpha\beta}^{-1}(q) = ig_{\alpha\beta}q^2 - \Pi_{\alpha\beta}(q). \quad (2.7)$$

In Fig. 1 we show the SDE satisfied by the gluon self-energy. It reads

$$\Delta^{-1}(q^2)P_{\alpha\beta}(q) = q^2P_{\alpha\beta}(q) + i \sum_{i=1}^6 (a_i)_{\alpha\beta}. \quad (2.8)$$

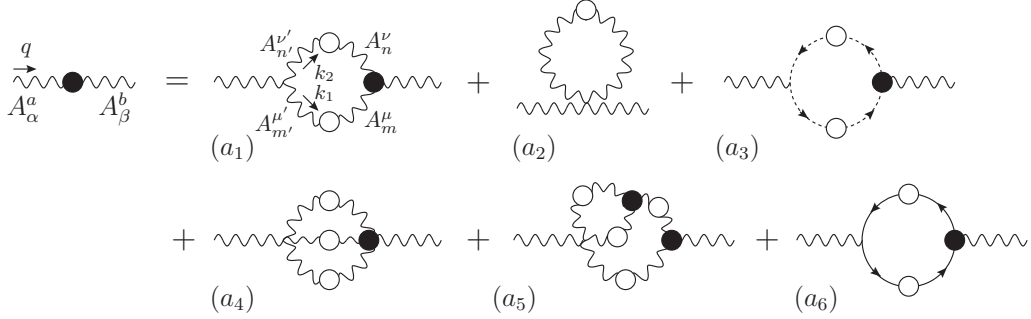


FIG. 1: Schwinger-Dyson equation satisfied by the gluon self-energy. The symmetry factors of the diagrams are $s(a_1, a_2, a_5) = 1/2$, $s(a_3, a_6) = -1$, $s(a_4) = 1/6$. White blobs represent connected Green's functions while black blobs represent one particle irreducible ones.

Of course, in addition to the SDE for the gluon propagator, one must also include the corresponding SDE for the vertices; they are normally expressed as skeleton expansions in terms of the corresponding connected multi-particle kernels (the proper treatment of the vertices is presented in Section IV).

The main theoretical problem one encounters when dealing with the SDE given above is the fact that it cannot be truncated in a physically meaningful way. The most obvious manifestation of this drawback is the following: after the truncation the fundamental Eq. (1.1) is violated. To recognize the origin of this difficulty, note that Eq. (1.1) translates at the level of the SDE to the statement

$$q^\alpha \sum_{i=1}^6 (a_i)_{\alpha\beta} = 0. \quad (2.9)$$

The diagrammatic verification of (2.9), *i.e.*, through contraction of the individual graphs by q^α , is practically very difficult, essentially due to the complicated STIs satisfied by the vertices involved. The most typical example of such an STI is that of the conventional three-gluon vertex $\Gamma_{\alpha\mu\nu}(q, k_1, k_2)$ (all momenta entering), given by [31]

$$q^\alpha \Gamma_{\alpha\mu\nu}(q, k_1, k_2) = [q^2 D(q)] \left\{ \Delta^{-1}(k_2^2) P_\nu^\gamma(k_2) H_{\mu\gamma}(k_1, k_2) - \Delta^{-1}(k_1^2) P_\mu^\gamma(k_1) H_{\nu\gamma}(k_2, k_1) \right\}, \quad (2.10)$$

where the auxiliary function $H_{\alpha\beta}$ is defined in Fig. 2. The kernel \mathcal{K} appearing in this function is the conventional connected ghost-ghost-gluon-gluon kernel appearing in the usual QCD skeleton expansion [4, 32]. Notice also that $H_{\alpha\beta}(k, q)$ is related to the conventional gluon-ghost vertex $\Gamma_\beta(k, q)$ (with k the gluon and q the anti-ghost momentum) by $q^\alpha H_{\alpha\beta}(k, q) =$

$$H_{\alpha\beta}(k_1, k_2) = g_{\alpha\beta} +$$

FIG. 2: The auxiliary function H appearing in the three-gluon vertex STI. Gray blobs represent (connected) Schwinger-Dyson kernels (in this specific case the ghost-gluon kernel \mathcal{K} appearing in the usual QCD skeleton expansion).

$\Gamma_\beta(k, q)$ [4, 31–33].

In addition, some of the pertinent STIs are either too complicated, such as that of the conventional four-gluon vertex, or they cannot be cast in a particularly convenient form. For instance, in the case of the conventional gluon-ghost vertex, $\Gamma_\mu(q, p)$, the STI that one may obtain formally for $q^\mu \Gamma_\mu(q, p)$ is the sum of two terms one of which is $p^\mu \Gamma_\mu(q, p)$; this clearly limits its usefulness in applications.

The main practical consequence of these complicated STIs is that one cannot truncate (2.8) in any obvious way without violating the transversality of the resulting $\Pi_{\alpha\beta}(q)$. For example, keeping only graphs (a_1) and (a_2) is not correct even perturbatively, since the ghost loop is crucial for the transversality of $\Pi_{\alpha\beta}$ already at one-loop; adding (a_3) is still not sufficient for a SD analysis, because (beyond one-loop) $q^\alpha [(a_1) + (a_2) + (a_3)]_{\alpha\beta} \neq 0$.

B. The pinch technique

The PT [14, 15] is a particular algorithm for rearranging the perturbative series in such a way as to obtain new Green’s functions that are independent of the gauge-fixing parameter, and satisfy to all orders ghost-free, QED-like WIs, instead of the usual STIs. The original motivation for resorting to it was precisely to devise a truncation scheme for the SDE that would preserve manifestly the gauge-invariance of the answer at every step.

Let us emphasize from the beginning that, to date, there is no formal definition of the PT procedure at the level of the functional integral defining the theory. In particular, let us assume that the path integral has been defined using an arbitrary gauge-fixing procedure (*i.e.* linear covariant gauges); then, there is no known a priori procedure (such as, *e.g.*,

functional differentiation with respect to some combination of appropriately defined sources) that would furnish directly the gauge-independent PT Green's functions. The definition of the PT procedure is operational, and is intimately linked to the diagrammatic expansion of the theory (*i.e.* one must know the Feynman rules). In fact, the starting point of the PT construction can be any gauge-fixing scheme that furnishes a set of well-defined Feynman rules and gauge-independent physical observables. Specifically, one operates at a certain well-defined subset of diagrams, and the subsequent rearrangements give rise to the same gfp-independent PT answer, regardless of the gauge-fixing scheme chosen for deriving the Feynman rules. Note however that, as the present paper amply demonstrates (and as has already been emphasized in some of the earlier literature), the PT is not diagrammatic, in the sense that one does not need to operate on individual graphs but rather on a handful of classes of diagrams (each one containing an infinite number of individual graphs). This is the enormous advantage of formulating the PT at the SD level.

The aforementioned rearrangements of the PT are collectively implemented through the systematic use of the STIs satisfied by certain Green's functions and kernels; the latter constitute standard ingredients in the ordinary perturbative expansion or the SDE of the various n -point Green's functions. In the Feynman gauge, which is by far the most convenient choice, the relevant STIs are triggered by the action of a very special set of longitudinal momenta. Specifically, consider the subset of Feynman diagrams that have at least one *external* three-gluon vertex

$$\Gamma_{\alpha\mu\nu}^{amn}(q, k_1, k_2) = -igf^{amn}\Gamma_{\alpha\mu\nu}(q, k_1, k_2). \quad (2.11)$$

By “external” we mean a vertex that has one of its legs irrigated by a physical momentum, to be denoted by q , as opposed to a virtual momentum, that is being integrated over in the Feynman graph [30] (a detailed discussion of why only external vertices can pinch while all other three-gluon vertices inside the loops should remain unchanged is provided in Appendix A). Then $\Gamma_{\alpha\mu\nu}(q, k_1, k_2)$ is decomposed as [14]

$$\begin{aligned} \Gamma_{\alpha\mu\nu}(q, k_1, k_2) &= \Gamma_{\alpha\mu\nu}^F(q, k_1, k_2) + \Gamma_{\alpha\mu\nu}^P(q, k_1, k_2), \\ \Gamma_{\alpha\mu\nu}^F(q, k_1, k_2) &= (k_1 - k_2)_\alpha g_{\mu\nu} + 2q_\nu g_{\alpha\mu} - 2q_\mu g_{\alpha\nu}, \\ \Gamma_{\alpha\mu\nu}^P(q, k_1, k_2) &= k_{2\nu} g_{\alpha\mu} - k_{1\mu} g_{\alpha\nu}. \end{aligned} \quad (2.12)$$

Evidently the above decomposition assigns a special role to the leg carrying the physical

momentum q , and allows $\Gamma_{\alpha\mu\nu}^F(q, k_1, k_2)$ to satisfy the tree-level WI

$$q^\alpha \Gamma_{\alpha\mu\nu}^F(q, k_2, k_1) = (k_2^2 - k_1^2)g_{\mu\nu}, \quad (2.13)$$

where the rhs is the difference of two (tree-level) inverse propagators in the Feynman gauge. Note that $\Gamma_{\alpha\mu\nu}^F(q, k_1, k_2)$ (i) is Bose-symmetric only with respect to the μ and ν legs, and (ii) it *coincides* with the BFM three-gluon vertex involving a background gluon, $\widehat{A}_\alpha(q)$, and two quantum gluons, $A_\mu(k_1)$ and $A_\nu(k_2)$, in the Feynman gauge (*i.e.*, when the quantum gauge-fixing parameter, ξ_Q , is chosen to be $\xi_Q = 1$). The term $\Gamma_{\alpha\mu\nu}^P(q, k_1, k_2)$, which in configuration space corresponds to a pure divergence, plays the central role in the PT construction; indeed, the main thrust of most PT demonstrations (in this article and many others before) is to essentially track down the precise action of the momenta contained inside $\Gamma_{\alpha\mu\nu}^P$. Specifically, $\Gamma_{\alpha\mu\nu}^P$ contains the longitudinal “pinching” momenta, which will get contracted with the kernels and Green’s functions nested inside the remaining part of the diagram, triggering the corresponding STIs; this, in turn, will produce the highly non-trivial rearrangements of the various terms characteristic of the PT. Quite remarkably, all these rearrangements finally amount to the modification of the ghost sector of the theory, reproducing dynamically the corresponding ghost sector of the BFM, leaving no residual terms behind.

The simplest example that demonstrates the action of the pinching momenta is the one-loop construction of the PT gluon self-energy (see subsection IID): the STI triggered inside the conventional one-loop diagram (a) in Fig.3 is simply the tree-level version of Eq. (2.10), namely

$$k_1^\mu \Gamma_{\alpha\mu\nu}(q, k_1, k_2) = q^2 P_{\alpha\nu}(q) - k_2^2 P_{\alpha\nu}(k_2), \quad (2.14)$$

$$k_2^\nu \Gamma_{\alpha\mu\nu}(q, k_1, k_2) = k_1^2 P_{\alpha\mu}(k_1) - q^2 P_{\alpha\mu}(q). \quad (2.15)$$

The terms proportional to an inverse propagator of the *external* leg (*i.e.*, to q^2), will cancel (when embedded into a physical process!) against similar contributions from other graphs (*e.g.*, vertex-graphs), also produced by the corresponding action of the pinching momenta inside them; in this case the pinching momenta literary “pinch out” internal quark lines (hence the name of the technique). Thus, *effectively*, inside a physical process, this particular subset of pinching contributions can be discarded altogether; this is the shortcut introduced in the “intrinsic” [15]. The remaining pinching terms, namely those proportional to the *internal* leg, are *instrumental* for obtaining the PT answer; in particular, they symmetrize

the original R_ξ ghost sector, so that it will finally coincide with the BFM ghost sector at $\xi_Q = 1$ (see again subsection IID).

C. Pinch technique and background field method: some conceptual issues

As mentioned in the Introduction, the (gauge-independent) PT n -point functions *coincide* with the BFM n -point functions when the latter are computed at the special value $\xi_Q = 1$ (BFG). Even though this correspondence (and its correct interpretation) has been addressed in various places in the literature, it may be useful to present a brief overview of some of the main subtleties associated with it.

- i.* The objective of the PT construction is not to derive diagrammatically the BFG, but rather to exploit the underlying BRST symmetry in order to expose a large number of cancellations, and eventually define gauge-independent Green's functions satisfying abelian WIs. In fact, it was after more than a decade of independent PT activity (when practically all one loop calculations had been carried out both in QCD and the electroweak sector) when the aforementioned correspondence was discovered (i.e. the PT results already existed, and then it was realized that they coincide with the results of the BFG). Thus, while it is a remarkable and extraordinarily useful result that the PT Green's functions can also be calculated in the BFG, this needs a very extensive demonstration. Therefore, the correspondence must be verified at the end of the PT construction and should not be assumed beforehand.
- ii.* It is well known that, at any order, the S -matrix \tilde{S} of the BFM, is equal to that in the conventional linear (R_ξ) gauges, *i.e.*, $\tilde{S} = S$. There is no way, however, to deduce from this equality the PT-BFG correspondence. Writing $S = \Gamma\Delta\Gamma + B$ and $\tilde{S} = \tilde{\Gamma}\tilde{\Delta}\tilde{\Gamma} + \tilde{B}$, using that the box diagrams are equal in both schemes, *i.e.*, $B = \tilde{B}$, and, finally, observing that the PT does not change the unique S -matrix, one can deduce that $\Gamma\Delta\Gamma = \hat{\Gamma}\hat{\Delta}\hat{\Gamma}$, and hence that $\hat{\Gamma}\hat{\Delta}\hat{\Gamma} = \tilde{\Gamma}\tilde{\Delta}\tilde{\Gamma}$. But from this does *not* follow that $\hat{\Delta} = \tilde{\Delta}$ nor that $\hat{\Gamma} = \tilde{\Gamma}$; one must *prove explicitly* the equality for *individual* Green's functions.
- iii.* We emphasize that the PT is a way of enforcing gauge independence (and several other physical properties) for off-shell Green's functions; the BFM, in a general gauge, is not. This is reflected in the fact that the BFM n -point functions are gauge-invariant,

in the sense that they satisfy (by construction) QED-like WIs, but are *not* gauge-independent, *i.e.*, they depend explicitly on ξ_Q . Had the BFM n -point functions been ξ_Q -independent, in addition to being gauge-invariant, there would be no need for introducing independently the PT.

- iv.* Notice that the ξ_Q -dependent BFM Green's functions are not physically equivalent. This is best seen in theories with spontaneous symmetry breaking: the dependence of the BFM Green's functions on ξ_Q gives rise to *unphysical* thresholds inside these Green's functions for $\xi_Q \neq 1$, a fact which limits their usefulness for resummation purposes [21]. Only the case of the BFG is free from unphysical poles; that's because then (and only then) the BFM results collapse to the physical PT Green's functions.
- v.* The PT procedure has no a-priori knowledge of the BFM built into it, despite the fact that the splitting of the regular three gluon vertex given in (2.12) suggests such a preference. Indeed, while Γ^F *coincides* with the BFG vertex, it only furnishes one piece of the final answer. As already mentioned, the non-trivial part of the PT construction resides in what happens when the Γ^P part of the vertex gets contracted with the Green's functions and kernels nested inside the corresponding SD diagram. The correspondence with the BFG works finally only because the WI triggered by Γ^P conspire in such a way as to reproduce dynamically the BFM ghost sector at $\xi_Q = 1$, and nothing more. There is no a-priori way of knowing that this will indeed happen, and hence the need for the detailed demonstration presented in the next sections.
- vi.* Amplifying the previous point, notice that the PT works perfectly well in the context of non-covariant gauges (in fact it was first carried out in such a gauge), where the ghosts are decoupled from the S -matrix. Spectacularly enough, the PT procedure produces completely dynamically the necessary ghost sector, from the STIs that are triggered.
- vii.* Perhaps the most compelling fact that demonstrates that the PT and the BFM are intrinsically two completely disparate methods is the following: one can apply the PT within the BFM. For example, the PT can be used to combine pieces of Feynman graphs in the background Landau gauge, just as in any other gauge, and the usual PT results (those of the BFG) emerge. Operationally this is easy to understand: away

from $\xi_Q = 1$ even in the BFM there are longitudinal (pinching momenta) that will initiate the pinching procedure. Ultimately, the BFG is singled out because of the total absence, in this particular gauge, of any such longitudinal momenta.

viii. We emphasize that the PT construction goes through unaltered under circumstances where the BFM Feynman rules cannot even be applied. Specifically, if instead of an S -matrix element one were to consider a different observable, such as a current-current correlation function or a Wilson loop (as was in fact done by Cornwall in the original formulation [14], and more recently in [20]) one could not start out using the background Feynman rules, because *all* fields appearing inside the first non-trivial loop are quantum ones. Instead, by following the PT rearrangement inside these physical amplitudes the unique PT answer emerges again.

D. The pinch technique as a gauge-invariant truncation scheme

Let us now see how the standard one-loop PT construction contains the seed of a gauge-invariant truncation scheme for the SDE of the gluon self-energy. This exercise may seem trivial at first, in the sense that no truncation is really needed, given that the two diagrams comprising the full answer are elementary to calculate. However, it illustrates exactly how the PT rearrangement furnishes a transverse one-loop approximation for the conventional gluon self-energy, even if the (modified) ghost loop is omitted.

In what follows we will use dimensional regularization, and will employ the short-hand notation $\int_k = \int d^d k / (2\pi)^d$, where $d = 4 - \epsilon$ is the space-time dimension. The conventional one-loop self-energy in the Feynman gauge, to be denoted by $\Pi_{\alpha\beta}^{(1)}(q)$, is given by the diagrams (a) and (b) in Fig. 3 (we set the “seagull”-type contributions directly to zero, using the standard result $\int_k k^{-2} = 0$). As is well known, neither (a) nor (b) is transverse, and it is only their sum that furnishes a transverse answer for $\Pi_{\alpha\beta}^{(1)}(q)$. Specifically, setting

$$f(q^2) = iC_A \frac{g^2}{48\pi^2} \Gamma\left(\frac{\epsilon}{2}\right) \left(\frac{q^2}{\mu^2}\right)^{-\frac{\epsilon}{2}}, \quad (2.16)$$

with C_A the Casimir eigenvalue of the adjoint representation ($C_A = N$ for $SU(N)$), and dropping irrelevant constants, we have

$$(a)_{\alpha\beta} = \frac{1}{4} f(q^2) (19q^2 g_{\alpha\beta} - 22q_\alpha q_\beta),$$

$$\begin{aligned}
\Pi_{\alpha\beta}(q) &= \text{(a)} + \text{(b)} \\
&=^{\text{PT}} \text{(\hat{a})} + \text{(\hat{b})} - 2 \text{(c)} q^2 P_{\alpha\beta}(q)
\end{aligned}$$

FIG. 3: The conventional one-loop gluon self-energy before (first line) and after (second line) the PT rearrangement. A gray circle at the end of an external gluon line denotes that the corresponding gluon behaves as if it were a background gluon.

$$\begin{aligned}
(b)_{\alpha\beta} &= \frac{1}{4} f(q^2) (q^2 g_{\alpha\beta} + 2q_\alpha q_\beta), \\
\Pi_{\alpha\beta}^{(1)}(q) &= 5q^2 f(q^2) P_{\alpha\beta}(q).
\end{aligned} \tag{2.17}$$

The application of the PT amounts to carrying out the following rearrangement of the two elementary three-gluon vertices

$$\begin{aligned}
\Gamma_{\alpha\mu\nu} \Gamma_\beta^{\mu\nu} &= [\Gamma_{\alpha\mu\nu}^{\text{F}} + \Gamma_{\alpha\mu\nu}^{\text{P}}] [\Gamma_\beta^{\text{F}\mu\nu} + \Gamma_\beta^{\text{P}\mu\nu}] \\
&= \Gamma_{\alpha\mu\nu}^{\text{F}} \Gamma_\beta^{\text{F}\mu\nu} + \Gamma_{\alpha\mu\nu}^{\text{P}} \Gamma_\beta^{\mu\nu} + \Gamma_{\alpha\mu\nu} \Gamma_\beta^{\text{P}\mu\nu} - \Gamma_{\alpha\mu\nu}^{\text{P}} \Gamma_\beta^{\text{P}\mu\nu}.
\end{aligned} \tag{2.18}$$

Then, using the elementary WIs of Eq.s (2.14) and (2.15) we have that

$$\Gamma_{\alpha\mu\nu}^{\text{P}} \Gamma_\beta^{\mu\nu} + \Gamma_{\alpha\mu\nu} \Gamma_\beta^{\text{P}\mu\nu} = -4q^2 P_{\alpha\beta}(q) - 2k_\alpha k_\beta - 2(k+q)_\alpha (k+q)_\beta, \tag{2.19}$$

$$\Gamma_{\alpha\mu\nu}^{\text{P}} \Gamma_\beta^{\text{P}\mu\nu} = 2k_\alpha k_\beta + (k_\alpha q_\beta + q_\alpha k_\beta), \tag{2.20}$$

where some terms have been set to zero by virtue of the dimensional regularization result $\int_k k^{-2} = 0$. Thus, one can cast $\Pi_{\alpha\beta}^{(1)}(q)$ in the following form:

$$\Pi_{\alpha\beta}^{(1)}(q) = \frac{C_A g^2}{2} \left[\int_k \frac{\Gamma_{\alpha\mu\nu}^{\text{F}} \Gamma_\beta^{\text{F}\mu\nu}}{k^2 (k+q)^2} - 2 \int_k \frac{(2k+q)_\alpha (2k+q)_\beta}{k^2 (k+q)^2} \right] - 2C_A g^2 \int_k \frac{q^2 P_{\alpha\beta}(q)}{k^2 (k+q)^2}. \tag{2.21}$$

It is elementary to verify that each of the two terms in the square bracket on the rhs of (2.21) are transverse; thus the PT rearrangement has created three manifestly transverse structures. That in itself might not be so important, if it were not for the fact that these structures admit a special diagrammatic representation and a unique field-theoretic interpretation.

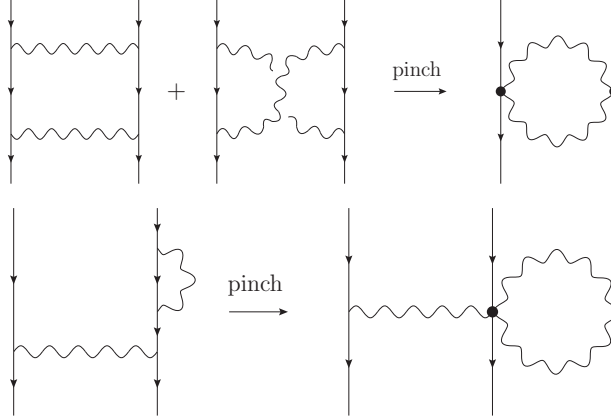


FIG. 4: Schematic representation of the pinching contributions one needs to consider away from the Feynman gauge $\xi = 1$.

Specifically, the two terms in the square bracket correspond precisely to diagrams (\hat{a}) and (\hat{b}) defining the one-loop gluon self-energy in the BFG, to be denoted by $\tilde{\Pi}_{\alpha\beta}^{(1)}(q)|_{\xi_Q=1}$; note in particular the symmetrized gluon-ghost coupling. Thus, *it is as if the external gluons in (a) and (b) had been converted dynamically into background ones*. As explained in [13], the third term on the rhs of (2.21) is the one-loop expression of a special auxiliary Green’s function, to be defined shortly; it corresponds to diagram (c) in Fig. 3, and is generated from the first term on the rhs of (2.14). The one-loop PT self-energy, to be denoted by $\hat{\Pi}_{\alpha\beta}^{(1)}(q)$, is obtained by simply dropping this last term from the rhs of (2.21); this defines the “intrinsic” PT [15]. The completely equivalent way of saying this, corresponding to the “S-matrix” PT [14], is that the term corresponding to graph (c) cancels exactly against a propagator-like contribution extracted from the vertex graphs contributing to the full S-matrix element that one considers. Notice that this is true only in the Feynman gauge: away from $\xi = 1$ additional pinching contributions need to be considered, *e.g.*, the ones coming from box and self-energy correction diagrams (Fig. 4).

To see how the aforementioned cancellation comes about, let us now imagine that the gluon self-energy $\Pi_{\alpha\beta}^{(1)}(q)$ is embedded into a physical process, such as the S-matrix element for the quark-quark elastic scattering process $\bar{\psi}(r_1)\psi(r_2) \rightarrow \bar{\psi}(p_1)\psi(p_2)$, with $q = r_1 - r_2 = p_2 - p_1$ being the momentum transfer. The one-loop quark-gluon vertex consists of the two graphs shown in Fig. 5. Let us concentrate on the non-Abelian diagram (d), and carry out

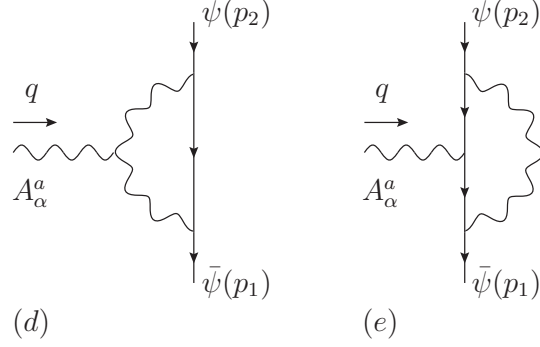


FIG. 5: The one-loop quark-gluon vertex appearing in the quark-quark elastic scattering process.

the vertex decomposition of Eq. (2.12) [15]:

$$\begin{aligned}
(d) &= \frac{1}{2}g^3 C_A t^a \int_k \frac{\Gamma_{\alpha\mu\nu} \gamma^\nu S^{(0)}(\not{k} + \not{p}_2) \gamma^\mu}{k^2(k+q)^2} \\
&= \frac{1}{2}g^3 C_A t^a \left[\int_k \frac{\Gamma_{\alpha\mu\nu}^F \gamma^\nu S^{(0)}(\not{k} + \not{p}_2) \gamma^\mu}{k^2(k+q)^2} + \int_k \frac{\Gamma_{\alpha\mu\nu}^P \gamma^\nu S^{(0)}(\not{k} + \not{p}_2) \gamma^\mu}{k^2(k+q)^2} \right]. \quad (2.22)
\end{aligned}$$

The first term on the rhs of the second line is the pure vertex-like part of (d), while the second term is purely propagator-like, as can be easily established using the elementary WI

$$k_\nu \gamma^\nu = (\not{k} + \not{p} - m) - (\not{p} - m) \quad (2.23)$$

The first term on the rhs of (2.23) removes (pinches out) the internal bare quark propagator $S_0(\not{k} + \not{p})$, whereas the second vanishes on shell, since $\bar{u}(p_2)(\not{p}_2 - m) = 0$ and $(\not{p}_1 - m)u(p_1) = 0$. Thus,

$$\int_k \frac{\Gamma_{\alpha\mu\nu}^P \gamma^\nu S^{(0)}(\not{k} + \not{p}_2) \gamma^\mu}{k^2(k+q)^2} \xrightarrow{\text{Dirac Eq. PT}} 2i \int_k \frac{1}{k^2(k+q)^2} \gamma_\alpha. \quad (2.24)$$

The self-energy-like contribution from the two vertex graphs (mirror graph included), to be denoted by $\Pi_{\alpha\beta}^{(1)P}(q)$, is given by (longitudinal pieces may be added for free, due to current conservation)

$$\Pi_{\alpha\beta}^{(1)P}(q) = 2C_A g^2 \int_k \frac{q^2 P_{\alpha\beta}(q)}{k^2(k+q)^2}. \quad (2.25)$$

The PT one-loop quark-gluon vertex, to be denoted by $\widehat{\Gamma}_\alpha^a(p_1, p_2)$, is given by [18]

$$\begin{aligned}
i\widehat{\Gamma}_\alpha^a(p_1, p_2) &= g^2 t^a \left[\frac{C_A}{2} \int_k \frac{\Gamma_{\alpha\mu\nu}^F \gamma^\nu S^{(0)}(\not{k} + \not{p}_2) \gamma^\mu}{k^2(k+q)^2} \right. \\
&\quad \left. - \left(\frac{C_A}{2} - C_f \right) \int_k \frac{\gamma^\mu S^{(0)}(\not{k} + \not{p}_2) \gamma^\alpha S^{(0)}(\not{k} + \not{p}_1) \gamma_\mu}{k^2} \right], \quad (2.26)
\end{aligned}$$

where C_f is the Casimir eigenvalue of the fundamental representation [$C_f = (N^2 - 1)/2N$ for $SU(N)$]. Now it is easy to derive the QED-like WI that the $\widehat{\Gamma}_\alpha^a(p_1, p_2)$ satisfies. Using (2.13), we have that

$$\begin{aligned} q^\alpha \widehat{\Gamma}_\alpha^a(p_1, p_2) &= -ig^3 t^a C_f \left[\int_k \frac{\gamma^\mu S^{(0)}(k + \not{p}_2) \gamma_\mu}{k^2} - \int_k \frac{\gamma^\mu S^{(0)}(k + \not{p}_1) \gamma_\mu}{k^2} \right] \\ &=igt^a [\Sigma(\not{p}_1) - \Sigma(\not{p}_2)], \end{aligned} \quad (2.27)$$

where $\Sigma(\not{p})$ is the one-loop quark self-energy in the Feynman gauge [20, 27].

Returning to the gluon self-energy, $\widehat{\Pi}_{\alpha\beta}^{(1)}(q)$ is defined as

$$\widehat{\Pi}_{\alpha\beta}^{(1)}(q) = \Pi_{\alpha\beta}^{(1)}(q) + \Pi_{\alpha\beta}^{\text{P}(1)}(q). \quad (2.28)$$

After carrying out the integrals one obtains

$$\begin{aligned} (\widehat{a})_{\alpha\beta} &= 10q^2 f(q^2) P_{\alpha\beta}(q), \\ (\widehat{b})_{\alpha\beta} &= q^2 f(q^2) P_{\alpha\beta}(q), \\ (c)_{\alpha\beta} &= -6q^2 f(q^2) P_{\alpha\beta}(q), \end{aligned} \quad (2.29)$$

and thus [15]

$$\begin{aligned} \widehat{\Pi}_{\alpha\beta}^{(1)}(q) &= (\widehat{a})_{\alpha\beta} + (\widehat{b})_{\alpha\beta} \\ &= 11q^2 f(q^2) P_{\alpha\beta}(q) = \widetilde{\Pi}_{\alpha\beta}^{(1)}(q)|_{\xi_Q=1}. \end{aligned} \quad (2.30)$$

Note that the second line of (2.30) expresses the PT-BFG correspondence at one loop [26].

Then, Eq. (2.21) assumes the alternative form

$$\Pi_{\alpha\beta}^{(1)}(q) = \widehat{\Pi}_{\alpha\beta}^{(1)}(q) + (c)_{\alpha\beta}. \quad (2.31)$$

As has been explained in detail in [34], and as we will see in the following sections, Eq. (2.31) is the one-loop version of a general identity [35], which we will call ‘‘Background-Quantum’’ identity (BQI) [34], relating the conventional and the BFM self-energies in terms of an auxiliary Green’s function, corresponding to graph (c). This identity is valid to all orders in perturbation theory, as well as non-perturbatively, and may be obtained either formally, by resorting to the Batalin-Vilkovisky (BV) formalism, or diagrammatically, as a by-product of the PT rearrangement of the conventional SD series; as we will see, in this latter case no reference to the BV formalism is necessary.

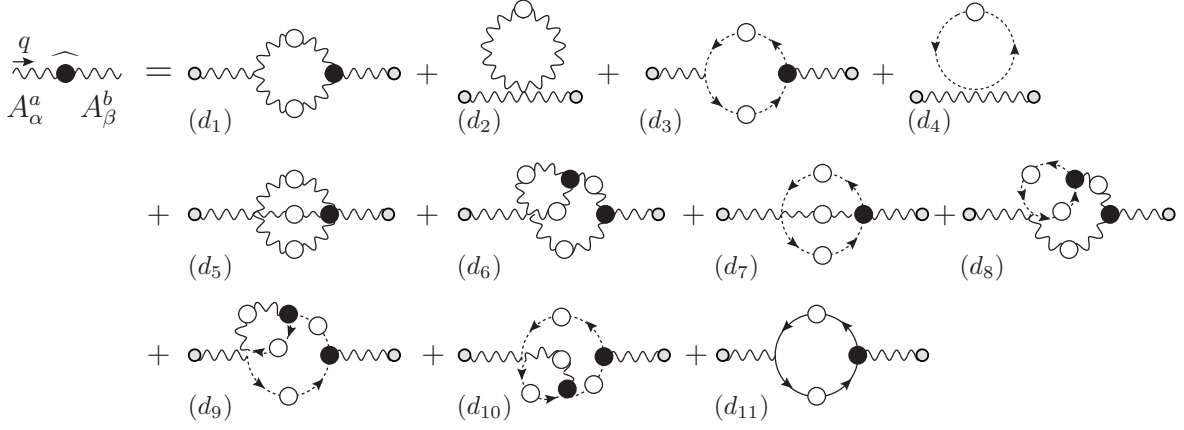


FIG. 6: The new Schwinger-Dyson series projected out dynamically by the PT algorithm. The symmetry factors are in this case $s(d_1, d_2, d_6) = 1/2$, $s(d_5) = 1/6$, and all the remaining diagrams have $s = -1$.

Let us now focus on $\Pi_{\alpha\beta}^{(1)}(q)$ and imagine for a moment that no ghost loops may be considered when computing it, *i.e.*, the graphs $(\widehat{b})_{\alpha\beta}$ must be omitted; in a SDE context this “omission” would amount to a “truncation” of the series. One may still obtain a *transverse* approximation for $\Pi_{\alpha\beta}^{(1)}(q)$ with no ghost-loop, given by

$$\Pi_{\alpha\beta}^{(1)}(q) = (\widehat{a})_{\alpha\beta} + (c)_{\alpha\beta} = 4q^2 f(q^2) P_{\alpha\beta}(q). \quad (2.32)$$

Interestingly enough, the PT rearrangement offers already at one-loop the ability to truncate gauge-invariantly, *i.e.*, preserving the transversality of the truncated answer.

E. The new Schwinger-Dyson series

The implementation of the PT at the level of the SDE has been studied first in the context of scalar QED [36]. The corresponding construction in the case of quarkless QCD has been recently carried out in a short communication [13], where we restricted ourselves to the SDE of the gluon propagator. As has been explained there, the PT rearrangement gives rise *dynamically* to a new SD series (see Fig. 6), with the following characteristics: on the rhs we have graphs that are made out of new vertices, but contain inside them the same gluon propagator as before, namely $\Delta_{\alpha\beta}(q)$. The new vertices, to be denoted by $\widehat{\Gamma}_{\alpha\mu\nu}^{amn}$, $\widehat{\Gamma}_{\alpha}^{anm}$, $\widehat{\Gamma}_{\alpha\mu\nu\rho}^{amnr}$, $\widehat{\Gamma}_{\alpha\mu}^{amnr}$, correspond precisely to the Feynman rules of the BFM in the Feynman gauge, *i.e.*, as already seen explicitly in the one-loop case, it is as if the external gluon had

FIG. 7: Diagrammatic representation of the auxiliary functions H and Λ .

been converted dynamically into a background gluon. The lhs is composed from the sum of three terms: in addition to the term $\Delta^{-1}(q^2)P_{\alpha\beta}(q)$, present there from the beginning, we have two additional contributions, $2G(q^2)\Delta^{-1}(q^2)P_{\alpha\beta}(q)$ and $G^2(q^2)\Delta^{-1}(q^2)P_{\alpha\beta}(q)$, which appear during the PT rearrangement of the rhs (and are subsequently carried to the lhs). The quantity $G(q^2)$ is a special function, defined in terms of the gluon and ghost propagators as well as the auxiliary function $H_{\alpha\beta}$ of Fig. 2. Specifically, define the following two-point function $\Lambda_{\alpha\beta}(q)$, (we suppress color indices)

$$\Lambda_{\alpha\beta}(q) = C_A \int_k H_{\mu\alpha}^{(0)} D(k) \Delta^{\mu\nu}(q-k) H_{\nu\beta}(q-k, -q), \quad (2.33)$$

with the diagrammatic representation shown in Fig. 7. Then, $G(q^2)$ is defined as i times the component of $\Lambda_{\alpha\beta}(q)$ multiplying $g_{\alpha\beta}$, namely

$$\Lambda_{\alpha\beta}(q) = ig_{\alpha\beta}G(q^2) + \dots, \quad (2.34)$$

where the omitted terms are proportional to $q_\alpha q_\beta$. Thus, the term appearing on the lhs of the new SDE is $\Delta^{-1}(q^2)[1 + G(q^2)]^2 P_{\alpha\beta}(q)$. So, one may write schematically

$$\Delta^{-1}(q^2)[1 + G(q^2)]^2 P_{\alpha\beta}(q) = q^2 P_{\alpha\beta}(q) + i \sum_{1=1}^{11} (d_i)_{\alpha\beta}, \quad (2.35)$$

or, equivalently, casting it into a more conventional form with the inverse of the unknown quantity isolated on the lhs, as

$$\Delta^{-1}(q^2)P_{\alpha\beta}(q) = \frac{q^2 P_{\alpha\beta}(q) + i \sum_{1=1}^{11} (d_i)_{\alpha\beta}}{[1 + G(q^2)]^2}. \quad (2.36)$$

This new SD series has a very special structure. Let us first separate the diagrams on the rhs into four obvious categories: one-loop (dressed) gluonic contributions $[(d_1)$ and $(d_2)]$, one-loop ghost contributions $[(d_3)$ and $(d_4)]$, two-loop gluonic contributions $[(d_5)$ and $(d_6)]$, and two-loop ghost contributions $[(d_7)$, (d_8) , (d_9) and $(d_{10})]$. It turns out that, by virtue of the all-order WI satisfied by the full vertices $\hat{\Gamma}_{\alpha\mu\nu}^{amn}$, $\hat{\Gamma}_{\alpha}^{anm}$, $\hat{\Gamma}_{\alpha\mu\nu\rho}^{amnr}$, $\hat{\Gamma}_{\alpha\mu}^{amnr}$ appearing in the

various diagrams, the contribution of each of the four subgroups is *individually* transverse. Specifically, the four fundamental all-order WIs are given by

$$q^\alpha \widehat{\Gamma}_{\alpha\mu\nu}^{amn}(q, k_1, k_2) = gf^{amn} [\Delta_{\mu\nu}^{-1}(k_1) - \Delta_{\mu\nu}^{-1}(k_2)], \quad (2.37)$$

$$q^\alpha \widehat{\Gamma}_\alpha^{anm}(q, k_1, k_2) = igf^{amn} [D^{-1}(k_1) - D^{-1}(k_2)], \quad (2.38)$$

$$\begin{aligned} q^\alpha \widehat{\Gamma}_{\alpha\mu\nu\rho}^{amnr}(q, k_1, k_2, k_3) &= gf^{adr} \Gamma_{\nu\rho\mu}^{drm}(q + k_2, k_3, k_1) + gf^{adn} \Gamma_{\nu\mu\rho}^{dmr}(q + k_3, k_1, k_2) \\ &+ gf^{adm} \Gamma_{\mu\nu\rho}^{dnr}(q + k_1, k_2, k_3), \end{aligned} \quad (2.39)$$

$$\begin{aligned} q^\alpha \widehat{\Gamma}_{\alpha\mu}^{amnr}(q, k_1, k_2, k_3) &= -gf^{ame} \Gamma_\mu^{enr}(q + k_1, k_2, k_3) - gf^{ane} \Gamma_\mu^{mer}(k_1, q + k_2, k_3) \\ &- gf^{are} \Gamma_\mu^{mne}(k_1, k_2, q + k_3). \end{aligned} \quad (2.40)$$

Using these WIs one may show after some elementary operations that [37]

$$\begin{aligned} q^\alpha [(d_1) + (d_2)]_{\alpha\beta} &= 0, \\ q^\alpha [(d_3) + (d_4)]_{\alpha\beta} &= 0, \\ q^\alpha [(d_5) + (d_6)]_{\alpha\beta} &= 0, \\ q^\alpha [(d_7) + (d_8) + (d_9) + (d_{10})]_{\alpha\beta} &= 0. \end{aligned} \quad (2.41)$$

[Notice that the one-loop dressed fermionic contributions (d_{11}) trivially satisfy this transversality property.]

As has been pointed out in [13], this special property has far-reaching practical consequences for the treatment of the SD series. Specifically, it furnishes a systematic truncation scheme that preserves the transversality of the answer. For example, keeping only the diagrams in the first group, we obtain the truncated SDE

$$\Delta^{-1}(q^2) P_{\alpha\beta}(q) = \frac{q^2 P_{\alpha\beta}(q) + i[(d_1) + (d_2)]_{\alpha\beta}}{[1 + G(q^2)]^2}, \quad (2.42)$$

and from the first equation of (2.41) we know that $[(d_1) + (d_2)]_{\alpha\beta}$ is transverse, *i.e.*, $[(d_1) + (d_2)]_{\alpha\beta} = (d-1)^{-1} [(d_1) + (d_2)]_\mu^\mu P_{\alpha\beta}(q)$. Thus, the transverse projector $P_{\alpha\beta}(q)$ appears *exactly* on both sides of (2.42); one may subsequently isolate the scalar cofactors on both sides obtaining a scalar equation of the form

$$\Delta^{-1}(q^2) = \frac{q^2 + \frac{i}{(d-1)} [(d_1) + (d_2)]_\mu^\mu}{[1 + G(q^2)]^2}. \quad (2.43)$$

A truncated equation similar to (2.42) may be written for any other of the four groups, or for sums of these groups, without compromising the transversality of the answer. The price

one has to pay for this advantageous situation is that one must consider in addition the equation determining $G(q^2)$, *i.e.*, the $g_{\alpha\beta}$ part of Eq. (2.33). This price is, however, rather modest, given that Eq. (2.33) may be approximated introducing, for example, a dressed-loop expansion (see Fig.2), without jeopardizing the transversality of $\Pi_{\alpha\beta}(q)$, given that $[1 + G(q^2)]^2$ affects only the size of the scalar prefactor.

In going from Eq. (2.35) to Eq. (2.36) one essentially chooses to retain the original propagator $\Delta(q)$ as the unknown quantity, to be dynamically determined from the SDE. There is, of course, an alternative strategy: one may define a new “variable” from the quantity appearing on the lhs (2.35), namely

$$\widehat{\Delta}(q) \equiv [1 + G(q^2)]^{-2} \Delta(q), \quad (2.44)$$

which leads to a new form for (2.35),

$$\widehat{\Delta}^{-1}(q^2)P_{\alpha\beta}(q) = q^2 P_{\alpha\beta}(q) + i \sum_{i=1}^{11} (d_i)_{\alpha\beta}. \quad (2.45)$$

Obviously, the special transversality properties established above holds as well for Eq. (2.45); for example, one may truncate it gauge-invariantly as

$$\widehat{\Delta}^{-1}(q^2)P_{\alpha\beta}(q) = q^2 P_{\mu\nu}(q) + i[(d_1) + (d_2)]_{\alpha\beta}. \quad (2.46)$$

Should one opt for treating $\widehat{\Delta}(q)$ as the new unknown quantity, then an additional step must be carried out: one must use (2.44) to rewrite the entire rhs of (2.45) in terms of $\widehat{\Delta}$ instead of Δ , *i.e.*, carry out the replacement $\Delta \rightarrow [1 + G]^2 \widehat{\Delta}$ *inside* every diagram on the rhs of Eq. (2.45) that contains Δ 's.

Let us discuss further these two versions of the SDE. Eq. (2.42) furnishes a gauge-invariant approximation for the conventional gluon self-energy $\Delta(q)$, whereas Eq. (2.45) is the gauge-invariant approximation for the effective PT self-energy $\widehat{\Delta}$. The crucial point is that one may switch from one to the other by means of Eq. (2.44). For practical purposes this means for example, that one may get a gauge-invariant approximation not just for the PT quantity (background Feynman gauge) but also for the *conventional* self-energy computed in the Feynman gauge. Eq. (2.44), which is the all-order generalization of the one-loop relation given in Eq. (2.31), plays an instrumental role in this entire construction, allowing one to convert the SDE series into a dynamical equation for either $\widehat{\Delta}(q)$ or $\Delta(q)$.

III. THE FORMAL MACHINERY

The extension of the PT algorithm to the SDEs of QCD is a challenging exercise, mainly due to the large amount of different Green's functions one needs to manipulate in the process. Most of these Green's functions are generated when longitudinal momenta trigger the STIs satisfied by specific subsets of fully dressed vertices appearing in the ordinary perturbative expansion. Due to the non-linearity of the BRST transformation [see Eq. (3.8) below] they involve composite operators; specifically, they are of the type $\langle 0|T[s\Phi(x)\cdots]|0\rangle$ with s the BRST operator and Φ a generic QCD field.

It turns out that the most efficient framework for dealing with this type of quantities is the BV formalism, allowing the construction of these auxiliary (ghost) Green's functions in terms of a well-defined set of Feynman rules. In addition, this formalism furnishes a set of useful identities (the BQIs mentioned in the previous section), relating Green's functions involving background fields to Green's functions involving quantum fields.

In this section, we fix our conventions, present the QCD Lagrangian and its gauge-fixing procedure (concentrating, in particular, on the conventional R_ξ gauges and the BFM), and briefly review the BV formalism. Then, we proceed to describe how one can extract from the master equations the all-order STIs and BQIs needed in the coming PT construction, postponing their actual derivation to the Appendix D and E. We will also describe how to derive the so-called Faddeev-Popov equations (see also Appendix C). Finally, in the process of describing all the above topics, we will introduce a particularly compact notation for Green's functions, which encodes unambiguously all relevant information (*i.e.*, the particle content, Lorentz and color structure, and momenta flow).

A. QCD Lagrangian and gauge fixing schemes

Throughout the paper we will adopt the conventions of the book by Peskin & Schröder [38]. The QCD Lagrangian density is given by

$$\mathcal{L} = \mathcal{L}_I + \mathcal{L}_{\text{GF}} + \mathcal{L}_{\text{FPG}}. \quad (3.1)$$

\mathcal{L}_I represents the gauge invariant $SU(3)$ Lagrangian, namely

$$\mathcal{L}_I = -\frac{1}{4}F_a^{\mu\nu}F_{\mu\nu}^a + \bar{\psi}_f^i(i\gamma^\mu\mathcal{D}_\mu - m)_{ij}\psi_f^j, \quad (3.2)$$

where $a = 1, \dots, 8$ (respectively $i, j = 1, 2, 3$) is the color index for the adjoint (respectively fundamental) representation, while “f” represents the flavor index. The field strength is

$$F_{\mu\nu}^a = \partial_\mu A_\nu^a - \partial_\nu A_\mu^a + g f^{abc} A_\mu^b A_\nu^c, \quad (3.3)$$

and the covariant derivative is defined according to

$$(\mathcal{D}_\mu)_{ij} = \partial_\mu(\mathbb{I})_{ij} - ig A_\mu^a (t^a)_{ij}, \quad (3.4)$$

with g the (strong) coupling constant. Finally, the $SU(3)$ generators t^a satisfy the commutation relations

$$[t^a, t^b] = i f^{abc} t^c, \quad (3.5)$$

with f^{abc} the totally antisymmetric $SU(3)$ structure constants.

\mathcal{L}_{GF} and \mathcal{L}_{FPG} represent respectively the (covariant) gauge fixing Lagrangian and its associated Faddeev-Popov ghost term. The most general way of writing these terms is through the expressions

$$\mathcal{L}_{\text{GF}} = -\frac{\xi}{2}(B^a)^2 + B^a \mathcal{F}^a, \quad (3.6)$$

$$\mathcal{L}_{\text{FPG}} = -\bar{c}^a s \mathcal{F}^a. \quad (3.7)$$

In the formulas above \mathcal{F}^a is the gauge fixing function, and the B^a are auxiliary, non-dynamical fields (the so called Nakanishi-Lautrup multipliers) that can be eliminated through their (trivial) equations of motion; c^a (respectively, \bar{c}^a) are the ghost (respectively, anti-ghost) fields, and, finally, s is the BRST operator, with the BRST transformations of the QCD fields given by

$$\begin{aligned} s A_\mu^a &= \partial_\mu c^a + g f^{abc} A_\mu^b c^c & s c^a &= -\frac{1}{2} g f^{abc} c^b c^c, \\ s \psi_f^i &= ig c^a (t^a)_{ij} \psi_f^j & s \bar{c}^a &= B^a, \\ s \bar{\psi}_f^i &= -ig c^a \bar{\psi}_f^j (t^a)_{ji} & s B^a &= 0. \end{aligned} \quad (3.8)$$

We thus see that the sum of the gauge fixing and Faddeev-Popov terms can be written as a total BRST variation:

$$\mathcal{L}_{\text{GF}} + \mathcal{L}_{\text{FPG}} = s \left(\bar{c}^a \mathcal{F}^a - \frac{\xi}{2} \bar{c}^a B^a \right). \quad (3.9)$$

This is of course expected, since it is well known that total BRST variations cannot appear in the physical spectrum of the theory. For our purposes, the gauge-fixing functions of interest

are the ones corresponding to the R_ξ (renormalizable ξ gauges) and the BFM, which we describe in what follows.

1. In the usual R_ξ gauges, the gauge fixing function is chosen to be $\mathcal{F}_{R_\xi}^a = \partial^\mu A_\mu^a$; therefore one finds

$$\mathcal{L}_{\text{GF}} = \frac{1}{2\xi}(\partial^\mu A_\mu^a)^2, \quad (3.10)$$

$$\mathcal{L}_{\text{FPG}} = \partial^\mu \bar{c}^a \partial_\mu c^a + g f^{abc} (\partial^\mu \bar{c}^a) A_\mu^b c^c \quad (3.11)$$

2. In the case of the BFM, one starts by splitting the gluon field into a background part, \widehat{A}_μ^a , and a quantum part, A_μ^a . Notice that the BRST variation of the background field will be zero, but the latter will enter in the variation of the quantum one, since

$$sA_\mu^a = \partial_\mu c^a + g f^{abc} (A_\mu^b + \widehat{A}_\mu^b) c^c. \quad (3.12)$$

The gauge fixing function is

$$\begin{aligned} \mathcal{F}_{\text{BFM}}^a &= (\widehat{\mathcal{D}}^\mu A_\mu)^a \\ &= \partial^\mu A_\mu^a + g f^{abc} \widehat{A}_\mu^b A_c^\mu, \end{aligned} \quad (3.13)$$

which gives in turn

$$\mathcal{L}_{\text{GF}} = \frac{1}{2\xi}(\partial^\mu A_\mu^a)^2 + \frac{1}{\xi} g f^{abc} (\partial^\mu A_\mu^a) \widehat{A}_\nu^b A_c^\nu + \frac{1}{2\xi} g^2 f^{abe} f^{cde} \widehat{A}_\mu^a A_b^\mu \widehat{A}_\nu^c A_d^\nu, \quad (3.14)$$

$$\begin{aligned} \mathcal{L}_{\text{FPG}} &= \partial^\mu \bar{c}^a \partial_\mu c^a + g f^{abc} (\partial^\mu \bar{c}^a) A_\mu^b c^c + g f^{abc} (\partial^\mu \bar{c}^a) \widehat{A}_\mu^b c^c - g f^{abc} \bar{c}^a \widehat{A}_\mu^b (\partial^\mu c^c) \\ &\quad - g^2 f^{abe} f^{cde} \bar{c}^a \widehat{A}_\mu^b (A_c^\mu + \widehat{A}_\mu^c) c^d. \end{aligned} \quad (3.15)$$

We thus see the appearance of the characteristic ghost sector for the interaction with background gluons, consisting in a symmetric $\widehat{A}c\bar{c}$ ghost vertex and a four particle $\widehat{A}Ac\bar{c}$ one.

B. Green's functions: conventions

The Green's functions of the theory can be constructed in terms of time-ordered products of free fields $\Phi_1^0 \cdots \Phi_n^0$ and vertices of the interaction Lagrangian \mathcal{L}_{int} (constructed from the

pieces of \mathcal{L} which are not bilinear in the fields) through the standard Gell-Man–Low formula for the 1PI truncated Green’s functions

$$\begin{aligned}\Gamma_{\Phi_1 \dots \Phi_n}(x_1, \dots, x_n) &= \langle T[\Phi_1(x_1) \dots \Phi_n(x_n)] \rangle^{\text{1PI}} \\ &= \langle T[\Phi_1^0(x_1) \dots \Phi_n^0(x_n)] \exp(-i \int d^4x \mathcal{L}_{\text{int}}) \rangle^{\text{1PI}}.\end{aligned}\quad (3.16)$$

The complete set of Green’s functions can be handled most efficiently by introducing a generating functional, which in Fourier space reads

$$\Gamma[\Phi] = \sum_{n=0}^{\infty} \frac{(-i)^n}{n!} \int \prod_{i=0}^n d^4p_i \delta^4\left(\sum_{j=1}^n p_j\right) \Phi_1(p_1) \dots \Phi_n(p_n) \Gamma_{\Phi_1 \dots \Phi_n}(p_1, \dots, p_n), \quad (3.17)$$

with p_i the (in-going) momentum of the Φ_i field. Since in perturbation theory $\Gamma_{\Phi_1 \dots \Phi_n}$ is a formal power series in \hbar , we will denote its m -loop contribution as $\Gamma_{\Phi_1 \dots \Phi_n}^{(m)}$. Then, in terms of the generating functional $\Gamma[\Phi]$ any of the Green’s function of the theory can be obtained by means of functional derivatives:

$$\Gamma_{\Phi_1 \dots \Phi_n}(p_1, \dots, p_n) = i^n \frac{\delta^n \Gamma}{\delta \Phi_1(p_1) \delta \Phi_2(p_2) \dots \delta \Phi_n(p_n)} \Big|_{\Phi_i=0}, \quad (3.18)$$

where $\Phi(p)$ denotes the Fourier transform of $\Phi(x)$ and our convention on the external momenta is summarized in Fig. 8. From the definition given in Eq. (3.18) it follows that the Green’s functions $i^{-n} \Gamma_{\Phi_1 \dots \Phi_n}$ are simply given by the corresponding Feynman diagrams in Minkowski space. Finally, notice that upon inversion of two (adjacent) fields we have

$$\Gamma_{\Phi_1 \dots \Phi_i \Phi_{i+1} \dots \Phi_n}(p_1, \dots, p_i, p_{i+1}, \dots, p_n) = \pm \Gamma_{\Phi_1 \dots \Phi_{i+1} \Phi_i \dots \Phi_n}(p_1, \dots, p_{i+1}, p_i, \dots, p_n), \quad (3.19)$$

with the minus appearing only when both fields Φ_i and Φ_{i+1} obey Fermi statistics.

The Green’s functions constructed so far are sufficient for building all possible amplitudes involved in the S -matrix computation; however, due to the non-linearity of the BRST transformations [Eq. (3.8)], they do not cover the complete set of Green’s functions appearing in the STIs of the theory (and therefore needed for its renormalization, as well as the PT construction).

C. A brief introduction to the Batalin-Vilkovisky formalism

In this subsection we review briefly the BV formalism [39], which allows one to obtain both the STIs as well as the BQIs of the theory at hand. In order to simplify the notation

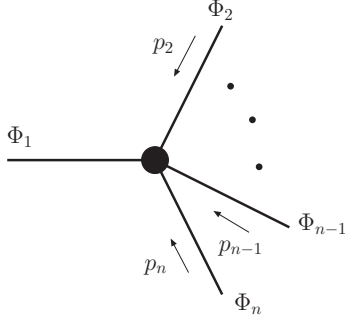


FIG. 8: Our conventions for the (1PI) Green's functions $\Gamma_{\Phi_1 \dots \Phi_n}(p_1, \dots, p_n)$. All momenta p_2, \dots, p_n are assumed to be incoming, and are assigned to the corresponding fields starting from the rightmost one. The momentum of the leftmost field Φ_1 is determined through momentum conservation ($\sum_i p_i = 0$) and will be suppressed.

	A_μ^m	ψ_f^i	$\bar{\psi}_f^i$	c^m	\bar{c}^m	B^m	A_μ^{*m}	ψ_f^{*i}	$\bar{\psi}_f^{*i}$	c^{*m}	\bar{c}^{*m}	\hat{A}_μ^m	Ω_μ^m
Ghost ch.	0	0	0	1	-1	0	-1	-1	-1	-2	0	0	1
Stat.	B	F	F	F	F	B	F	B	B	B	B	B	F
Dim.	1	$\frac{3}{2}$	$\frac{3}{2}$	0	2	2	3	$\frac{5}{2}$	$\frac{5}{2}$	4	2	1	1

TABLE I: Ghost charge, statistics (B for Bose, F for Fermi), and mass dimension of the QCD fields, anti-fields and background sources.

(and since they will not play any role in what follows) we will suppress from now on all spinor indices (both flavor and color).

Let us then start by introducing for each field Φ appearing in the theory a corresponding anti-field, to be denoted by Φ^* . The anti-field Φ^* has opposite statistics with respect to Φ ; its ghost charge, $\text{gh}(\Phi^*)$, is related to the ghost charge $\text{gh}(\Phi)$ of the field Φ by $\text{gh}(\Phi^*) = -1 - \text{gh}(\Phi)$. For convenience, we summarize the ghost charges and statistics of the various QCD fields and anti-fields in Table I. Next, we add to the original gauge invariant Lagrangian a term coupling the anti-fields with the BRST variation of the corresponding fields, to get

$$\begin{aligned} \mathcal{L}_{\text{BV}} &= \mathcal{L}_{\text{I}} + \mathcal{L}_{\text{BRST}}, \\ \mathcal{L}_{\text{BRST}} &= \sum_{\Phi} \Phi^* s\Phi \end{aligned}$$

$$\begin{aligned}
&= A_\mu^{*a}(\partial^\mu c^a + g f^{abc} A_b^\mu c^c) - \frac{1}{2} g f^{abc} c^{*a} c^b c^c + i g \bar{\psi}^* c^a t^a \psi - i g c^a \bar{\psi} t^a \psi^* \\
&+ \bar{c}^{*a} B^a
\end{aligned} \tag{3.20}$$

Then, the action $\Gamma^{(0)}[\Phi, \Phi^*]$ constructed from \mathcal{L}_{BV} , will satisfy the master equation

$$\int d^4x \sum_{\Phi} \frac{\delta \Gamma^{(0)}}{\delta \Phi^*} \frac{\delta \Gamma^{(0)}}{\delta \Phi} = 0. \tag{3.21}$$

To verify this, observe that, on one hand, the terms in $\delta \Gamma^{(0)}/\delta \Phi$ that are independent from the anti-fields Φ^* are zero due the BRST (actually the gauge) invariance of the action

$$\int d^4x \sum_{\Phi} s\Phi \frac{\delta \Gamma_I^{(0)}}{\delta \Phi} = \int d^4x (s\Gamma_I^{(0)}[\Phi]) = 0; \tag{3.22}$$

on the other hand, terms in $\delta \Gamma^{(0)}/\delta \Phi$ that are linear in the anti-fields vanish due to the nilpotency of the BRST operator

$$\int d^4x \sum_{\Phi, \Phi'} s\Phi' \frac{\delta(s\Phi)}{\delta \Phi'} = \int d^4x \sum_{\Phi} s^2\Phi = 0. \tag{3.23}$$

Now, since the anti-fields are external sources, we must constrain them to suitable values before we can use the action $\Gamma^{(0)}$ in calculations of S -matrix elements [25]. To that end, we introduce an arbitrary fermionic functional, $\Psi[\Phi]$, with ghost charge -1, and set for all the anti-fields Φ^*

$$\Phi^* = \frac{\delta \Psi[\Phi]}{\delta \Phi}. \tag{3.24}$$

Then the action becomes

$$\begin{aligned}
\Gamma^{(0)}[\Phi, \delta \Psi/\delta \Phi] &= \Gamma_I^{(0)}[\Phi] + (s\Phi) \frac{\delta \Psi[\Phi]}{\delta \Phi} \\
&= \Gamma_I^{(0)}[\Phi] + s\Psi[\Phi],
\end{aligned} \tag{3.25}$$

and therefore, choosing the functional Ψ to satisfy the relation

$$s\Psi = \int d^4x (\mathcal{L}_{\text{GF}} + \mathcal{L}_{\text{FPG}}), \tag{3.26}$$

we see that the action $\Gamma^{(0)}$ (obtained from \mathcal{L}_{BV}) is equivalent to the gauge-fixed action obtained from the original Lagrangian \mathcal{L} of Eq. (3.1). The functional Ψ is often referred to as the ‘‘gauge fixing fermion’’.

The BRST symmetry is crucial for endowing a theory with a unitary S -matrix and gauge-independent physical observables; therefore, it must be implemented to all orders. For doing

so we establish the quantum corrected version of the master equation (3.21) in the form of the STI functional

$$\begin{aligned}
\mathcal{S}(\Gamma)[\Phi] &= \int d^4x \sum_{\Phi} \frac{\delta\Gamma}{\delta\Phi^*} \frac{\delta\Gamma}{\delta\Phi} \\
&= \int d^4x \left\{ \frac{\delta\Gamma}{\delta A_m^{*\mu}} \frac{\delta\Gamma}{\delta A_\mu^m} + \frac{\delta\Gamma}{\delta c^{*m}} \frac{\delta\Gamma}{\delta c^m} + \frac{\delta\Gamma}{\delta\psi^*} \frac{\delta\Gamma}{\delta\bar{\psi}} + \frac{\delta\Gamma}{\delta\psi} \frac{\delta\Gamma}{\delta\bar{\psi}^*} + B^m \frac{\delta\Gamma}{\delta\bar{c}^m} \right\} \\
&= 0,
\end{aligned} \tag{3.27}$$

where $\Gamma[\Phi, \Phi^*]$ is now the effective action.

In order to simplify the structure of the STI generating functional of Eq. (3.27), let us notice that the anti-ghost \bar{c}^a and the multiplier B^a have *linear* BRST transformations; therefore they do not present the usual complications (due to non-linearity) of the other QCD fields. Together with their corresponding anti-field, they enter bi-linearly in the action, and one can write the complete action (which we now explicitly indicate it with a C subscript) as a sum of a minimal and non-minimal sector

$$\Gamma_C^{(0)}[\Phi, \Phi^*] = \Gamma^{(0)}[A, A^*, \psi, \psi^*, \bar{\psi}, \bar{\psi}^*, c, c^*] + \bar{c}^{*a} B^a. \tag{3.28}$$

The last term has no effect on the master equation (3.21), which is satisfied by $\Gamma^{(0)}$ alone; the fields $\{A_\mu^a, A_\mu^{*a}, \psi, \psi^*, \bar{\psi}, \bar{\psi}^*, c^a, c^{*a}\}$ are then often called *minimal variables* while \bar{c}^a and B^a are referred to as non-minimal variables or “trivial pairs”. Equivalently one can introduce the minimal (or reduced) action by subtracting from the complete one the local term corresponding to the gauge-fixing Lagrangian, *i.e.*,

$$\Gamma = \Gamma_C - \int d^4x \mathcal{L}_{\text{GF}}. \tag{3.29}$$

In either cases, the result is that the STI functional is now written as

$$\mathcal{S}(\Gamma)[\Phi] = \int d^4x \left\{ \frac{\delta\Gamma}{\delta A_m^{*\mu}} \frac{\delta\Gamma}{\delta A_\mu^m} + \frac{\delta\Gamma}{\delta c^{*m}} \frac{\delta\Gamma}{\delta c^m} + \frac{\delta\Gamma}{\delta\psi^*} \frac{\delta\Gamma}{\delta\bar{\psi}} + \frac{\delta\Gamma}{\delta\psi} \frac{\delta\Gamma}{\delta\bar{\psi}^*} \right\} = 0. \tag{3.30}$$

In practice, the STIs generated from the functional of Eq. (3.30) coincide with the one obtained by the complete one after the implementation of the Faddeev-Popov equation described in the next subsection [40]. One should also keep in mind that the Green’s functions involving unphysical fields generated by the minimal functional coincide with the ones generated by the complete functional only up to constant terms proportional to the gauge fixing parameter, *e.g.*, $\Gamma_{A_\mu A_\nu}(q) = \Gamma_{A_\mu A_\nu}^C(q) - i\xi^{-1}q_\mu q_\nu$. We will discuss further the differences

between employing the complete and minimal generating functionals in the Appendix D and E.

Taking functional derivatives of $\mathcal{S}(\Gamma)[\Phi]$ and setting afterwards all fields and anti-fields to zero will generate the complete set of the all-order STIs of the theory; this is in exact analogy to what happens with the effective action, where taking functional derivatives of $\Gamma[\Phi]$ and setting afterwards all fields to zero generates the Green's functions of the theory, see Eq. (3.18). However, in order to reach meaningful expressions, one needs to keep in mind that:

1. $\mathcal{S}(\Gamma)$ has ghost charge 1;
2. functions with non-zero ghost charge vanish, since the ghost charge is a conserved quantity.

Thus, in order to extract non-zero identities from Eq. (3.30) one needs to differentiate the latter with respect to a combination of fields, containing either one ghost field, or two ghost fields and one anti-field. The only exception to this rule is when differentiating with respect to a ghost anti-field, which needs to be compensated by three ghost fields. In particular, identities involving one or more gauge fields are obtained by differentiating Eq. (3.30) with respect to the set of fields in which one gauge boson has been replaced by the corresponding ghost field. This is due to the fact that the linear part of the BRST transformation of the gauge field is proportional to the ghost field: $sA_\mu^a|_{\text{linear}} = \partial_\mu c^a$. For completeness we notice that, for obtaining STIs involving Green's functions that contain ghost fields, one ghost field must be replaced by two ghost fields, due to the non linearity of the BRST ghost field transformation [$sc^a \propto f^{abc}c^b c^c$, see Eq. (3.8)]. The last technical point to be clarified is the dependence of the STIs on the (external) momenta. One should notice that the integral over d^4x present in Eq. (3.30), together with the conservation of momentum flow of the Green's functions, implies that no momentum integration is left over; as a result, the STIs will be expressed as a sum of products of (at most two) Green's functions.

An advantage of working with the BV formalism is the fact that the STI functional of Eq. (3.30) is valid in any gauge, *i.e.*, it will not be affected when switching from one gauge to another. In particular, if we want to consider the BFM gauge, the only additional step we need to take is to implement the equations of motion for the background fields at the quantum level. This latter step is achieved most efficiently by extending the BRST

symmetry to the background gluon field, through the relations

$$s\widehat{A}_\mu^m = \Omega_\mu^m, \quad s\Omega_\mu^m = 0, \quad (3.31)$$

where Ω_μ^m represents a (classical) vector field with the same quantum numbers as the gluon, ghost charge +1 and Fermi statistics (see also Table I). The dependence of the Green's functions on the background fields is then controlled by the modified STI functional

$$\mathcal{S}'(\Gamma')[\Phi] = \mathcal{S}(\Gamma')[\Phi] + \int d^4x \Omega_\mu^m \left(\frac{\delta\Gamma'}{\delta\widehat{A}_\mu^m} - \frac{\delta\Gamma'}{\delta A_\mu^m} \right) = 0, \quad (3.32)$$

where Γ' denotes the effective action that depends on the background sources Ω_μ^m (with $\Gamma \equiv \Gamma'|_{\Omega=0}$), and $\mathcal{S}(\Gamma')[\Phi]$ is the STI functional of Eq. (3.30). Differentiation of the STI functional (3.32) with respect to the background source and background or quantum fields will then provide the so called BQIs, which relate 1PI Green's functions involving background fields with the ones involving quantum fields. The BQIs are particularly useful in the PT context, since they allow for a direct comparison between PT and BFM Green's functions.

Finally, the background gauge invariance of the BFM effective action implies that Green's functions involving background fields satisfy linear WIs when contracted with the momentum corresponding to a background leg [see, *e.g.*, Eq.s (2.37) – (2.40)]. These WIs are generated by taking functional differentiations of the WI functional

$$\mathcal{W}_\vartheta[\Gamma'] = \int d^4x \sum_{\Phi, \Phi^*} (\delta_{\vartheta(x)}\Phi) \frac{\delta\Gamma'}{\delta\Phi} = 0, \quad (3.33)$$

where $\vartheta^a(x)$ are the local infinitesimal parameters corresponding to the $SU(3)$ generators t^a that now play the role of the ghost field. The transformations $\delta_\vartheta\Phi$ are thus given by

$$\begin{aligned} \delta_\vartheta A_\mu^a &= g f^{abc} A_\mu^b \vartheta^c & \delta_\vartheta \widehat{A}_\mu^a &= \partial_\mu \vartheta^a + g f^{abc} \widehat{A}_\mu^b \vartheta^c, \\ \delta_\vartheta c^a &= -g f^{abc} c^b \vartheta^c & \delta_\vartheta \bar{c}^a &= -g f^{abc} \bar{c}^b \vartheta^c, \\ \delta_\vartheta \psi_f^i &= i g \vartheta^a (t^a)_{ij} \psi_f^j & \delta_\vartheta \bar{\psi}_f^i &= -i g \vartheta^a \bar{\psi}_f^j (t^a)_{ji}, \end{aligned} \quad (3.34)$$

and the background transformations of the anti-fields $\delta_\vartheta\Phi^*$ coincide with the gauge transformations of the corresponding quantum gauge fields according to their specific representation. Notice that, in order to obtain the WI satisfied by the Green's functions involving background gluons \widehat{A} , one has to differentiate the functional (3.33) with respect to the corresponding parameter ϑ .

All the STIs and BQIs needed for the PT construction carried out in the rest of this paper, together with the method of constructing the auxiliary functions appearing in these identities, are reported in Appendix D and E, respectively.

D. Faddeev-Popov equation(s)

The final ingredient needed for carrying out the PT program for SDEs is the derivation of the so-called Faddeev-Popov equation (FPE). The FPE depends crucially on the form of the ghost Lagrangian, which, in turn, depends on the gauge fixing function [see Eq. (3.7)]. In what follows we will first present the corresponding derivation in the R_ξ gauges, and then in the BFM.

To derive the FPE in the R_ξ gauges, one observes that in the QCD action the only term proportional to the anti-ghost fields comes from the Faddeev-Popov lagrangian density, which can be rewritten as

$$\mathcal{L}_{\text{FPG}}^{R_\xi} = -\bar{c}^m \partial^\mu (s A_\mu^m) = -\bar{c}^m \partial^\mu \frac{\delta \Gamma}{\delta A_\mu^{*m}}. \quad (3.35)$$

Differentiation of the action with respect to \bar{c}^a then yields the FPE in the form of the identity

$$\frac{\delta \Gamma}{\delta \bar{c}^m} + \partial^\mu \frac{\delta \Gamma}{\delta A_\mu^{*m}} = 0, \quad (3.36)$$

so that, taking the Fourier transform, we arrive at

$$\frac{\delta \Gamma}{\delta \bar{c}^m} + i q^\mu \frac{\delta \Gamma}{\delta A_\mu^{*m}} = 0. \quad (3.37)$$

Thus, in the R_ξ case, the FPE amounts to the simple statement that the contraction of a leg corresponding to a gluon anti-field (A_μ^{*m}) by its own momentum (q^μ) converts it to an anti-ghost leg (\bar{c}^m). Functional differentiation of this identity with respect to QCD fields (but not background sources and fields, see below) furnishes useful identities, that will be used extensively in our construction.

For obtaining FPEs for Green's functions involving BFM gluons and sources, one has to modify Eq. (3.37), in order to account for the presence of extra terms in the BFM gauge fixing function (and therefore in the BFM Faddeev-Popov ghost Lagrangian). Eq. (3.35) gets then modified into

$$\frac{\delta \Gamma'}{\delta \bar{c}^m} + \left(\widehat{\mathcal{D}}^\mu \frac{\delta \Gamma'}{\delta A_\mu^*} \right)^m - (\mathcal{D}^\mu \Omega_\mu)^m - g f^{mrs} \widehat{A}_\mu^r \Omega_s^\mu = 0. \quad (3.38)$$

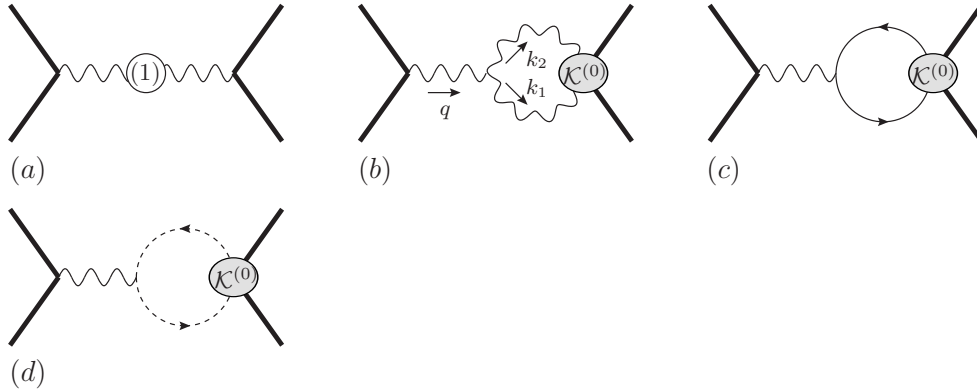


FIG. 9: The S -matrix one-loop PT setting for constructing the gluon propagator. The external particles are left unspecified since they can be both quarks as well as gluons. The kernels $\mathcal{K}^{(0)}$ appearing in diagram (b) are the tree-level version of the one shown in Figs 11 and 15 (depending on the external particles chosen) and therefore contains only the 1PR terms shown there. Three diagrams having the kernels on the opposite side are not shown.

Notice that by undoing the splitting of the field A into background and quantum parts (that is using $A + \hat{A} \rightarrow A$) the equation above assumes the more compact form

$$\frac{\delta\Gamma'}{\delta\bar{c}^m} + \left(\hat{\mathcal{D}}^\mu \frac{\delta\Gamma'}{\delta A_\mu^*} \right)^m - (\mathcal{D}^\mu \Omega_\mu)^m = 0. \quad (3.39)$$

The specific FPEs needed for the PT construction are reported in Appendix C.

E. The (one-loop) PT algorithm in the BV language

Before entering into the intricacies of the SDEs, it is important to make contact between the PT algorithm and the BV formalism. This is best done at the one-loop level, since in this case all calculations are rather straightforward and it is relatively easy to compare the standard diagrammatic results with those coming from the BV formalism. This comparison will (i) help us identify the pieces that will be generated when applying the PT algorithm, and (ii) establish the rules for distributing the pieces obtained in (i) among the different Green's functions appearing in the calculation.

The starting point is the embedding of the (one-loop) gluon propagator into an S -matrix element (Fig. 9), exactly as done in subsection IID. Then, carrying out the PT decomposition $\Gamma = \Gamma^P + \Gamma^F$ on the tree-level three-gluon vertex of diagram (b) [see Eq. (2.12)], we

find

$$(b) = (b)^F + (b)^P, \quad (3.40)$$

$$(b)^P = -\frac{1}{2}g f^{am'n'} \int_{k_1} (g_{\alpha\nu'} k_{1\mu'} - g_{\alpha\mu'} k_{2\nu'}) \Delta_{m'm}^{(0)\mu'\mu}(k_1) \Delta_{n'n}^{(0)\nu'\nu}(k_2) \mathcal{K}_{A_\mu^m A_\nu^p \psi \bar{\psi}}^{(0)}(k_2, p_2, -p_1). \quad (3.41)$$

Of course, k_1 and k_2 are not independent, since $k_2 = q - k_1$; thus, we have

$$\begin{aligned} & f^{am'n'} g_{\alpha\mu'} \int_{k_1} k_{2\nu'} \Delta_{m'm}^{(0)\mu'\mu}(k_1) \Delta_{n'n}^{(0)\nu'\nu}(k_2) \mathcal{K}_{A_\mu^m A_\nu^p \psi \bar{\psi}}^{(0)}(k_2, p_2, -p_1) \\ &= f^{am'n'} g_{\alpha\mu'} \int_{k_1} k_{1\nu'} \Delta_{m'm}^{(0)\mu'\mu}(k_2) \Delta_{n'n}^{(0)\nu'\nu}(k_1) \mathcal{K}_{A_\mu^m A_\nu^p \psi \bar{\psi}}^{(0)}(k_1, p_2, -p_1) \\ &= -f^{am'n'} g_{\alpha\nu'} \int_{k_1} k_{1\mu'} \Delta_{m'm}^{(0)\mu'\mu}(k_1) \Delta_{n'n}^{(0)\nu'\nu}(k_2) \mathcal{K}_{A_\mu^m A_\nu^p \psi \bar{\psi}}^{(0)}(k_2, p_2, -p_1), \end{aligned} \quad (3.42)$$

and we see that the contributions of the two longitudinal momenta add up, thus removing the 1/2 symmetry factor (this is clearly an all-order result, since the above derivation does not depend on the various Green's functions and kernels being at tree-level). Therefore we obtain

$$(b)^P = -g f^{am'n} g_\alpha^\nu \int_{k_1} \frac{1}{k_1^2} \frac{1}{k_2^2} k_1^\mu \mathcal{K}_{A_\mu^m A_\nu^p \psi \bar{\psi}}^{(0)}(k_2, p_2, -p_1). \quad (3.43)$$

On the other hand, using the results

$$k_1^2 D_{mm'}^{(0)}(k_1) = \delta^{mm'}, \quad \Gamma_{c m' A_\nu^p A_d^{*\rho}}^{(0)} = g g_\nu^\rho f^{m'dn}, \quad \Gamma_{c m' A_d^{*\rho} \psi \bar{\psi}}^{(0)} = 0, \quad (3.44)$$

we find that the STI of Eq. (D.29) reduces to

$$\begin{aligned} k_1^\mu \mathcal{K}_{A_\mu^m A_\nu^p \psi \bar{\psi}}^{(0)}(k_2, p_2, -p_1) &= -g g_\nu^\gamma f^{dmn} \Gamma_{A_\gamma^d \psi \bar{\psi}}^{(0)}(p_2, -p_1) + \Gamma_{\psi \bar{\psi}}^{(0)}(p_1) \mathcal{K}_{A_\nu^p c m \bar{\psi}^*}^{(0)}(p_2, k_1, -p_1) \\ &+ \mathcal{K}_{A_\nu^p \psi^* \bar{\psi} c m}^{(0)}(p_2, -p_1, k_1) \Gamma_{\psi \bar{\psi}}^{(0)}(p_2). \end{aligned} \quad (3.45)$$

At this point the calculation is over and one needs to reshuffle the pieces generated. First of all, notice that when the external legs are on-shell the last two terms of the above STI drop out, by virtue of the (all-order) equations of motion

$$\Gamma_{\psi \bar{\psi}}^{(0)}(p_2) u(p_2) \Big|_{\not{p}_2=m} = 0, \quad (3.46)$$

$$\bar{u}(p_1) \Gamma_{\psi \bar{\psi}}^{(0)}(p_1) \Big|_{\not{p}_1=m} = 0. \quad (3.47)$$

Thus, making use of Eq. (E.9) we are finally left with the result

$$\begin{aligned} (b)^P &= g^2 C_A \delta^{ad} g_\alpha^\gamma \int_{k_1} \frac{1}{k_1^2} \frac{1}{k_2^2} \Gamma_{A_\gamma^d \psi \bar{\psi}}^{(0)}(p_2, -p_1) \\ &= -\Gamma_{\Omega_\alpha^a A_d^{*\gamma}}^{(1)}(-q) \Gamma_{A_\gamma^d \psi \bar{\psi}}^{(0)}(p_2, -p_1). \end{aligned} \quad (3.48)$$

Notice that, as explicitly shown in Appendix E, the auxiliary function $\Gamma_{\Omega_\alpha A_\beta^*}$ [see Eq. (E.9) and Fig. 24] coincide with the function $\Lambda_{\alpha\beta}$ [see Eq. (2.33) and Fig. 7] to all orders

$$\Lambda_{\alpha\beta}(q) \equiv \Gamma_{\Omega_\alpha A_\beta^*}(q). \quad (3.49)$$

Thus the scalar function $G(q^2)$ introduced earlier in Section II E corresponds also to (i times) the $g_{\alpha\beta}$ part of $\Gamma_{\Omega_\alpha A_\beta^*}$.

We can now define the PT (on-shell) quark-gluon vertex, by considering the corresponding Green's function embedded in the diagrams

$$\begin{aligned} (b)^F + (c) &= (b) + (c) - (b)^P \\ \Rightarrow i\widehat{\Gamma}_{A_\alpha^a \psi \bar{\psi}}^{(1)}(p_2, -p_1) &= i\Gamma_{A_\alpha^a \psi \bar{\psi}}^{(1)}(p_2, -p_1) + \Gamma_{\Omega_\alpha^a A_d^{*\gamma}}^{(1)}(-q)\Gamma_{A_\gamma^d \psi \bar{\psi}}^{(0)}(p_2, -p_1), \end{aligned} \quad (3.50)$$

while the PT self-energy will given by the combination

$$(a) + 2(b)^P \Rightarrow \widehat{\Pi}_{\alpha\beta}^{(1)}(q) = \Pi_{\alpha\beta}^{(1)}(q) + \Pi_{\alpha\beta}^{P(1)}(q). \quad (3.51)$$

The factor of 2 comes from the mirror diagram of (b) having the kernel on the left side, and we have defined [with the aid of Eq. (D.10)]

$$\begin{aligned} \delta^{ab}\Pi_{\alpha\beta}^{P(1)}(q) &= -2\Gamma_{\Omega_\alpha^a A_d^{*\gamma}}^{(1)}(q)q^2 P_{\gamma\beta}(q)\delta^{bd} \\ &= 2i\Gamma_{\Omega_\alpha^a A_d^{*\gamma}}^{(1)}(q)\Gamma_{A_\gamma^d A_\beta^b}^{(0)}(q). \end{aligned} \quad (3.52)$$

We can now proceed to the comparison of the PT Green's function with that of the BFG, by resorting to the BQIs. Clearly, Eq. (3.50) represents the one-loop version of the BQI of Eq. (E.13), and we immediately conclude that

$$\widehat{\Gamma}_{A_\alpha^a \psi \bar{\psi}}^{(1)}(p_2, -p_1) \equiv \Gamma_{\widehat{A}_\alpha^a \psi \bar{\psi}}^{(1)}(p_2, -p_1). \quad (3.53)$$

For the self-energy we have instead [recall that $-\Gamma_{A_\mu^m A_\nu^p}(k) = \Pi_{\mu\nu}(k)$]

$$\delta^{ab}\widehat{\Pi}_{\alpha\beta}^{(1)}(q) = -\Gamma_{A_\alpha^a A_\beta^b}^{(1)}(q) + 2i\Gamma_{\Omega_\alpha^a A_d^{*\gamma}}^{(1)}(q)\Gamma_{A_\gamma^d A_\beta^b}^{(0)}(q), \quad (3.54)$$

which represents the one-loop version of the BQI of Eq. (E.4), *i.e.*, we have

$$\delta^{ab}\widehat{\Pi}_{\alpha\beta}^{(1)}(q) = -\Gamma_{\widehat{A}_\alpha^a \widehat{A}_\beta^b}^{(1)}(q). \quad (3.55)$$

The procedure just described goes through almost unaltered when choosing the external legs of the process to be gluons. In this case

$$(b)^P = -gf^{amnn}g_\alpha^\nu \int_{k_1} \frac{1}{k_1^2} \frac{1}{k_2^2} k_1^\mu \mathcal{K}_{A_\mu^m A_\nu^p A_\rho^r A_\sigma^s}^{(0)}(k_2, p_2, -p_1). \quad (3.56)$$

and one has from the STI of Eq. (D.36) the result

$$\begin{aligned}
k_1^\mu \mathcal{K}_{A_\mu^m A_\nu^p A_\rho^s A_\sigma^s}^{(0)}(k_2, p_2, -p_1) &= -gg_\nu^\gamma f^{dmn} \Gamma_{A_\gamma^d A_\rho^r A_\sigma^s}^{(0)}(p_2, -p_1) \\
&+ \mathcal{K}_{c^m A_\nu^p A_\sigma^s A_d^{*\gamma}}^{(0)}(k_2, -p_1, p_2) \Gamma_{A_\gamma^d A_\rho^r}^{(0)}(p_2) \\
&+ \mathcal{K}_{c^m A_\nu^p A_\rho^r A_d^{*\gamma}}^{(0)}(k_2, p_2, -p_1) \Gamma_{A_\gamma^d A_\sigma^s}^{(0)}(p_1) \\
&+ \mathcal{K}_{c^m A_\rho^r A_\sigma^s A_d^{*\gamma}}^{(0)}(p_2, -p_1, k_2) \Gamma_{A_\gamma^d A_\nu^p}^{(0)}(k_2). \tag{3.57}
\end{aligned}$$

As before, the second and third terms drop out when the external gluons are taken to be on-shell; thus we are left with the terms

$$\begin{aligned}
(b)^P &= -\Gamma_{\Omega_\alpha^a A_d^{*\gamma}}^{(1)}(-q) \Gamma_{A_\gamma^d A_\rho^r A_\sigma^s}^{(0)}(p_2, -p_1) - gf^{amn} g_\alpha^\nu \int_{k_1} \frac{1}{k_1^2} \frac{1}{k_2^2} \mathcal{K}_{c^m A_\rho^r A_\sigma^s A_d^{*\gamma}}^{(0)}(p_2, -p_1, k_2) \Gamma_{A_\gamma^d A_\nu^p}^{(0)}(k_2) \\
&= -\Gamma_{\Omega_\alpha^a A_d^{*\gamma}}^{(1)}(-q) \Gamma_{A_\gamma^d A_\rho^r A_\sigma^s}^{(0)}(p_2, -p_1) + (b'). \tag{3.58}
\end{aligned}$$

The first term is exactly the PT propagator-like piece encountered in the quark case; this is the essence of the process independence of the PT. Notice, however, that the second term was not present before. The action of this term will be discussed in detail in Section IV B; here it suffices to note that it is a vertex-like piece (as is evident from the structure of the kernel appearing in it) and, therefore, it ought to be allotted to the PT three-gluon vertex. Thus we can define the PT (on-shell) three-gluon vertex and propagator as before, *i.e.*,

$$\begin{aligned}
(b)^F + (b') + (c) + (d) &= (b) + (c) + (d) + (b') - (b)^P \\
\Rightarrow i\widehat{\Gamma}_{A_\alpha^a A_\rho^r A_\sigma^s}^{(1)}(p_2, -p_1) &= i\Gamma_{A_\alpha^a A_\rho^r A_\sigma^s}^{(1)}(p_2, -p_1) + \Gamma_{\Omega_\alpha^a A_d^{*\gamma}}^{(1)}(-q) \Gamma_{A_\gamma^d A_\rho^r A_\sigma^s}^{(0)}(p_2, -p_1), \\
(a) + 2(b)^P &\Rightarrow \widehat{\Pi}_{\alpha\beta}^{(1)}(q) = \Pi_{\alpha\beta}^{(1)}(q) + \Pi_{\alpha\beta}^{P(1)}(q). \tag{3.59}
\end{aligned}$$

The comparison with the BQI of Eq. (E.17) shows then that

$$\widehat{\Gamma}_{A_\alpha^a A_\rho^r A_\sigma^s}^{(1)}(p_2, -p_1) = \Gamma_{\widehat{A}_\alpha^a \widehat{A}_\rho^r \widehat{A}_\sigma^s}^{(1)}(p_2, -p_1), \tag{3.60}$$

and again we find

$$\delta^{ab} \widehat{\Pi}_{\alpha\beta}^{(1)}(q) = -\Gamma_{\widehat{A}_\alpha^a \widehat{A}_\beta^b}^{(1)}(q). \tag{3.61}$$

The (one-loop) procedure described above carries over practically unaltered to the corresponding SDEs. This is due to the fact that: (*i*) the pinching momenta will be always determined from the tree-level decomposition of Eq. (2.12); (*ii*) their action is completely fixed by the structure of the STIs they trigger [Eq.s (D.29) and (D.36) for the vertices at

hand]; (*iii*) the kernels appearing in these STIs are the same appearing in the corresponding BQIs; thus, it is always possible to write the result of the action of pinching momenta in terms of auxiliary Green's functions appearing in the BQIs.

The only operational difference is that, in the case of the SDEs for the quark-gluon vertex and the three-gluon vertex, *all three* external legs will be *off-shell*. This is of course unavoidable, given that these (fully dressed) vertices are nested in the SDE of the off-shell gluon self-energy [see Fig.6, diagrams (d_{11}) and (d_1), respectively], and their legs inside the diagrams are irrigated by the virtual off-shell momenta. As a result, the equations of motion employed above [*viz.* Eq. (3.47)] should not be used in this case; therefore, the corresponding terms, proportional to inverse self-energies, do not drop out, and form part of the resulting BQI.

Thus the PT rules for the construction of SDEs may be summarized as follows:

- i.* For the SDEs of vertices, with *all three* external legs *off-shell*, the pinching momenta, coming from the only external three-gluon vertex undergoing the decomposition (2.12), generate four types of terms: one of them, corresponding to the term (b') in Eq. (3.58), is a genuine vertex-like contribution that must be included in the final PT answer for the vertex under construction, while the remaining three-terms will form part of the emerging BQIs (and thus would be discarded from the PT vertex). These latter terms have a very characteristic structure, which facilitates their identification in the calculation. Specifically, one of them is always proportional to the auxiliary function $\Gamma_{\Omega A^*}$, while the other two are proportional to the inverse propagators of the fields entering into the two legs that did not undergo the decomposition of (2.12).
- ii.* In the case of the new SDE for the gluon propagator the pinching momenta will only generate pieces proportional to $\Gamma_{\Omega A^*}$, which should be discarded from the PT answer for the gluon two-point function (since they are exactly those that cancel against the contribution coming from the corresponding vertices).

IV. PT GREEN'S FUNCTIONS FROM SCHWINGER-DYSON EQUATIONS

After the introduction of the useful tools and basic rules required for the application of the PT program to the (non-perturbative) case of SDEs, we are ready to describe in detail the

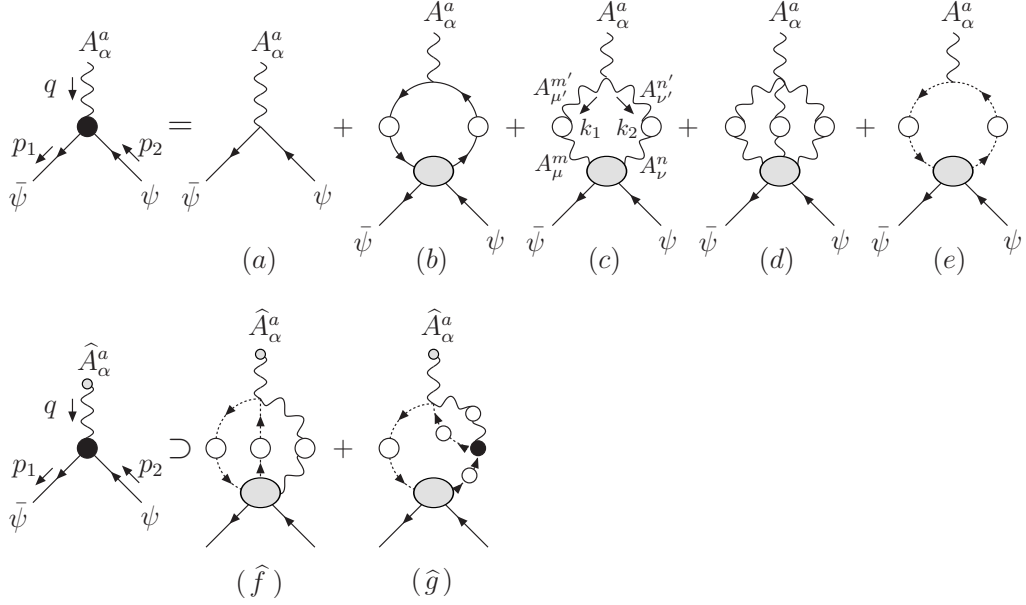


FIG. 10: The SDE for the quark-gluon vertex. The symmetry factors of the R_ξ diagrams (first line) are: $s(a, b) = 1$. $s(c) = 1/2$, $s(d) = 1/6$ and $s(e) = -1$. For the key diagram (c) we show explicitly the kinematics chosen. In the second line we show the additional topologies present in the BFM version of the equation [$s(\hat{f}, \hat{g}) = -1$], generated dynamically by the PT procedure.

actual construction, starting from the corresponding SDEs written in the Feynman gauge of the R_ξ . We will first derive the new SDEs for the two vertices, $\hat{\Gamma}_{A\psi\bar{\psi}}$ and $\hat{\Gamma}_{AAA}$, given that the calculations are easier to work out, and will then address the more complicated case of the SDE for the PT gluon propagator $\hat{\Gamma}_{AA}$.

A. Quark-Gluon vertex

The SDE of the quark-gluon vertex, shown in Fig. 10, is the simplest one as far as the PT construction is concerned, capturing at the same time several of the essential steps that appear during the application of the PT algorithm to the SDEs of QCD.

We start by carrying out the decomposition of Eq. (2.12) on the tree-level vertex appearing in (c), the only diagram we will touch in our construction. Let us concentrate on the Γ^P part; one has

$$(c)^P = -\frac{1}{2} g f^{am'n'} \int_{k_1} (g_{\alpha\nu'} k_{1\mu'} - g_{\alpha\mu'} k_{2\nu'}) \Delta_{m'm}^{\mu'\mu}(k_1) \Delta_{n'n}^{\nu'\nu}(k_2) \mathcal{K}_{A_\mu^m A_\nu^n \psi \bar{\psi}}(k_2, p_2, -p_1)$$

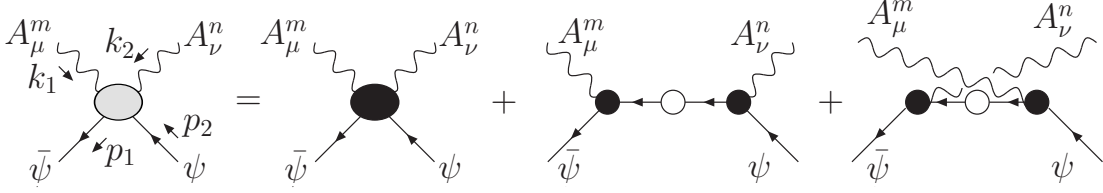


FIG. 11: Skeleton expansion of the kernel appearing in the SDE for the trilinear quark-gluon vertex [see diagram (c) of Fig. 10]. Black, white, and gray blobs denote 1PI functions, connected functions, and SD kernels, respectively.

$$= g f^{am'n'} g_{\alpha\nu'} \int_{k_1} \frac{1}{k_1^2} \Delta_{n'n}^{\nu\nu'}(k_2) k_1^\mu \mathcal{K}_{A_\mu^m A_\nu^n \psi \bar{\psi}}(k_2, p_2, -p_1), \quad (4.1)$$

where the kernel $\mathcal{K}_{AA\psi\bar{\psi}}$ is shown in Fig. 11. Using the STI of the kernel $\mathcal{K}_{A_\mu^m A_\nu^n \psi \bar{\psi}}$ given in Eq. (D.29), we obtain from (4.1) four terms, to be denoted by (s_1) , (s_2) , (s_3) and (s_4) , *i.e.*,

$$(c)^P = (s_1) + (s_2) + (s_3) + (s_4), \quad (4.2)$$

with

$$\begin{aligned} (s_1) &= g f^{am'n'} g_{\alpha\nu'} \int_{k_1} D^{m'm}(k_1) \Delta_{n'n}^{\nu\nu'}(k_2) \Gamma_{c^m A_\nu^n A_d^{*\gamma}}(k_2, -k_1 - k_2) \Gamma_{A_\gamma^d \psi \bar{\psi}}(p_2, -p_1), \\ (s_2) &= g f^{am'n'} g_{\alpha\nu'} \Gamma_{\psi \bar{\psi}}(p_1) \int_{k_1} D^{m'm}(k_1) \Delta_{n'n}^{\nu\nu'}(k_2) \mathcal{K}_{A_\nu^n \psi c^m \bar{\psi}^*}(p_2, k_1, -p_1), \\ (s_3) &= g f^{am'n'} g_{\alpha\nu'} \int_{k_1} D^{m'm}(k_1) \Delta_{n'n}^{\nu\nu'}(k_2) \mathcal{K}_{A_\nu^n \psi^* \bar{\psi} c^m}(p_2, -p_1, k_1) \Gamma_{\psi \bar{\psi}}(p_2), \\ (s_4) &= g f^{am'n'} g_{\alpha\nu'} \int_{k_1} D^{m'm}(k_1) \Delta_{n'n}^{\nu\nu'}(k_2) \Gamma_{c^m A_d^{*\gamma} \psi \bar{\psi}}(k_2, p_2, -p_1) \Gamma_{A_\gamma^d A_\nu^n}(k_2). \end{aligned} \quad (4.3)$$

Next, using Eq.s (E.9), (E.14) and (E.15), it is fairly straightforward to demonstrate that

$$\begin{aligned} (s_1) &= -\Gamma_{\Omega_\alpha^a A_d^{*\gamma}}(-q) \Gamma_{A_\gamma^d \psi \bar{\psi}}(p_2, -p_1), \\ (s_2) &= -\Gamma_{\psi \bar{\psi}}(p_1) \Gamma_{\psi \Omega_\alpha^a \bar{\psi}^*}(q, -p_1), \\ (s_3) &= -\Gamma_{\psi^* \bar{\psi} \Omega_\alpha^a}(-p_1, q) \Gamma_{\psi \bar{\psi}}(p_2). \end{aligned} \quad (4.4)$$

Evidently, (s_1) gives rise to the PT propagator-like term, while (s_2) and (s_3) generate the terms that in the usual S -matrix PT would vanish on-shell, due to the (all-order) spinor equations of motion $\Gamma_{\psi \bar{\psi}}(p_2) u(p_2)|_{\not{p}_2=m} = 0$, and $\bar{u}(p_1) \Gamma_{\psi \bar{\psi}}(p_1)|_{\not{p}_1=m} = 0$. Of course, in our case we are not allowed to use the equations of motion, given that the quark legs are considered to be off-shell.

$$iD^{mn} = (iD^{mn})^{(0)} + (iD^{mm'})^{(0)} \times (-\Gamma'_{c^m \bar{c}^{n'}}) \times (iD^{n'})$$

FIG. 12: The Schwinger-Dyson equation (4.9) satisfied by the ghost propagator.

Let us finally look at the term (s_4) , and show how it combines with the remaining R_ξ diagrams to generate the BFM quark-gluon vertex $\Gamma_{\hat{A}\psi\bar{\psi}}$. To this end, using Eq. (D.11) and the FPE satisfied by the 1PI function $\Gamma_{cA^*\psi\bar{\psi}}$, we write $(s_4) = (s_{4a}) + (s_{4b})$, with

$$\begin{aligned} (s_{4a}) &= -igf^{am'd}g_{\alpha\gamma} \int_{k_1} D^{m'm}(k_1)\Gamma_{c^mA_d^*\gamma\psi\bar{\psi}}(k_2, p_2, -p_1), \\ (s_{4b}) &= gf^{am'n'}g_{\alpha\nu'} \int_{k_1} \delta^{dn'} \frac{k_2^{\nu'}}{k_2^2} D^{m'm}(k_1)\Gamma_{c^m\bar{c}^d\psi\bar{\psi}}(k_2, p_2, -p_1). \end{aligned} \quad (4.5)$$

The general structure of these two terms suggests that (s_{4a}) should give rise to the ghost quadrilinear vertex, while (s_{4b}) , when added to diagram (e), should symmetrize the trilinear ghost gluon coupling. It turns out that this expectation is essentially correct, but its realization is not immediate, mainly due to the fact that (s_{4b}) contains a tree-level instead of a full ghost propagator $[(k_2^2)^{-1}$ instead of $D(k_2)]$, while (s_{4a}) can reproduce, at most, diagram (\hat{f}) of Fig. 10, but not (\hat{g}). The solution to this apparent mismatch is rather subtle: one must employ the SDE satisfied by the *ghost propagator*, shown in Fig 12. This SDE is common to both the R_ξ -gauge and the BFM, given that there are no background ghosts.

To see how this works in detail, add and subtract to Eq. (4.5) the missing term (see Fig. 13), obtaining

$$\begin{aligned} (s_{4a}) &= -igf^{am'd}g_{\alpha\gamma} \int_{k_1} D^{m'm}(k_1) \left[\Gamma_{c^mA_d^*\gamma\psi\bar{\psi}}(k_2, p_2, -p_1) \right. \\ &\quad \left. - \Gamma'_{c^gA_d^*\gamma}(k_2)iD^{gg'}(k_2)\Gamma_{c^m\bar{c}^{g'}\psi\bar{\psi}}(k_2, p_2, -p_1) \right] \\ &= -igf^{am'd}g_{\alpha\gamma} \int_{k_1} D^{mm'}(k_1)\mathcal{K}_{c^{m'}A_d^*\gamma\psi\bar{\psi}}(k_2, p_2, -p_1) \end{aligned} \quad (4.6)$$

$$\begin{aligned} (s_{4b}) &= -gf^{am'n'}g_{\alpha\nu'} \int_{k_1} \left[\delta^{dn'} \frac{k_2^{\nu'}}{k_2^2} - \Gamma'_{c^gA_{\nu'}^{n'}}(k_2)D^{gd}(k_2) \right] \times \\ &\quad \times D^{m'm}(k_1)\Gamma_{c^m\bar{c}^d\psi\bar{\psi}}(k_2, p_2, -p_1), \end{aligned} \quad (4.7)$$

where the auxiliary function Γ'_{cA^*} has been defined in Eq. (E.7), and is given by Γ_{cA^*} minus

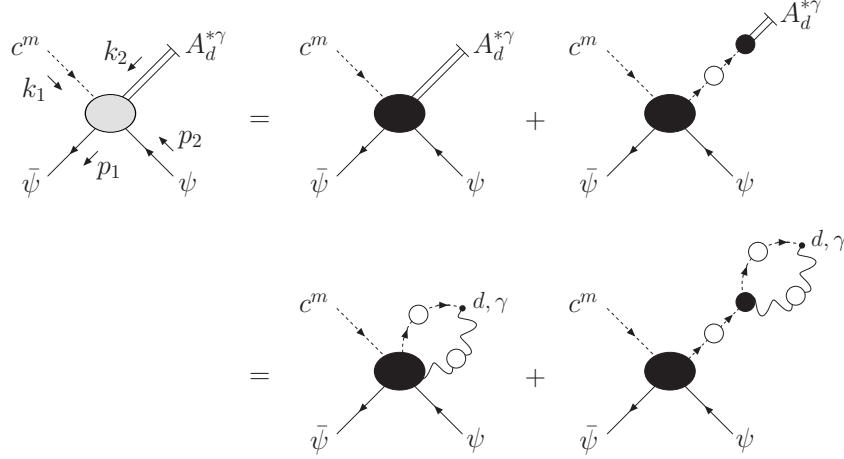


FIG. 13: Diagrammatic decomposition of the kernel $\mathcal{K}_{c^m A_d^{*\gamma} \psi \bar{\psi}}$. The second term is the one added (and subtracted) to the original sum $(s_{4a}) + (s_{4b})$ of Eq. (4.5). After replacing the gluon anti-field $A_d^{*\gamma}$ by the corresponding composite operator (second line), taking into account the extra structure provided by the $(c)^P$ term, this kernel furnishes the BFM terms $(\hat{f}) + (\hat{g})$ [see Eq. (4.8).]

its tree-level part. Using Eq. (E.5), we can then rewrite (s_{4a}) as

$$\begin{aligned}
(s_{4a}) &= i g^2 f^{am'd} f^{dse} g_{\alpha\sigma} \int_{k_1} \int_{k_3} D^{m'm}(k_1) D^{ee'}(k_3) \Delta_{ss'}^{\sigma\sigma'}(k_4) \times \\
&\times \left[\Gamma_{c^m A_{\sigma'}^{s'} \bar{c}^{e'} \psi \bar{\psi}}(k_3, k_4, p_2, -p_1) - i \Gamma_{c^g A_{\sigma'}^{s'} \bar{c}^{e'}}(k_3, k_4) D^{gg'}(k_2) \Gamma_{c^m \bar{c}^{g'} \psi \bar{\psi}}(k_2, p_2, -p_1) \right] \\
&= (\hat{f}) + (\hat{g}).
\end{aligned} \tag{4.8}$$

We next turn to (s_{4b}) and consider the ghost SD equation of Fig. 12. One has

$$i D^{dn'}(k_2) = i \frac{\delta^{dn'}}{k_2^2} + i \frac{\delta^{dg}}{k_2^2} [-\Gamma'_{c^g \bar{c}^{g'}}(k_2)] i D^{g'n'}(k_2), \tag{4.9}$$

where, as before, $\Gamma'_{c^g \bar{c}^{g'}}$ is given by $\Gamma_{c^g \bar{c}^{g'}}$ minus its tree-level part. Multiplying the above equation by k_2^2 , using the FPE (C.1) and factoring out a $k_{2\nu'}$ we get the relation

$$\begin{aligned}
k_{2\nu'} D^{dn'}(k_2) &= \delta^{dn'} \frac{k_{2\nu'}}{k_2^2} - \Gamma'_{c^d A_{\nu'}^{*g}}(k_2) D^{gn'}(k_2) \\
&= \delta^{dn'} \frac{k_{2\nu'}}{k_2^2} - \Gamma'_{c^g A_{\nu'}^{*n'}}(k_2) D^{gd}(k_2).
\end{aligned} \tag{4.10}$$

Therefore, we obtain

$$(s_{4b}) = -g f^{am'n'} \int_{k_1} k_{2\alpha} D^{m'm}(k_1) D^{n'n}(k_2) \Gamma_{c^m \bar{c}^n \psi \bar{\psi}}(k_2, p_2, -p_1). \tag{4.11}$$

Adding this last contribution to diagram (e) we finally arrive at

$$\begin{aligned}
(e) + (s_{4b}) &= g f^{am'n'} \int_{k_1} (k_1 - k_2)_\alpha D^{m'm}(k_1) D^{n'n}(k_2) \mathcal{K}_{c^m \bar{c}^n \psi \bar{\psi}}(k_2, p_2, -p_1) \\
&= (\widehat{e}).
\end{aligned} \tag{4.12}$$

Next, observe that the graphs (a), (b), and (d) of Fig. 10 can be converted to hatted ones automatically (see the corresponding tree-level Feynman in Appendix F), and that $(c)^F = (\widehat{c})$ since in the BFG $\Gamma^F = \Gamma_{\widehat{A}AA}^{(0)}$. Thus,

$$\begin{aligned}
i\Gamma_{A_\alpha^a \psi \bar{\psi}}(p_2, -p_1) &= -\Gamma_{\Omega_\alpha^a A_d^{*\gamma}}(-q) \Gamma_{A_\gamma^d \psi \bar{\psi}}(p_2, -p_1) - \Gamma_{\psi^* \bar{\psi} \Omega_\alpha^a}(-p_1, q) \Gamma_{\psi \bar{\psi}}(p_2) \\
&\quad - \Gamma_{\psi \bar{\psi}}(p_1) \Gamma_{\psi \Omega_\alpha^a \bar{\psi}^*}(q, -p_1) + [(\widehat{a}) + (\widehat{b}) + (\widehat{c}) + (\widehat{d}) + (\widehat{e}) + (\widehat{f}) + (\widehat{g})]_\alpha^a.
\end{aligned} \tag{4.13}$$

The sum of diagrams in the brackets is nothing but the kernel expansion of the SDE governing the vertex $\Gamma_{\widehat{A} \psi \bar{\psi}}$, *i.e.*,

$$i\Gamma_{\widehat{A} \psi \bar{\psi}}(p_2, -p_1) = [(\widehat{a}) + (\widehat{b}) + (\widehat{c}) + (\widehat{d}) + (\widehat{e}) + (\widehat{f}) + (\widehat{g})]_\alpha^a. \tag{4.14}$$

After this identification, it is clear that Eq. (4.13) coincides with the full BQI of Eq. (E.13), namely

$$\begin{aligned}
i\Gamma_{\widehat{A} \psi \bar{\psi}}(p_2, -p_1) &= [i g_\alpha^\gamma \delta^{ad} + \Gamma_{\Omega_\alpha^a A_d^{*\gamma}}(-q)] \Gamma_{A_\gamma^d \psi \bar{\psi}}(p_2, -p_1) \\
&\quad + \Gamma_{\psi^* \bar{\psi} \Omega_\alpha^a}(-p_1, q) \Gamma_{\psi \bar{\psi}}(p_2) + \Gamma_{\psi \bar{\psi}}(p_1) \Gamma_{\psi \Omega_\alpha^a \bar{\psi}^*}(q, -p_1).
\end{aligned} \tag{4.15}$$

In summary, the application of the PT to the conventional SDE for the quark-gluon vertex (i) has converted the initial kernel expansion [graphs (a) to (e) in Fig. 10] into the graphs corresponding to the kernel expansion of the vertex $\Gamma_{\widehat{A} \psi \bar{\psi}}$; (ii) all other pinching terms extracted from the original diagram (c) are precisely the combinations of auxiliary Green's functions appearing in the BQI that relates the initial vertex $\Gamma_{A \psi \bar{\psi}}$ with the final vertex $\Gamma_{\widehat{A} \psi \bar{\psi}}$.

Notice at this point that the skeleton expansion of the multi-particle kernels appearing in the SDE for $\Gamma_{\widehat{A} \psi \bar{\psi}}$ is still written in terms of the conventional fully dressed vertices and propagators (involving only quantum fields). Thus, Eq. (4.14) is not manifestly dynamical, *i.e.*, it does not involve the same unknown quantities on the right and left hand side; this situation is exactly analogous to the gluon propagator case discussed in subsection II E.

Specifically, in order to convert (4.14) into a genuine SDE, one has two possibilities, both involving the use of the above BQI: (i) substitute the lhs of Eq. (4.15) into the rhs of Eq. (4.14) and solve for the conventional $\Gamma_{A\psi\bar{\psi}}$ vertex, or (ii) invert Eq. (4.15) and use it to convert every $\Gamma_{A\psi\bar{\psi}}$ vertex appearing in the rhs of Eq. (4.14) into a $\Gamma_{\widehat{A}\psi\bar{\psi}}$ vertex. It would seem that the latter option is operationally more cumbersome, especially taking into account that a similar procedure has to be followed for all the Green's functions that appear in the coupled system of SDEs that one considers.

B. Three-gluon vertex

The construction of the PT three-gluon vertex proceeds in a very similar way, with some additional subtleties that we will spell out in detail in what follows. We emphasize that the purpose of this exercise is to generate dynamically the vertex $\Gamma_{\widehat{A}AA}$ and *not* the fully Bose-symmetric vertex $\Gamma_{\widehat{A}\widehat{A}\widehat{A}}$ studied in [15, 29]. The reason is that it is the former vertex that appears in the SDEs for the gluon propagator [see, *e.g.*, diagram (d_1) in Fig. 6], making it the relevant object to consider at this level.

We start by considering the conventional [4] SDE for the three gluon vertex (Fig. 14), and carry out the standard $\Gamma^P + \Gamma^F$ decomposition to the tree-level vertex of diagram (c), which is the only one we will modify in our construction.

We then find

$$\begin{aligned}
(c)^P &= -\frac{1}{2}gf^{am'n'} \int_{k_1} (g_{\alpha\nu'} k_{1\mu'} - g_{\alpha\mu'} k_{2\nu'}) \Delta_{m'm}^{\mu'\mu}(k_1) \Delta_{n'n}^{\nu'\nu}(k_2) \mathcal{K}_{A_\mu^m A_\nu^n A_\rho^r A_\sigma^s}(k_2, p_2, -p_1) \\
&= gf^{amn'} g_{\alpha\nu'} \int_{k_1} \frac{1}{k_1^2} \Delta_{n'n}^{\nu'\nu}(k_2) k_1^\mu \mathcal{K}_{A_\mu^m A_\nu^n A_\rho^r A_\sigma^s}(k_2, p_2, -p_1),
\end{aligned} \tag{4.16}$$

and the kernel K_{AAAA} is shown in Fig. 15.

The next step is to apply the STI of Eq. (D.36), and scrutinize the various terms, denoted again by (s_1), (s_2), (s_3), and (s_4).

For the first three terms, we get the following results

$$\begin{aligned}
(s_1) &= gf^{am'n'} g_{\alpha\nu'} \int_{k_1} D^{m'm}(k_1) \Delta_{n'n}^{\nu'\nu}(k_2) \Gamma_{c^m A_\nu^n A_d^{*\gamma}}(k_2, -k_1 - k_2) \Gamma_{A_\gamma^d A_\rho^r A_\sigma^s}(p_2, -p_1) \\
&= -\Gamma_{\Omega_\alpha^a A_d^{*\gamma}}(-q) \Gamma_{A_\gamma^d A_\rho^r A_\sigma^s}(p_2, -p_1), \\
(s_2) &= gf^{am'n'} g_{\alpha\nu'} \int_{k_1} D^{m'm}(k_1) \Delta_{n'n}^{\nu'\nu}(k_2) \mathcal{K}_{c^m A_\nu^n A_\sigma^s A_d^{*\gamma}}(k_2, -p_1, p_2) \Gamma_{A_\gamma^d A_\rho^r}(p_2) \\
&= -\Gamma_{\Omega_\alpha^a A_\sigma^s A_d^{*\gamma}}(-p_1, p_2) \Gamma_{A_\gamma^d A_\rho^r}(p_2),
\end{aligned}$$

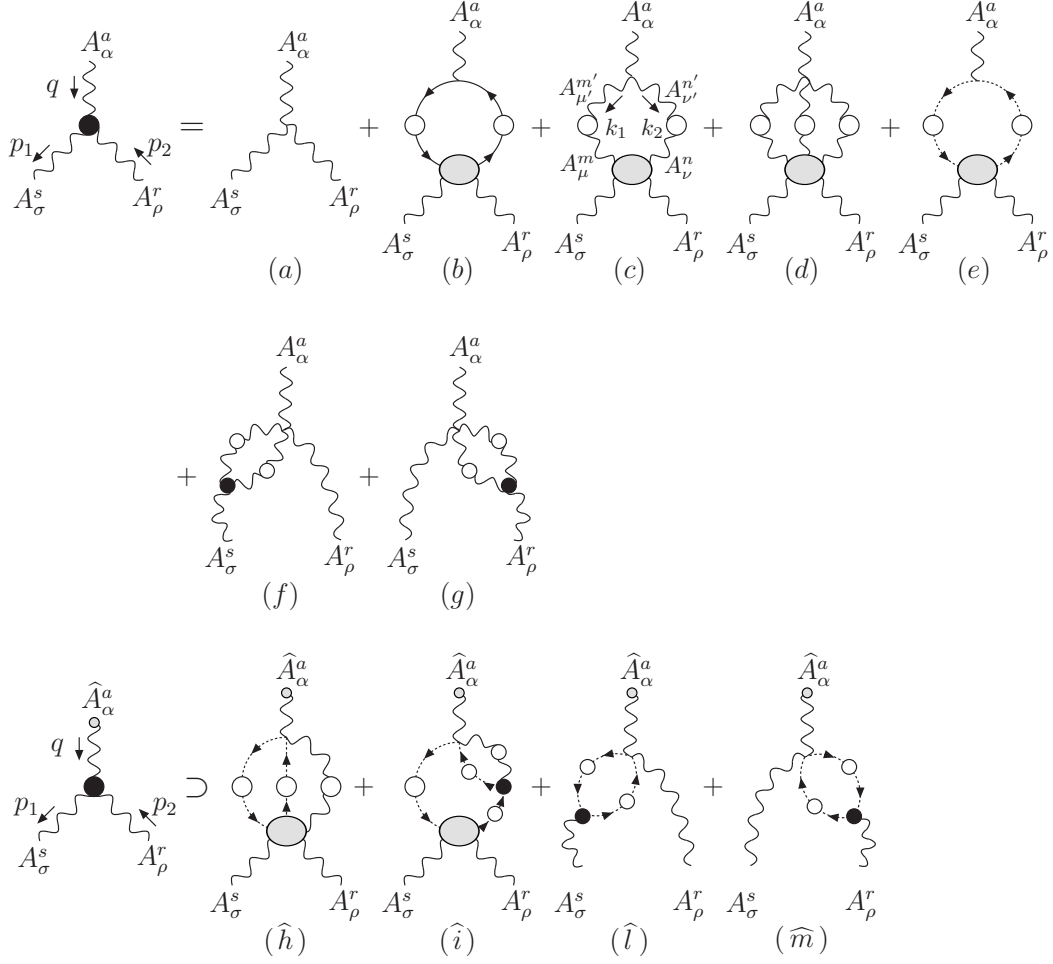


FIG. 14: The SDE of the three-gluon vertex. The symmetry factors of the R_ξ (first and second line of the figure) diagrams are $s(a, b) = 1$. $s(c) = 1/2$, $s(d) = 1/6$, $s(e) = -1$, $s(f, g) = 1/2$. In the third line we show the additional topologies present in the BFM version of the equation [$s(\hat{h}, \hat{i}, \hat{l}, \hat{m}) = -1$], generated during the PT procedure.

$$\begin{aligned}
(s_3) &= g f^{am'n'} g_{\alpha\nu'} \int_{k_1} D^{m'm}(k_1) \Delta_{n'n}^{\nu\nu'}(k_2) \mathcal{K}_{c^m A_\nu^r A_\rho^r A_d^{*\gamma}}(k_2, p_2, -p_1) \Gamma_{A_\gamma^d A_\sigma^s}(p_1) \\
&= -\Gamma_{\Omega_\alpha^a A_\rho^r A_d^{*\gamma}}(p_2, -p_1) \Gamma_{A_\gamma^d A_\sigma^s}(p_1).
\end{aligned} \tag{4.17}$$

As in the case of the quark-gluon vertex, (s_1) represents the propagator-like contribution that in the S -matrix PT would be allotted to the new two point function $\hat{\Gamma}_{AA}$. Notice that this term is equal (modulo the external vertex) to the one found in the quark-gluon vertex case; this is the manifestation of the well-known property of the process-independence of the PT algorithm (as already noticed in our previous one-loop analysis): the propagator-like contributions do not depend on the details of the external (embedding) particles. As for (s_2)

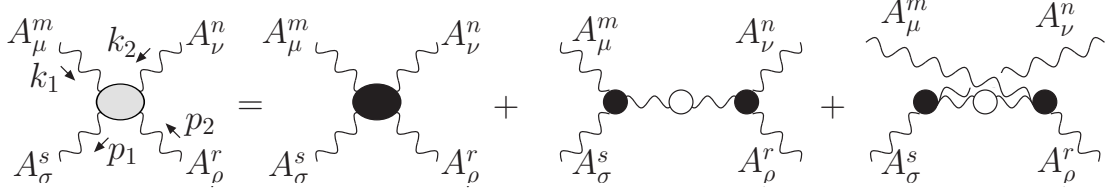


FIG. 15: Skeleton expansion of the kernel appearing in the SDE for the three-gluon vertex [diagram (c) of Fig. 14]

and (s_3) , they correspond again to terms that would vanish on-shell, but now are retained in the final answer due to the off-shell condition of the external legs.

Finally, one has to consider the term (s_4) , given by

$$(s_4) = g f^{am'n'} g_{\alpha\nu'} \int_{k_1} D^{m'm}(k_1) \Delta_{n'n}^{\nu'\nu}(k_2) \mathcal{K}_{c^m A_d^* \gamma A_\rho^r A_\sigma^s}(p_2, -p_1, k_2) \Gamma_{A_\gamma^d A_\nu^n}(k_2), \quad (4.18)$$

which again can be written as the sum of the following two terms

$$(s_{4a}) = -i g f^{am'd} g_{\alpha\gamma} \int_{k_1} D^{m'm}(k_1) \mathcal{K}_{c^m A_d^* \gamma A_\rho^r A_\sigma^s}(k_2, p_2, -p_1), \quad (4.19)$$

$$(s_{4b}) = -g f^{am'n'} g_{\alpha\nu'} \int_{k_1} \delta^{dn'} \frac{k_2^{\nu'}}{k_2^2} D^{m'm}(k_1) \mathcal{K}_{c^m \bar{c}^d A_\rho^r A_\sigma^s}(k_2, p_2, -p_1). \quad (4.20)$$

The kernel $\mathcal{K}_{c\bar{c}AA}$ is defined by replacing in Eq. (D.39) every anti-field leg A^* by the corresponding anti-ghost field \bar{c} . As before, (s_{4b}) has a tree-level ghost propagator, while (s_{4a}) misses a diagram that we need to add and subtract to solve the two problems simultaneously. Even so, we are still missing the diagrams (\hat{l}) and (\hat{m}) of Fig. 14; they will be generated by the tree-level contribution appearing in the SDE of the auxiliary function Γ_{cAA^*} . In order to isolate this contribution as early as possible, let us write

$$\begin{aligned} \mathcal{K}_{c^m A_d^* \gamma A_\rho^r A_\sigma^s}(k_2, p_2, -p_1) &= \mathcal{K}'_{c^m A_d^* \gamma A_\rho^r A_\sigma^s}(k_2, p_2, -p_1) \\ &+ i \Gamma_{c^m A_\sigma^s \bar{c}^{e'}}(-p_1, \ell) i D^{ee'}(\ell) i \Gamma_{c^{e'} A_\rho^r A_d^* \gamma}^{(0)}(p_2, k_2) \\ &+ i \Gamma_{c^e A_\sigma^s A_d^* \gamma}^{(0)}(-p_1, k_2) i D^{ee'}(\ell') i \Gamma_{c^m A_\rho^r \bar{c}^{e'}}(p_2, -\ell') \\ &= \mathcal{K}'_{c^m A_d^* \gamma A_\rho^r A_\sigma^s}(k_2, p_2, -p_1) - i g f^{dre'} g_\rho^\gamma \Gamma_{c^m A_\sigma^s \bar{c}^{e'}}(-p_1, \ell) D^{ee'}(\ell) \\ &- i g f^{dse} g_\sigma^\gamma D^{ee'}(\ell') \Gamma_{c^m A_\rho^r \bar{c}^{e'}}(p_2, -\ell'), \end{aligned} \quad (4.21)$$

where the prime denotes that the Γ_{cAA^*} that appears in the 1PR terms starts at one-loop. We then find (see also Fig. 16)

$$(s_{4a}) = -i g f^{am'd} g_{\alpha\gamma} \int_{k_1} D^{m'm}(k_1) \mathcal{K}'_{c^m A_d^* \gamma A_\rho^r A_\sigma^s}(k_2, p_2, -p_1)$$

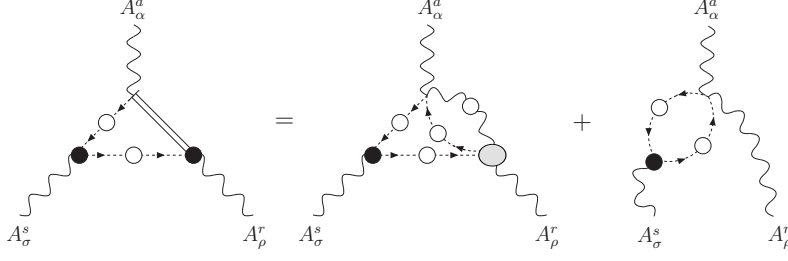


FIG. 16: The 1PR terms appearing in $\mathcal{K}_{c^m A_d^{*\gamma} A_\rho^r A_\sigma^s}$ contain a tree-level contribution generating the missing BFM topologies. Here we show the case for (\widehat{l}) ; a symmetric term generates (\widehat{m}) . The first term on the rhs is part of the skeleton expansion of diagram (\widehat{h}) of Fig. 14. Notice that the lhs is simply a pictorial representation of the rhs, taking advantage of the notation introduced in Fig.13; the anti-fields are static sources and do not propagate.

$$\begin{aligned}
& - g^2 f^{am'd} f^{dre'} g_{\alpha\rho} \int_{k_1} D^{m'm}(k_1) D^{e'e}(\ell) \Gamma_{c^m A_\sigma^s \bar{c}e'}(-p_1, \ell) \\
& - g^2 f^{am'd} f^{dse'} g_{\alpha\sigma} \int_{k_1} D^{m'm}(k_1) D^{e'e}(\ell') \Gamma_{c^m A_\rho^r \bar{c}e'}(p_2, -\ell') \\
& = (s'_{4a}) + (\widehat{l}) + (\widehat{m}).
\end{aligned} \tag{4.22}$$

For generating the remaining terms one proceeds as in the quark case, writing (see Fig. 17)

$$\begin{aligned}
(s'_{4a}) & = -ig f^{am'd} g_{\alpha\gamma} \int_{k_1} D^{m'm}(k_1) \left[\mathcal{K}'_{c^m A_d^{*\gamma} A_\rho^r A_\sigma^s}(k_2, p_2, -p_1) \right. \\
& \quad \left. - \Gamma'_{c^g A_d^{*\gamma}}(k_2) i D^{gg'}(k_2) \mathcal{K}_{c^m \bar{c}g' A_\rho^r A_\sigma^s}(k_2, p_2, -p_1) \right] \\
& = -ig f^{am'd} g_{\alpha\gamma} \int_{k_1} D^{m'm}(k_1) \mathcal{K}_{c^m A_d^{*\gamma} A_\rho^r A_\sigma^s}^{\text{full}}(k_2, p_2, -p_1)
\end{aligned} \tag{4.23}$$

$$\begin{aligned}
(s_{4b}) & = -g f^{am'n'} g_\alpha^{\nu'} \int_{k_1} \left[\delta^{dn'} \frac{k_{2\nu'}}{k_2^2} - \Gamma'_{c^e A_{\nu'}^{*n'}}(k_2) D^{ed}(k_2) \right] \times \\
& \quad \times D^{m'm}(k_1) \mathcal{K}_{c^m \bar{c}d A_\rho^r A_\sigma^s}(k_2, p_2, -p_1).
\end{aligned} \tag{4.24}$$

Then, using Eq. (E.5) (which can be safely done now, since tree-level contribution has been already taken into account) and Eq. (4.10), one finds

$$(s'_{4a}) = (\widehat{h}) + (\widehat{i}) \tag{4.25}$$

$$(s_{4b}) = -g f^{am'n'} \int_{k_1} k_{2\alpha} D^{m'm}(k_1) D^{n'n}(k_2) \mathcal{K}_{c^m \bar{c}n A_\rho^r A_\sigma^s}(k_2, p_2, -p_1), \tag{4.26}$$

so that

$$(s_{4b}) + (e) = (\widehat{e}). \tag{4.27}$$

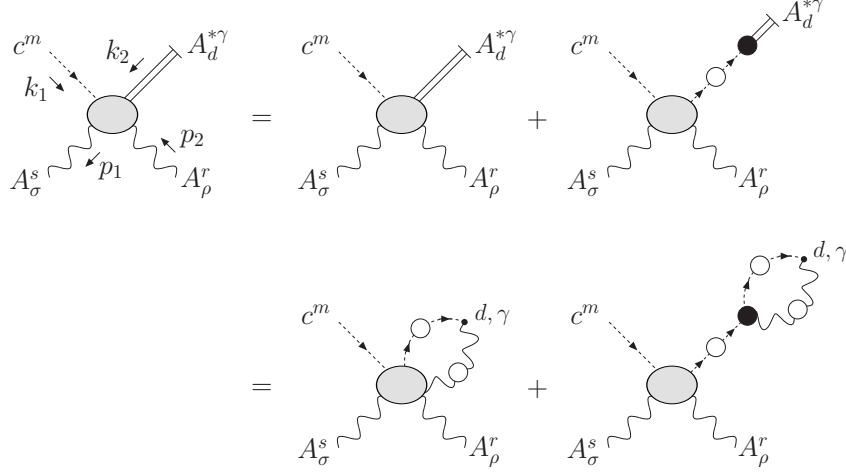


FIG. 17: Diagrammatic decomposition of the SD kernel $\mathcal{K}_{c^m A_d^{*\gamma} A_\rho^r A_\sigma^s}^{\text{full}}$ defined in Eq. (4.23). The first term represents the kernel $\mathcal{K}'_{c^m A_d^{*\gamma} A_\rho^r A_\sigma^s}$; therefore the Γ_{cAA^*} appearing in the corresponding 1PR terms start at one-loop. The second term is the one added (and subtracted) to the original sum (s'_{4a}) + (s_{4b}). After replacing the gluon anti-field $A_d^{*\gamma}$ with the corresponding composite operator (second line), this kernel generates the BFM terms $(\hat{h}) + (\hat{i})$.

Using the tree-level Feynman rules (see Appendix F), it is straightforward to establish that the graphs (b), (d), (f), and (g) can be converted to hatted ones automatically, and that $(c)^F = (\hat{c})$. Thus, collecting all the pieces we have, and using the standard PT decomposition (2.12) on the tree-level contribution (a), we get

$$\begin{aligned}
i\Gamma_{A_\alpha^a A_\rho^r A_\sigma^s}(p_2, -p_1) &= -\Gamma_{\Omega_\alpha^a A_d^{*\gamma}}(-q)\Gamma_{A_\gamma^d A_\rho^r A_\sigma^s}(p_2, -p_1) - \Gamma_{\Omega_\alpha^a A_\sigma^s A_d^{*\gamma}}(-p_1, p_2)\Gamma_{A_\gamma^d A_\rho^r}(p_2) \\
&- \Gamma_{\Omega_\alpha^a A_\rho^r A_d^{*\gamma}}(p_2, -p_1)\Gamma_{A_\gamma^d A_\sigma^s}(p_1) + [(\hat{a}) + (\hat{b}) + (\hat{c}) + (\hat{d}) + (\hat{e}) \\
&+ (\hat{f}) + (\hat{g}) + (\hat{h}) + (\hat{i}) + (\hat{l}) + (\hat{m})]_{\alpha\rho\sigma}^{ars} - igf^{ars}\Gamma^P(p_2, -p_1). \quad (4.28)
\end{aligned}$$

As in the previous case, the sum of diagrams in the brackets is nothing but the kernel expansion of the SDE governing the vertex $\Gamma_{\hat{A}AA}$, *i.e.*,

$$\begin{aligned}
i\Gamma_{\hat{A}_\alpha^a A_\rho^r A_\sigma^s}(p_2, -p_1) &= [(\hat{a}) + (\hat{b}) + (\hat{c}) + (\hat{d}) + (\hat{e}) \\
&+ (\hat{f}) + (\hat{g}) + (\hat{h}) + (\hat{i}) + (\hat{l}) + (\hat{m})]_{\alpha\rho\sigma}^{ars}. \quad (4.29)
\end{aligned}$$

This in turn implies that Eq. (4.28) represents the BQI of Eq. (E.17) up to the last (tree-level) term in the rhs. Of course this tree-level discrepancy is to be expected since the PT algorithm cannot possibly work at tree-level if the external legs are amputated, as is the

case in the SDEs we are considering. To be sure, if we start from the tree-level $\Gamma_{AAA}^{(0)}$ only, *i.e.*, without hooking (two of) the external legs to (conserved) external currents, we can still carry out the decomposition of Eq. (2.12), but the Γ^P term will have nothing to act upon.

Notice finally that the discussion following Eq. (4.15) the SDE for the gluon-quark vertex applies with minimal modification to the three-gluon vertex case discussed here.

C. The gluon propagator

In this section we turn to the SDE of the gluon self-energy. From the technical point of view the construction is somewhat more involved compared to that presented for the vertices, simply because the PT decomposition of Eq. (2.12) must be carried out on both sides of the self-energy diagram. Put in a different way, now we must convert to background gluons not one but two external gluons. To the best of our knowledge, the most efficient procedure to follow consists of the three basic steps described below [13].

1. First step

The starting point is diagram (a_1) of Fig.1. Following the PT procedure, we decompose the tree-level three-gluon vertex according to (2.12) and concentrate on the pinch part. We then get

$$\begin{aligned}
(a_1)^P &= -\frac{i}{2} g f^{am'n'} \int_{k_1} (g_{\alpha\nu'} k_{1\mu'} - g_{\alpha\mu'} k_{2\nu'}) \Delta_{m'm}^{\mu'\mu}(k_1) \Delta_{n'n}^{\nu'\nu}(k_2) \Gamma_{A_\mu^m A_\nu^n A_\beta^b}(k_2, -q) \\
&= i g f^{amn'} g_{\alpha\nu'} \int_{k_1} \frac{1}{k_1^2} \Delta_{n'n}^{\nu'\nu}(k_2) k_1^\mu \Gamma_{A_\mu^m A_\nu^n A_\beta^b}(k_2, -q).
\end{aligned} \tag{4.30}$$

At this point the application of the STI of Eq. (D.9) together with Eq. (D.11) and the FPE (C.5), results in the following terms

$$\begin{aligned}
(a_1)^P &= i g f^{am'n'} g_{\alpha\nu'} \int_{k_1} D^{m'm}(k_1) \Delta_{n'n}^{\nu'\nu}(k_2) \Gamma_{c^m A_\nu^n A_d^{*\gamma}}(k_2, -q) \Gamma_{A_\alpha^d A_\beta^b}(q) \\
&+ g f^{am'd} g_{\alpha\gamma} \int_{k_1} D^{m'm}(k_1) \Gamma_{c^m A_\beta^b A_d^{*\gamma}}(-q, k_2) \\
&- i g f^{am'n'} g_{\alpha\nu'} \int_{k_1} \delta^{dn'} \frac{k_2^{\nu'}}{k_2^2} D^{m'm}(k_1) \Gamma_{c^m A_\beta^b \bar{c}^d}(-q, k_2) \\
&= (s_1) + (s_2) + (s_3).
\end{aligned} \tag{4.31}$$

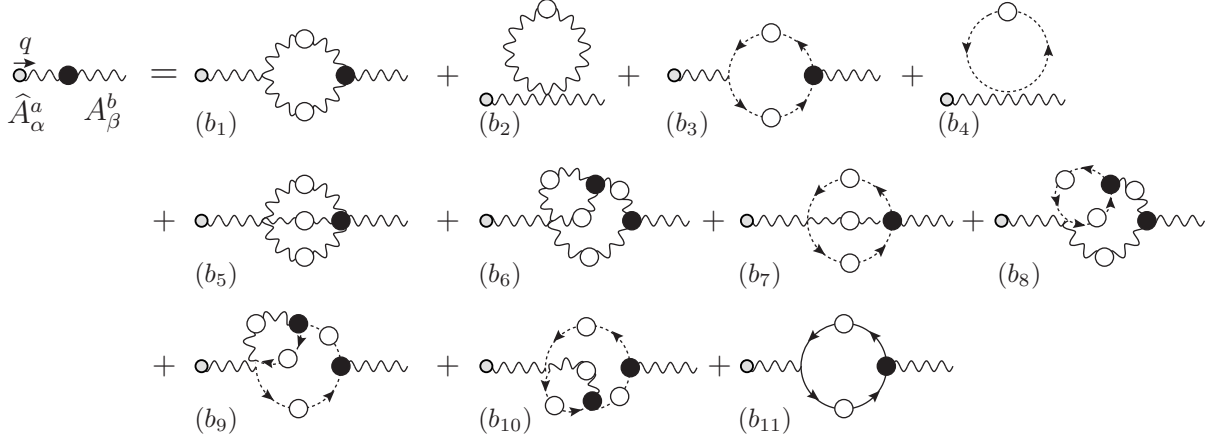


FIG. 18: Schwinger-Dyson equation satisfied by the gluon self-energy $-\Gamma_{\hat{A}A}$. The symmetry factors of the diagrams are $s(b_1, b_2, b_6) = 1/2$, $s(b_5) = 1/6$, and all the remaining diagrams have $s = -1$.

Clearly, using the SDE of the auxiliary function $\Gamma_{\Omega A^*}$, shown in Eq. (E.9), one has immediately that

$$(s_1) = -i\Gamma_{\Omega_\alpha A_d^{*\gamma}}(q)\Gamma_{A_\gamma^d A_\beta^b}(q). \quad (4.32)$$

This would be half of the pinching contribution coming from the vertex in the S -matrix PT.

As far as the (s_2) and (s_3) terms are concerned, let us start by adding and subtracting to them the expression needed to convert the tree-level ghost propagator of (s_3) into a full one; making use of the ghost SDE (4.10) we then get

$$\begin{aligned} (s_2) &= -gf^{am'd}g_{\alpha\gamma} \int_{k_1} iD^{m'm}(k_1) \left[i\Gamma_{c^m A_\beta^b A_d^{*\gamma}}(-q, k_2) + \Gamma'_{c^{g'} A_d^{*\gamma}}(k_2) D^{g'g}(k_2) \Gamma_{c^m A_\beta^b \bar{c}^g}(-q, k_2) \right] \\ (s_3) &= -igf^{am'n'} \int_{k_1} k_{2\alpha} D^{m'm}(k_1) D^{n'n}(k_2) \Gamma_{c^m A_\beta^b \bar{c}^n}(-q, k_2). \end{aligned} \quad (4.33)$$

The second term symmetrizes the trilinear ghost-gluon coupling, and one has

$$(s_3) + (a_3) = (b_3), \quad (4.34)$$

where (b_3) is shown in Fig. 18. The term (s_2) will finally generate all the remaining terms. To see how this happens, we denote by (s_{2a}) and (s_{2b}) the two terms appearing in the square brackets of (s_{2a}) , and concentrate on the first one. Making use of the SDE (E.8) satisfied by the auxiliary function Γ_{cAA^*} and the decomposition (E.11) of the kernel appearing in the latter, we get

$$(s_{2a}) = g^2 f^{am'd} f^{mdb} g_{\alpha\beta} \int_{k_1} D^{m'm}(k_1)$$

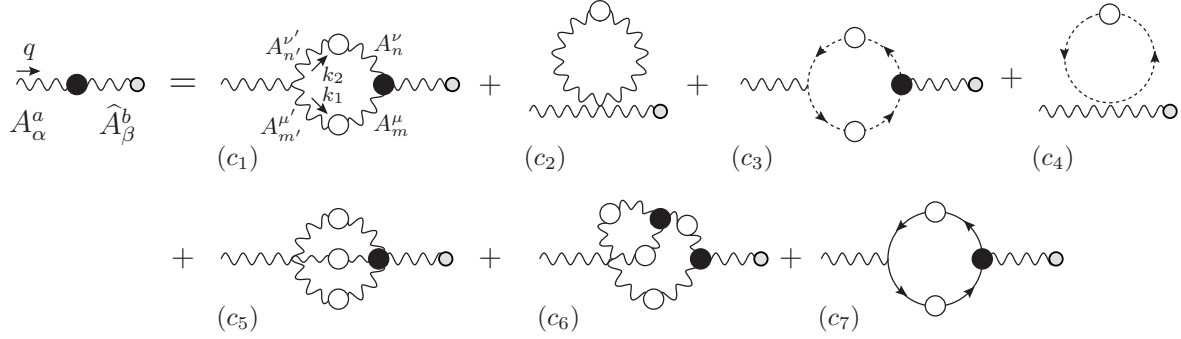


FIG. 19: Schwinger-Dyson equation satisfied by the gluon self-energy $-\Gamma_{A\hat{A}}$. The symmetry factors of the diagrams are $s(c_1, c_2, c_6) = 1/2$, $s(c_3, c_4, c_7) = -1$, $s(c_5) = 1/6$.

$$\begin{aligned}
& + g^2 f^{am'd} f^{dn's'} g_{\alpha\sigma'} \int_{k_1} \int_{k_3} D^{m'm}(k_1) \Delta_{s's}^{\sigma'\sigma}(k_3) D^{n'n}(k_4) \mathcal{K}_{c^m A_\beta^b A_\sigma^s \bar{c}^n}(-q, k_3, k_4) \\
& = (b_4) + (b_7) + (b_8) + (b_{10}).
\end{aligned} \tag{4.35}$$

Using instead the SDE satisfied by Γ_{cA^*} , shown in Eq. (E.7), we obtain

$$\begin{aligned}
(s_{2b}) & = ig^2 f^{am'd} f^{dse} g_\alpha^\sigma \int_{k_1} \int_{k_3} D^{m'm}(k_1) \Delta_{\sigma\sigma'}^{ss'}(k_3) D^{ee'}(k_4) \Gamma_{c^g A_{s'}^{\sigma'} \bar{c}^{e'}}(k_3, k_4) D^{g'g}(k_2) \times \\
& \quad \times \Gamma_{c^m A_\beta^b \bar{c}^g}(-q, k_2) \\
& = (b_9).
\end{aligned} \tag{4.36}$$

Finally, since diagrams (a_2) , (a_4) (a_5) and (a_6) carry over to the corresponding BFM ones (b_2) , (b_5) , (b_6) and (b_{11}) and $(a_1)^F = (b_1)$, we have the final identity

$$(s_2) + (s_3) + \left[(a_1)^F + \sum_{i=2}^6 (a_i) \right] = \sum_{i=1}^{11} (b_i), \tag{4.37}$$

and therefore

$$-\Gamma_{A_\alpha^a A_\beta^b}(q) = -i\Gamma_{\Omega_\alpha^a A_d^{*\gamma}}(q) \Gamma_{A_7^d A_\beta^b}(q) - \Gamma_{\hat{A}_\alpha^a A_\beta^b}(q), \tag{4.38}$$

which is the BQI of Eq. (E.2).

2. Second step

The second step in the propagator construction is to employ the obvious relation

$$\Gamma_{\hat{A}_\alpha^a A_\beta^b}(q) = \Gamma_{A_\alpha^a \hat{A}_\beta^b}(q), \tag{4.39}$$

that is to interchange the background and quantum legs (the SDE for the self-energy $-\Gamma_{AA\hat{A}}$ is shown in Fig. 19). This apparently trivial operation introduces a considerable simplification. First of all, it allows for the identification of the pinching momenta from the usual PT decomposition of the (tree-level) Γ appearing in diagram (c_1) of Fig. 19 [something not directly possible from diagram (b_1)]; thus, from the operational point of view, we remain on familiar ground. In addition, it avoids the need to employ the (formidably complicated) BQI for the four-gluon vertex; indeed, the equality between diagrams (c_5) , (c_6) , (c_7) of Fig. 19 and (d_5) , (d_6) , (d_{11}) of Fig. 6, respectively, is now immediate [as it was before, between the diagrams (a_4) , (a_5) , (a_6) and (b_5) , (b_6) , (b_{11}) , respectively].

3. Third step

We now turn to diagram (c_1) and concentrate on its pinching part, given by

$$(c_1)^P = igf^{amn'}g_{\alpha\nu'} \int_{k_1} \frac{1}{k_1^2} \Delta_{n'n}^{\nu\nu'}(k_2) k_1^\mu \Gamma_{A_\mu^m A_\nu^{\hat{a}} \hat{A}_\beta^b}(k_2, -q). \quad (4.40)$$

Notice the appearance of the full BFM vertex $\Gamma_{AA\hat{A}}$ instead of the standard Γ_{AAA} (in the R_ξ). The STI satisfied by the former vertex has been derived in Eq. (D.25). Now, the first three terms, (s_1) , (s_2) and (s_3) , appearing in this STI, will give rise to PT contributions exactly equal to those encountered in first step described above, the only difference being that the A_β^b field appearing there is now a background field \hat{A}_β^b . Thus, following exactly the reasoning described before, we find [see again Fig. 6 for the diagrams corresponding to each (d_i)]

$$(s_1) \rightarrow -i\Gamma_{\Omega_\alpha^a A_\epsilon^{*e}}(q) \Gamma_{A_\epsilon^e \hat{A}_\beta^b}(q), \quad (4.41)$$

$$(s_2) + (s_3) + (c_3) = (d_3) + (d_4) + (d_7) + (d_8) + (d_9) + (d_{10}). \quad (4.42)$$

For the term (s_4) we have instead

$$(s_4) \rightarrow g^2 f^{am'e} f^{ebm} g_{\alpha\mu'} g_{\beta\mu} \int_{k_1} \Delta_{m'm}^{\mu'\mu}(k_1). \quad (4.43)$$

Clearly this has a tadpole-like structure; in particular, it is immediate to prove that when added to (c_2) it will convert it into (d_2)

$$(s_4) + (c_2) = (d_2). \quad (4.44)$$

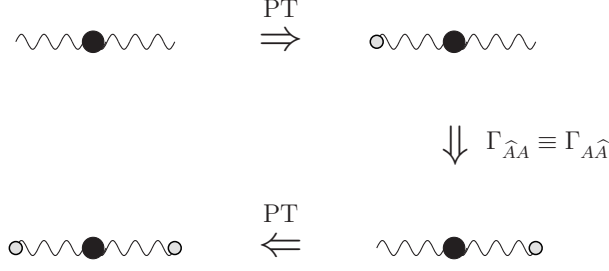


FIG. 20: Summary of the PT procedure employed in the text in order to construct the new PT SDE of the gluon propagator.

Thus, since as always $(c_1)^F = (d_1)$ we get

$$(s_2) + (s_3) + (s_4) + \left[(c_1)^F + \sum_{i=2}^7 (c_i) \right] = \sum_{i=1}^{11} (d_i), \quad (4.45)$$

and therefore

$$- \Gamma_{A_\alpha^a \hat{A}_\beta^b}(q) = -i\Gamma_{\Omega_\alpha^a A_\epsilon^{*e}}(q)\Gamma_{A_\epsilon^e \hat{A}_\beta^b}(q) - \Gamma_{\hat{A}_\alpha^a \hat{A}_\beta^b}(q), \quad (4.46)$$

which is the BQI of Eq. (E.3). This concludes our proof.

In Fig. 20 we summarize the steps that allowed the successful construction of the SDE for the PT propagator; putting together the three steps above, we have been able to generate the complete BQI of Eq. (E.4), namely

$$i\Gamma_{\hat{A}_\alpha^a \hat{A}_\beta^b}(q) = i\Gamma_{A_\alpha^a A_\beta^b}(q) + 2\Gamma_{\Omega_\alpha^a A_d^{*\gamma}}(q)\Gamma_{A_\gamma^d A_\beta^b}(q) - i\Gamma_{\Omega_\alpha^a A_d^{*\gamma}}(q)\Gamma_{A_\gamma^d A_\epsilon^e}(q)\Gamma_{\Omega_\beta^b A_\epsilon^{*e}}(q). \quad (4.47)$$

According to the PT rules put forward in Section III E, on the one hand the PT gluon two-point function $i\hat{\Gamma}_{AA}$ would coincide with the rhs of Eq. (4.47) after dropping the terms proportional to the auxiliary function $\Gamma_{\Omega A^*}$, since these would cancel anyway after adding the contribution coming from the corresponding vertices. On the other hand, recalling that $\Gamma_{\Omega_\alpha A_\beta^*}$ coincide with $\Lambda_{\alpha\beta}$, and observing that the only relevant part in the identity above of such functions is the one proportional to the metric tensor (due to the transversality of the gluon two-point function Γ_{AA}), it is immediate to show, using Eq. (2.6) and the relation $-\Gamma_{A_\alpha A_\beta} = \Pi_{\alpha\beta}$, that Eq. (4.47) can be cast in the form of the SDE shown in Eq. (2.36).

D. How to truncate the new SDEs

After constructing the new SDE series, let us focus on its truncation properties, both from the theoretical as well as the practical point of view.

As has been stated repeatedly, the main theoretical advantage of the new SD series is that it allows for a systematic gauge-invariant truncation, in the sense described in subsection II E. There we focused on how to truncate the SDE for the gluon self-energy, shown in Fig.6, by exploiting the fact that the various fully dressed graphs organize themselves into gauge-invariant subsets [those appearing in Eq.(2.41)]. The practical importance of this property is the following: one can reduce the number of coupled SDE that one must include in order to maintain the gauge (or BRST) symmetry of the theory intact, as reflected, for example in the validity of Eq.(1.1). Thus, in the case of pure Yang-Mills, within this new formulation, the minimum number of equations that one must consider is only two: The SDE for the gluon self-energy, given by the first gauge-invariant subset *only* (i.e., $[(d_1) + (d_2)]_{\alpha\beta}$ in Fig.6) and the SDE for the full three-gluon vertex, shown in Fig.14 (which is instrumental in assuring the gauge invariance of the subset chosen). This is to be contrasted to what happens within the conventional formulation: there the SDEs for *all* vertices must be considered, or else Eq. (1.1) is violated (which is what usually happens).

Notice an important point, however: the present analysis does *not* furnish a simple diagrammatic truncation, analogous to that of the gluon self-energy, for the SDE of the three gluon vertex $\Gamma_{\widehat{A}_\alpha A_\mu A_\nu}(k_1, k_2)$, shown in Fig.14. Thus, if one were to truncate the SDE for the three-gluon vertex by keeping any subset of the graphs appearing in Fig.14, one would violate the validity of the *all-order* WI of Eq. (2.37); this, in turn, would lead immediately to the violation of Eq. (1.1), thus making the entire truncation scheme collapse.

The strategy one should adopt is instead the following. Given that the proposed truncation scheme hinges crucially on the validity of Eq. (2.37), one should start out with an approximation that manifestly preserves it. The way to enforce this, familiar to the SDE practitioners already from the time of QED, is to resort to the “gauge-technique” [47], namely “solve” the WI of Eq. (2.37). Specifically, one must express the three-gluon vertex as a functional of the corresponding self-energies, in such a way that (by construction) its WI is automatically satisfied. For example, an Ansatz with this property would be

$$\Gamma_{\widehat{A}_\alpha A_\mu A_\nu}(k_1, k_2) = \Gamma_{\widehat{A}_\alpha A_\mu A_\nu}^{(0)}(k_1, k_2) - i \frac{(k_2 - k_1)_\alpha}{k_2^2 - k_1^2} [\Pi_{\mu\nu}(k_2) - \Pi_{\mu\nu}(k_1)]; \quad (4.48)$$

contracting the rhs with $q_\alpha = (k_1 + k_2)_\alpha$ yields automatically the WI of Eq. (2.37). Thus, the minimum amount of ingredients for initiating a *self-consistent* non-perturbative treatment is the SD for the gluon self-energy, consisting of $[(d_1) + (d_2)]_{\alpha\beta}$, supplemented by an Ansatz

for the three-gluon vertex like the one given in (4.48). Note that the “gauge-technique” leaves the transverse (*i.e.*, automatically conserved) part of the vertex undetermined. This is where the SDE for the vertex enters; it is used precisely to determine the transverse parts. Specifically, following standard techniques [29, 31], one must expand the vertex into a suitable tensorial basis, consisting of fourteen independent tensors, and then isolate the transverse subset. This procedure will lead to a large number of coupled integral equations, one for each of the form-factors multiplying the corresponding tensorial structures, which may or may not be tractable. However, at this point, one may simplify the resulting equations (*e.g.*, linearize, etc) without jeopardizing the transversality of $\Pi_{\mu\nu}$, which only depends on the “longitudinal” part of the vertex, *i.e.*, the one determined by (4.48). Thus, the transverse parts will be approximately determined, but gauge invariance, as captured by $q^\mu \Pi_{\mu\nu} = 0$, will remain exact.

Note by the way that the methodology described above constitutes, even to date, the standard procedure even in the context of QED, where the structure of the SDE is much simpler, given that the SDE for the photon contains one single graph [diagram (a_6) in Fig.1], and the photon-electron vertex satisfies automatically a naive all-order WI. Thus, while the PT approach described here replicates QED-like properties at the level of the SDEs of QCD, in our opinion a striking fact in itself, does not make QCD easier to solve than QED.

The reader should appreciate one additional point: any attempt to apply the approach described above in the context of the conventional SDE is bound to lead to the violation of the transversality of $\Pi_{\mu\nu}$, because (*i*) the vertices satisfy complicated STI’s instead of the WIs of Eq. (2.37)–(2.40), a fact that makes the application of the “gauge-technique” impractical, and (*ii*) even if one came up with the analogue of Eq. (4.48) for all vertices, one should still keep all self-energy diagrams in Fig.1 to guarantee that $q^\mu \Pi_{\mu\nu} = 0$. From this point of view, the improvement of the present approach over the standard formulation becomes evident.

Finally, one should be aware of the fact that there is no a-priori guarantee that the gauge-invariant subset kept (*i.e.*, $[(d_1) + (d_2)]_{\alpha\beta}$) capture necessarily most of the dynamics, or, in other words, that they represent the numerically dominant contributions (however, for a variety of cases it seems to be true [42]). But, the point is that one can *systematically* improve the picture by including more terms, without worrying that the initial approximation is plagued with artifacts, originating from the violation of the gauge invariance or of the BRST

symmetry.

V. CONCLUSIONS

In this article we have presented a detailed derivation of a new SD series for non-Abelian gauge theories, based on the PT and its correspondence with the BFM. The procedure we followed for constructing the PT SDE is identical to that followed in the perturbative construction, *without* any additional new assumption.

Our starting point is the conventional SDEs for the vertices and the gluon self-energy written in the Feynman gauge. The first step in the derivation is to simply carry out the PT decomposition of the elementary (tree-level) three-gluon vertex, $\Gamma_{\alpha\mu\nu}$ given in Eq. (2.12), to the external three-gluon vertices appearing in the corresponding diagrams of the standard SD series. The part of $\Gamma_{\alpha\mu\nu}$ denoted by $\Gamma_{\alpha\mu\nu}^P$ contains longitudinal momenta which get contracted with the kernels or the fully-dressed Green's functions appearing inside the diagram containing the original $\Gamma_{\alpha\mu\nu}$, triggering the corresponding STIs. These STIs, in turn, contain pieces that, according to the well-established PT criteria, either form part of the answer, in this case the diagrammatic expansion of the SDE for the corresponding Green's function, or they are discarded from it. In Section IV we have worked out in detail three cases: (i) the quark-gluon vertex, (ii) the three-gluon vertex, and (iii) the technically more involved case of the gluon self-energy. It turns out that the diagrams comprising the PT answer are identical to those corresponding to the BFG. Thus, the resulting new SDEs, generated after the characteristic PT rearrangements have taken place, and the PT criterion for identifying the answer has been employed, correspond to the BFM SDEs, written in the BFG. This is an important result, because it proves the PT-BFG correspondence at the level of the SDE of the theory; obviously, all results on this point presented in the literature so far are included in the result presented here, given that any order in perturbation theory is already contained in the SDEs we consider.

An additional important result, obtained from the same procedure, is the diagrammatic derivation of the BQIs, which, to date, have only been formally derived in the context of the BV formalism. The way that the terms comprising the BQIs appear in the present analysis is automatic: they are simply the leftovers of the PT construction, *i.e.*, the pieces that have been discarded from the PT answer.

As explained in detail in [13, 37], and mentioned also in Section II, the new SDE series for the gluon self-energy contains fully dressed vertices that satisfy simple, QED-like (*i.e.*, tree-level-like) WIs, instead of STIs. This fact allows for the truncation of the SDE series while maintaining the transversality of the answer at any step.

Returning to the construction of the gluon SDE, a crucial ingredient for the proof has been the interchange of background and quantum legs done in subsection IV C 2, *i.e.*, $\Gamma_{\hat{A}A} \rightarrow \Gamma_{A\hat{A}}$ (see also Fig. 20). As we have mentioned there this allowed us to (*i*) identify the pinching momenta from the usual PT decomposition, and (*ii*) avoid the use of some otherwise indispensable multi-leg BQIs. But more importantly it unveils a recursive pattern that can be used to generalize the construction to n -point Green's functions with n arbitrary. Work in this direction is already in progress.

As we have emphasized in the Introduction, the BFG is singled out dynamically when carrying out the PT rearrangement of a physical quantity, such as an S -matrix element or a Wilson loop. In particular, after the full cancellation of all (effectively propagator-like) gauge-dependent pieces has taken place, and after the vertices have been forced to obey Abelian WIs, the resulting self-energy contribution (to be identified with the PT self-energy) *coincides* with the BFM gluon self-energy, calculated in the BFG. In that sense the BFG is very special, because it captures the net gauge-independent and universal (*i.e.*, process-independent) contribution contained in any physical quantity. In practice, however, one would like to be able to truncate gauge-invariantly (*i.e.*, maintaining transversality) sets of SDEs written in different gauges. This becomes particularly relevant, for example, when one attempts to compare SDE predictions with lattice simulations, carried out usually in the Landau gauge. One of the most powerful features of this formalism, not explored in this article, is that it can be generalized to any other gauge choice. In particular, Eq. (2.36) maintains the same form, regardless of the gauge chosen. The way to accomplish this is to use the “generalized” PT, developed in [41]. The generalized PT modifies the starting point of the PT algorithm, namely Eq. (2.12), distributing differently the longitudinal momenta between $\Gamma_{\alpha\mu\nu}^F$ and $\Gamma_{\alpha\mu\nu}^P$. Specifically, the non-pinching part, *i.e.*, the analogue of $\Gamma_{\alpha\mu\nu}^F$, must satisfy, instead of (2.13), a WI whose rhs is the difference of two inverse tree-level propagators in the gauge one wishes to consider. The way this works is the following. One starts out with the conventional SDE in the chosen gauge, carrying out the generalized PT vertex decomposition. Then, the action of the corresponding $\Gamma_{\alpha\mu\nu}^P$ projects one to the

corresponding BFM gauge; this includes the covariant gauges, such as the Landau gauge, or even non-covariant gauges, such as axial or light-cone gauges (for the way how to use non-covariant gauges within the BFM framework, see [41]). This new SD series contains full vertices that, even though they are in a different gauge, satisfy the QED-like WIs given in Eq.s (2.37) – (2.41). Therefore, the truncation properties of this SDE are the same as those discussed in Section II for the case of the Feynman gauge. The analogy is completed by realizing that the BQIs in the corresponding gauge allow one to switch back and forth from the conventional to the BFM Green’s function. Thus, one may obtain, for example, transverse approximations for the gluon propagator in the conventional Landau gauge by studying the SDE written in the BFM Landau gauge, computing the $[1 + G(q^2)]^2$ in the same gauge, *i.e.*, employ Eq. (2.36) using for the diagrams on its rhs the BFM Feynman rules in the Landau gauge (see Appendix). This Landau gauge SDE has already been used in [42], in order to derive results for the gluon and ghost propagators that are in qualitative agreement with recent lattice data; as explained there, particular care is needed when taking the limit $\xi_Q \rightarrow 0$.

It would be important, both from the theoretical point of view as well as for the practical applications, to study in detail the renormalization properties of the new SDEs (for a general discussion see the Appendix B). For addressing this problem the intrinsically non-perturbative renormalization method known as “displacement operator formalism” [43] may prove to be particularly suitable.

It is also very appealing to believe that the SDE derived here may be actually obtained from a variational principle, *i.e.*, as a result of the extremization of an appropriate effective action, as happens in the case of the CJT formalism [3]. Calculations in this directions are already in progress.

Finally, it would be interesting to establish connections between the dynamics obtained from the SDEs derived here and results based on the non-perturbative BFM formalism developed in [44].

Acknowledgments

D.B. acknowledges the hospitality of the Physics Department of the University of Valencia, where part of this work was carried out. The research of J.P. is supported by the

Fundación General of the UV and by the MEC grant FPA 2005-01678.

Feynman diagrams have been drawn using JaxoDraw [45].

Appendix A: Which way to pinch and why

Historically, the basic conceptual difficulty associated with the generalization of the PT beyond one loop has been to determine the origin of the pinching momenta. Let us assume that, without loss of generality, one chooses from the beginning the conventional Feynman gauge. Then, the only sources of possible pinching momenta are the three-gluon vertices. The question is whether all such vertices must be somehow forced to pinch, or, in other words, whether the standard PT decomposition of Eq. (2.12) should be carried out to all available three-gluon vertices. The problem with such an operation, however, is the following: for the case of a three-gluon vertex nested inside a Feynman diagram, how does one choose which is the “special” momentum? Or, in other words, which way is one supposed to brake the Bose-symmetry of the vertex? Turns out that the solution to these questions is very simple [30]: one should apply Eq. (2.12) *only* to the vertices that have the physical momentum incoming (or outgoing) in one of their legs (not mixed with virtual momenta); the special leg is precisely the one carrying q , *i.e.*, the *physical* momentum transfer appearing in the problem. We will call such a vertex “external”. All other vertices are not to be touched, *i.e.*, they should not be decomposed in any way; such vertices have virtual momenta entering into every one of their three legs, and are called “internal” (see Fig.21).

The reason why all other three-gluon vertices inside the loops should remain unchanged (no splitting) can be best understood by resorting to the *absorptive construction* of the PT [21–23]. The basic philosophy behind the absorptive construction is to emulate as much as possible the text-book reconstruction of the real part of the vacuum polarization of QED (containing say a muon-loop) from the tree-level cross-section for $e^+e^- \rightarrow \mu^+\mu^-$, *i.e.*, the optical theorem, and a (once-subtracted) dispersion relation. As in QED, in the case of the PT the basic observation also happens already at one loop: the PT subamplitudes (self-energies, vertices, boxes) satisfy the optical theorem *individually*, in a way similar to what happens with scalar theories and QED.

Specifically, let us write $S = 1 + iT$, and consider the forward scattering process $q(p_1)\bar{q}(p_2) \rightarrow q(p_1)\bar{q}(p_2)$, with $s = q^2 = (p_1 + p_2)^2$. Restricting ourselves to only gluonic intermediate states, the PT amplitudes, at lowest order satisfy

$$\Im m \langle q\bar{q} | T^{[4]} | q\bar{q} \rangle_\ell = \frac{1}{2} \times \frac{1}{2} \int_{\text{PS}_{2g}} [\langle q\bar{q} | T^{[2]} | gg \rangle \langle gg | T^{[2]} | q\bar{q} \rangle^*]_\ell, \quad (\text{A.1})$$

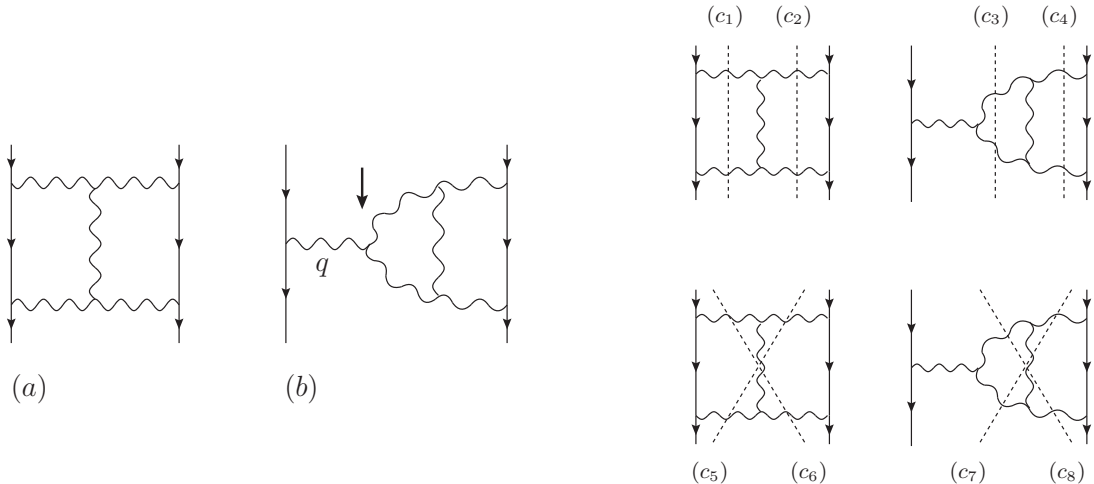


FIG. 21: Left panel: Some examples of external (indicated with an arrow) and internal vertices (all the remaining). Diagram (a) has only internal three-gluon vertices, while diagram (b) has two internal vertices and one external, indicated by the arrow. Right panel: The two- and three-particle Cutkosky cuts (cutting through gluons only).

with $\int_{\text{PS}_{2g}}$ denoting the two-body phase space for massless gluons. In the equation above the superscript $[n]$ denotes the order of the corresponding amplitude in the coupling constant g (when counting powers of g remember the couplings coming from the vertices with the external particles); the subscript $\ell = 1, 2, 3$ denotes, respectively, the propagator-, vertex-, and box-like parts of either side (to recover the full optical theorem, one simply sums both sides over ℓ). Finally, the extra factor of $\frac{1}{2}$ is statistical, since the final state gluons are considered as identical particles in the total rate.

The meaning of propagator-, vertex-, and box-like is clear as far as the lhs of Eq. (A.1) is concerned: one must determine the imaginary (absorptive) parts of the three one-loop PT subamplitudes obtained after casting the amplitude $q(p_1)\bar{q}(p_2) \rightarrow q(p_1)\bar{q}(p_2)$ into the PT form, following the standard PT rules. To get these absorptive parts one may carry the corresponding Cutkosky cuts to the various integrals, (including “unphysical” contributions coming from ghost loops) or, equivalently, study where the various logarithms develop imaginary parts.

Let us see now what propagator-, vertex-, and box-like means on the rhs, consisting of the squared amplitude for the tree-level process $q(p_1)\bar{q}(p_2) \rightarrow g(k_1)g(k_2)$ (with k_1 and k_2

integrated over all available phase space). A PT-rearranged squared amplitude means the following. Consider a normal squared amplitude, *i.e.*, the product of two regular amplitudes [remember that “product” means that they are also connected (multiplied) by the corresponding polarization tensors]. Then each amplitude must be first cast into its PT form, by again simply following the standard PT rules. However, this is not the end of the story as far as the PT-rearrangement of the square is concerned. One must go through the additional exercise of letting the longitudinal momenta coming from the polarization vectors trigger a particular cancellation between the s -channel and the t -channel graphs (known in the literature as the “ s - t cancellation”). That will finally identify the genuine propagator-, vertex-, and box-like pieces of the entire product.

Now the important step is the following: Suppose that one starts out with the rhs of Eq. (A.1), *i.e.*, one works at the level of the physical squared amplitude. The PT rearrangement of the rhs may furnish the PT rearranged amplitudes on the lhs, through an (appropriately subtracted) dispersion relation. Thus, the absorptive PT construction means to (i) PT-rearrange the rhs, (ii) impose the optical theorem (individually for each ℓ), and (iii) use analyticity to get the real parts of the PT amplitudes.

Let us now see how the PT absorptive construction gets generalized to higher orders, and, in particular, how it can furnish a unique way for defining the PT construction without any a-priori reference to the BFM and its special vertices.

At the next order in g^2 Eq. (A.1) becomes

$$\begin{aligned} \Im m \langle q\bar{q} | T^{[6]} | q\bar{q} \rangle_\ell &= \frac{1}{2} \left(\frac{1}{2!} \right) \int_{\text{PS}_{2g}} 2 \Re e [\langle gg | T^{[4]} | q\bar{q} \rangle^* \langle gg | T^{[2]} | q\bar{q} \rangle]_\ell \\ &+ \frac{1}{2} \left(\frac{1}{3!} \right) \int_{\text{PS}_{3g}} [\langle ggg | T^{[2]} | q\bar{q} \rangle^* \langle ggg | T^{[2]} | q\bar{q} \rangle]_\ell, \end{aligned} \quad (\text{A.2})$$

where now $\int_{\text{PS}_{3g}}$ denotes the three-body phase-space for massless gluons.

According to Eq. (A.2) then the imaginary parts of the two-loop PT Green’s functions (under construction) are related by the optical theorem to precisely identifiable and very special parts of the squared amplitudes for the processes $q\bar{q} \rightarrow gg$ and $q\bar{q} \rightarrow ggg$. In particular, the two-particle Cutkosky cuts of the two-loop PT self-energy are related to the propagator-like part of the *PT-rearranged* one-loop squared amplitude for $q\bar{q} \rightarrow gg$, while, at the same time, the three-particle Cutkosky cuts of the same quantity are related to the propagator-like part of the *PT-rearranged* tree-level squared amplitude for $q\bar{q} \rightarrow ggg$. The

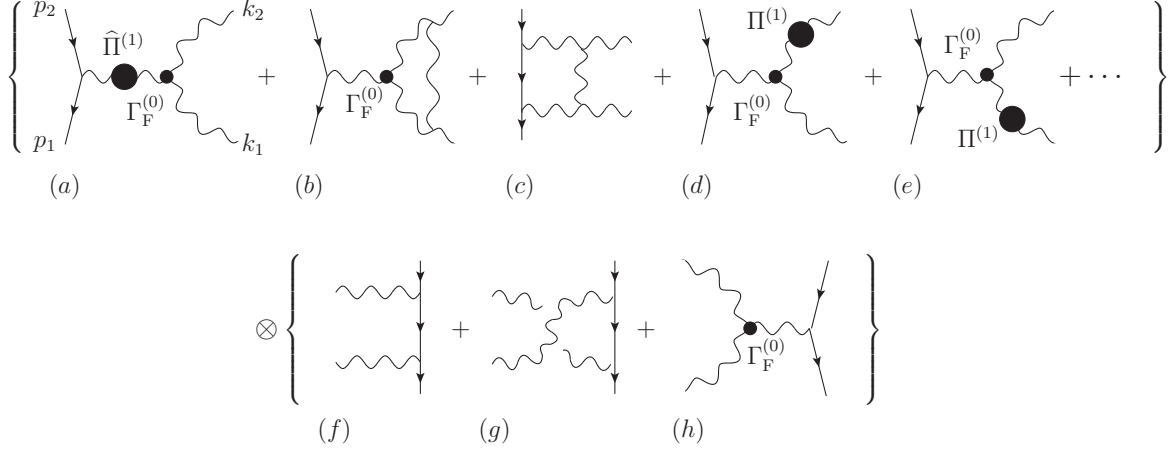


FIG. 22: The product of the PT-rearranged amplitudes of the process $q\bar{q} \rightarrow q\bar{q}$ at one-loop (up) and tree-level (down). The longitudinal momenta from the polarization tensors will produce additional cancellations between s -channel and t -channel graphs [30], furnishing finally the first term on the rhs of Eq. (A.2).

same holds for vertex- and box-like contributions. The processes appearing on the rhs of Eq. (A.2) are shown in Figs 22 and 23. The advantage of this formulation is the following: all the PT-rearranged (squared) amplitudes appearing on the rhs are at least one loop lower than the amplitude on the lhs. Therefore, one can actually reconstruct the lhs, by working directly on the rhs, because one knows how to pinch at lower orders.

To see how all this analysis makes finally contact with the main question at hand, namely which way to pinch in higher orders, let us focus on Fig. 22. There it is clear that the product involves the PT-rearranged *one-loop* on-shell amplitude for the process $q(p_1)\bar{q}(p_2) \rightarrow g(k_1)g(k_2)$, whose construction is absolutely fixed and well defined, and has been described in great detail in the literature [34, 46] In fact, it was the first explicit example [46] demonstrating the universality (process-independence) of the PT gluon self-energy: the resulting gluon self-energy does not depend on the embedding process (quarks to quarks or quarks to gluons or gluons to gluons, etc). The PT-rearranged *one-loop* $q(p_1)\bar{q}(p_2) \rightarrow g(k_1)g(k_2)$ is obtained following exactly the same PT procedure as for the process with only quarks as external particles. In particular, the three-gluon vertices in graphs (b) and (c) in Fig. 22 must be exactly as shown, *i.e.*, the one injected with q has undergone the PT decomposition (and has become Γ^F), while the ones injected with k_1 and

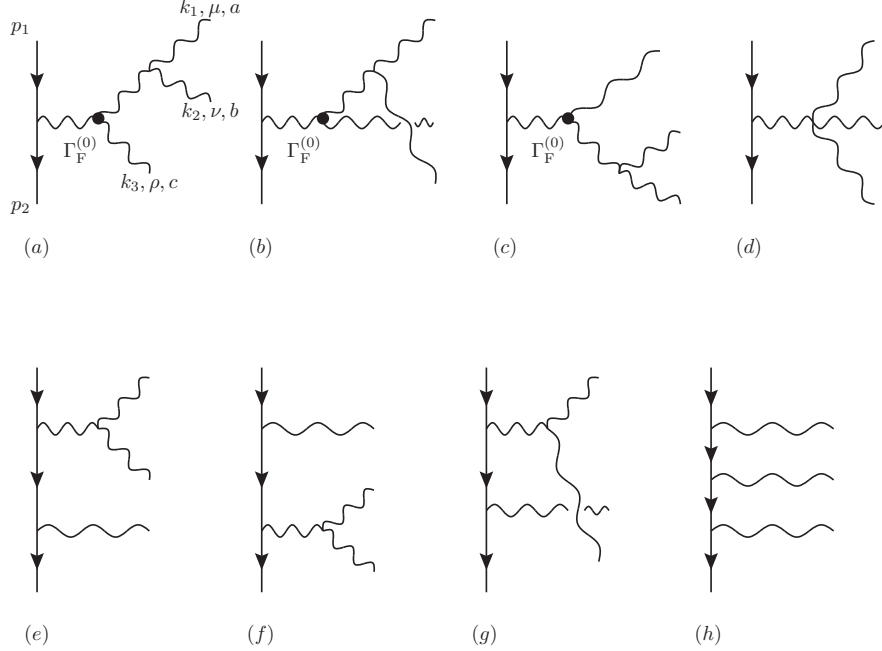


FIG. 23: The PT-rearranged tree-level amplitude for the process $q\bar{q} \rightarrow ggg$; squaring and further pinching triggered by the longitudinal momenta inside the polarization tensors [30] will furnish the second term on the rhs of Eq. (A.2).

k_2 remain unchanged. Let us now return to the two representative two-loop diagrams of Fig.21. After their PT rearrangement, the two-particle Cutkosky cut on (a) denoted by (c₂) in Fig. 21 must reproduce (c) \otimes [(f) + (g)] in Fig. 22, and cut (c₄) on (b) must reproduce (b) \otimes [(f) + (g)]. Obviously, if we were to modify the internal three-gluon vertices of (a) or (b) in Fig. 21 in any way, this identification would not work: one must modify *only* the vertex injected with q (turning it to Γ^F). This argument may be generalized to include all remaining two-particle and three-particle cuts, making the above conclusion completely airtight. Under the light of these observations it should be clear why, for example, the relevant full three-gluon vertex entering into the SD equation for the gluon self-energy (*viz.* Fig.6) is indeed $\Gamma_{\widehat{A}AA}$ (constructed in subsection IV B) and *not* the vertex $\Gamma_{\widehat{A}\widehat{A}\widehat{A}}$. The latter could not be consistently constructed inside loops, because any preferred direction (i.e. the direction determining the “would-be” background field) is immediately at odds with the unitarity-cut arguments developed above.

The arguments presented here do not postulate at any point the existence of any relation between the PT and the BFM. On the other hand, on hindsight, all conclusions drawn (for

example, the $\Gamma_{\widehat{AAA}}$ versus $\Gamma_{\widehat{AA}\widehat{A}}$ issue) are in complete agreement with the known PT/BFM correspondence. Specifically, switching now to the BFM language, the fact that internal vertices should not be touched is precisely what the unique set of BFM Feynman rules dictates: since one cannot have background fields propagating inside loops, all internal vertices have three *quantum* gluons merging. This is exactly what one finds, *e.g.*, when computing the two-loop gluon self-energy [17]: as a subset of the calculation one will have to consider the one-loop vertex $\Gamma_{\widehat{AAA}}^{(1)}$, but will never encounter the one-loop vertex $\Gamma_{\widehat{AA}\widehat{A}}^{(1)}$ (constructed in [15] and studied in [29]).

Appendix B: A brief discussion of renormalization

This appendix is meant to outline the general framework for dealing with the issue of renormalization in the context of the PT. The emphasis is put on the various conceptual and methodological issues involved, rather than an explicit proof of renormalizability. In particular, we consider this discussion necessary for convincing the reader that renormalization poses no problem whatsoever for the self-consistent implementation of the PT.

The analysis presented thus far assumes implicitly that the theory is renormalizable (as is QCD in $d = 4$) or superrenormalizable (as is QCD in $d = 3$), and that all momentum space integrals have been regularized by resorting to a regularization scheme that preserves the gauge symmetry (obviously there is little point in applying the PT to a theory that is ill-defined to begin with). Specifically, throughout the paper we have adopted the most widely used such scheme, namely dimensional regularization. Given that the original theory is renormalizable (by assumption) it should be clear that there is no step throughout the PT procedure that could jeopardize renormalizability. Indeed, all that the PT really does is to trigger STIs. The latter are a direct consequence of the original BRST symmetry of the theory; therefore, within a suitable regularization scheme (such as dimensional regularization) they will be preserved by renormalization (*i.e.*, they will not get deformed). It is important to emphasize that the latter property holds true for the BQIs as well; they too are a consequence of the BRST symmetry and (under the same assumptions) do not get deformed either. Notice that this is completely different from the case of the Nielsen identities [48], describing the gauge fixing parameter dependence of the bare Green's functions (we do not use them here). In this latter case, one needs to extend the BRST symmetry to include

the variation of the gauge fixing parameter. This, in turn, will spoil the original BRST invariance of the theory, implying that the latter identities get deformed by renormalization already at the one-loop level [43].

For concreteness let us assume that we start the PT procedure in the renormalizable (linear) Feynman gauge (RFG), as we have done throughout this article. Let us denote by Z_A the gluon wave-function renormalization, by Z_3 the vertex renormalization constant for the three-gluon vertex $\Gamma_{\alpha\mu\nu}$, by \bar{Z}_2 the usual ghost wave-function renormalization, and by \bar{Z}_1 the ghost-gluon vertex renormalization constant. Notice also that, the BRST symmetry demands that $Z_3/Z_A = \bar{Z}_1/\bar{Z}_2$. Then, the fundamental STIs employed when carrying out the PT survives renormalization, simply because all counterterms necessary to render it finite are already furnished by the usual counterterms of the RFG Lagrangian. This is, of course, a direct result of the basic assumption that the theory in the RFG is renormalizable: once all counterterms have been supplied in the RFG, the STI which is studied in the same gauge, will continue being valid.

The actual implementation of the renormalization procedure proceeds along the lines described in [30] for the two-loop case. One should start out with the counterterms that are necessary to renormalize individually the conventional Green's functions in the RFG. Then, one should show that, by simply rearranging these counterterms following the PT rules, one can renormalize the PT Green's functions. Notice also that, due to the validity of the Abelian WIs, the renormalization constants before and after the PT rearrangements are related to the gauge coupling renormalization as follows:

$$Z_g^2 = Z_1^2 Z_2^{-2} Z_A^{-1} = \widehat{Z}_1^2 \widehat{Z}_2^{-2} \widehat{Z}_A^{-1} = \widehat{Z}_A^{-1}. \quad (\text{B.1})$$

After rearranging the original RFG counterterms in such a way as to render the PT Green's functions finite, one should be able to verify that the resulting counterterms are in fact identical to those obtained when carrying out the BFM renormalization program as explained by Abbott [17], i.e. by renormalizing only the background gluons, the coupling constant g , and the quantum gauge-fixing parameter ξ_Q . Thus, the relevant renormalization constants are given by

$$g_0 = Z_g g, \quad \widetilde{A}_0 = Z_{\widetilde{A}}^{1/2} \widetilde{A}, \quad \xi_Q^0 = Z_{\xi_Q} \xi_Q, \quad Z_{\xi_Q} = Z_A. \quad (\text{B.2})$$

The renormalization of ξ_Q is necessary due to the fact that the longitudinal part of the quantum gluon propagator is not renormalized. As pointed out by Abbott, in the context of

the BFM this step may be avoided if the calculation is carried out with an arbitrary ξ_Q rather than the BFG $\xi_Q = 1$. Of course, as we have seen, the PT brings us effectively to $\xi_Q = 1$; thus, when interpreting the resulting counterterm from the BFM point of view, one should keep in mind that gauge-fixing parameter renormalization is necessary. The renormalization of ξ_Q not only affects the propagator-lines, but also the longitudinal parts of the external vertices; it renormalizes precisely the Γ^P part, as can be seen from the corresponding BFM Feynman rule for the three-gluon vertex (see Appendix F).

All the above ingredients must be combined appropriately in order to demonstrate the renormalizability of the new SDE; we shall not pursue this point any further.

Appendix C: Faddeev-Popov Equations

As a first example of the use of the FPE introduced in Section III D, let us differentiate the functional equation (3.37) with respect to the ghost field c^b ; after setting the fields/anti-fields to zero we get (relabeling the color and Lorentz indices)

$$\Gamma_{c^m \bar{c}^n}(q) + iq^\nu \Gamma_{c^m A_\nu^{*n}}(q) = 0, \quad (\text{C.1})$$

which can be used to relate the auxiliary function $\Gamma_{c^m A_\nu^{*n}}(q)$ with the full ghost propagator $D^{ab}(q)$. Due to Lorentz invariance, we can in fact write $\Gamma_{c^m A_\nu^{*n}}(q) = q_\nu \Gamma_{c^m A^{*n}}(q)$, and therefore

$$\Gamma_{c^m \bar{c}^n}(q) = -iq^\nu \Gamma_{c^m A_\nu^{*n}}(q) = -iq^2 \Gamma_{c^m A^{*n}}(q). \quad (\text{C.2})$$

On the other hand, due to our definition of the Green's functions [see Eq. (3.18)], one has that

$$iD^{mr}(q)\Gamma_{c^r \bar{c}^n}(q) = \delta^{mn}, \quad (\text{C.3})$$

and therefore we get the announced relation:

$$\begin{aligned} \Gamma_{c^m A_\nu^{*n}}(q) &= q_\nu \Gamma_{c^m A^{*n}}(q) \\ &= q_\nu [q^2 D^{mn}(q)]^{-1}. \end{aligned} \quad (\text{C.4})$$

As a second example, let us differentiate Eq. (3.37) twice, once with respect to A_μ^n and once with respect to c^r , and then set the fields/anti-fields to zero; in this way we get the identity

$$\Gamma_{c^r A_\nu^n \bar{c}^m}(k, q) + iq^\mu \Gamma_{c^r A_\nu^n A_\mu^{*m}}(k, q) = 0, \quad (\text{C.5})$$

which is particularly useful for the PT construction. Notice that this identity is the equivalent of the one introduced in Section II A relating the conventional H function with the trilinear gluon-ghost vertex. All these identities can be easily checked at tree-level; for example, using the Feynman rules presented in Appendix F, we have

$$iq^\mu \Gamma_{c^r A_\nu^n A_\mu^{*m}}^{(0)}(k, q) = igf^{mnr} q_\nu = -\Gamma_{c^r A_\nu^n \bar{c}^m}^{(0)}(k, q). \quad (\text{C.6})$$

Differentiation of the functional (3.38) with respect to a BFM source Ω and a quantum gluon field A or a ghost field c and a background gluon \widehat{A} , provides instead the identities ($k_1 + k + q = 0$)

$$\Gamma_{\Omega^r A_\nu^n \bar{c}^m}(k, q) + iq^\mu \Gamma_{\Omega^r A_\nu^n A_\mu^{*m}}(k, q) = gf^{mnr} g_{\nu\rho}, \quad (\text{C.7})$$

$$\Gamma_{c^r \widehat{A}_\nu^n \bar{c}^m}(k, q) + iq^\mu \Gamma_{c^r \widehat{A}_\nu^n A_\mu^{*m}}(k, q) = -igf^{mne} \Gamma_{c^r A_\nu^{*e}}(-k_1), \quad (\text{C.8})$$

that can be easily checked at tree-level.

Appendix D: Slavnov-Taylor Identities

STIs are obtained by functional differentiation of the STI functional of Eq. (3.30) with respect to suitable combinations of fields chosen following the rules discussed in Section III C.

1. STIs for quark proper vertices

We begin by deriving the STI satisfied by the trilinear quark-gluon vertex (see, *e.g.*, [4, 33]). From our general discussion of Section III C, for obtaining this identity we need to consider the functional differentiation

$$\left. \frac{\delta^3 \mathcal{S}(\Gamma)}{\delta c^a(q) \delta \psi(p_2) \delta \bar{\psi}(-p_1)} \right|_{\Phi, \Phi^*=0} = 0 \quad q + p_2 = p_1, \quad (\text{D.1})$$

from which we obtain the equation

$$\Gamma_{c^a A_d^{*\gamma}}(-q) \Gamma_{A_d^q \psi \bar{\psi}}(p_2, -p_1) + \Gamma_{\psi^* \bar{\psi} c^m}(-p_1, q) \Gamma_{\psi \bar{\psi}}(p_2) + \Gamma_{\psi \bar{\psi}}(p_1) \Gamma_{\psi c^m \bar{\psi}^*}(q, -p_1) = 0, \quad (\text{D.2})$$

where the two-point function $\Gamma_{\psi \bar{\psi}}(p)$ is defined through the identity

$$iS(p) \Gamma_{\psi \bar{\psi}}(p) = \mathbb{I}. \quad (\text{D.3})$$

Using then the relation of Eq. (C.4), we get the STI in its final form, namely

$$q^\alpha \Gamma_{A_\alpha^a \psi \bar{\psi}}(p_2, -p_1) = [q^2 D^{aa'}(q)] \left\{ \Gamma_{\psi^* \bar{\psi} c^{a'}}(-p_1, q) \Gamma_{\psi \bar{\psi}}(p_2) + \Gamma_{\psi \bar{\psi}}(p_1) \Gamma_{\psi c^{a'} \bar{\psi}^*}(q, -p_1) \right\}. \quad (\text{D.4})$$

The three-point auxiliary functions appearing in the equation above can be constructed using the Feynman rules reported in Appendix F. At tree-level the above identity can be trivially checked, with the rhs being proportional to two inverse quark propagators

$$\begin{aligned} q^\alpha \Gamma_{A_\alpha^a \psi \bar{\psi}}^{(0)}(p_2, -p_1) &= [q^2 D^{aa'}(q)]^{(0)} \left\{ \Gamma_{\psi^* \bar{\psi} c^{a'}}^{(0)}(-p_1, q) \Gamma_{\psi \bar{\psi}}^{(0)}(p_2) + \Gamma_{\psi \bar{\psi}}^{(0)}(p_1) \Gamma_{\psi c^{a'} \bar{\psi}^*}^{(0)}(q, -p_1) \right\} \\ &= g t^a [(\not{p}_1 - m) - (\not{p}_2 - m)]. \end{aligned} \quad (\text{D.5})$$

Contrary to the case of QED, where this generalizes directly to all orders, in the QCD case it is valid only to lowest order, due to the non-linearity of Eq. (D.4).

The STI satisfied by the quadrilinear quark-gluon vertex (induced beyond tree-level) can be derived by considering the following functional differentiation

$$\left. \frac{\delta^4 \mathcal{S}(\Gamma)}{\delta c^m(k_1) \delta A_\nu^n(k_2) \delta \psi(p_2) \delta \bar{\psi}(-p_1)} \right|_{\Phi, \Phi^*=0} = 0 \quad k_1 + k_2 + p_2 = p_1. \quad (\text{D.6})$$

Carrying out the functional differentiation and using again Eq. (C.4), we get

$$\begin{aligned} k_1^\mu \Gamma_{A_\mu^m A_\nu^n \psi \bar{\psi}}(k_2, p_2, -p_1) &= [k_1^2 D^{mm'}(k_1)] \left\{ \Gamma_{\psi^* \bar{\psi} c^{m'}}(-p_1, k_1) \Gamma_{A_\nu^n \psi \bar{\psi}}(p_2, -p_2 - k_2) \right. \\ &\quad + \Gamma_{A_\nu^n \psi \bar{\psi}}(p_1 - k_2, -p_1) \Gamma_{\psi c^{m'} \bar{\psi}^*}(k_1, -p_2 - k_1) + \Gamma_{c^{m'} A_\nu^n A_d^{*\gamma}}(k_2, -k_1 - k_2) \Gamma_{A_d^d \psi \bar{\psi}}(p_2, -p_1) \\ &\quad + \Gamma_{A_\nu^n \psi^* \bar{\psi} c^{m'}}(p_2, -p_1, k_1) \Gamma_{\psi \bar{\psi}}(p_2) + \Gamma_{\psi \bar{\psi}}(p_1) \Gamma_{A_\nu^n \psi c^{m'} \bar{\psi}^*}(p_2, k_1, p_1) \\ &\quad \left. + \Gamma_{c^{m'} A_d^{*\gamma} \psi \bar{\psi}}(k_2, p_2, -p_1) \Gamma_{A_\gamma^d A_\nu^n}(k_2) \right\}. \end{aligned} \quad (\text{D.7})$$

Clearly this identity starts at the one-loop level (recall that Γ s represent 1PI functions).

2. STIs for gluon proper vertices

Let us start by deriving the well-known STI for the trilinear gluon vertex [4, 31, 33]. By considering the functional differentiation

$$\left. \frac{\delta^3 \mathcal{S}(\Gamma)}{\delta c^a(q) \delta A_\mu^m(k_1) \delta A_\nu^n(k_2)} \right|_{\Phi, \Phi^*=0} = 0 \quad q + k_1 + k_2 = 0, \quad (\text{D.8})$$

and using Eq. (C.4) one obtains

$$q^\alpha \Gamma_{A_\alpha^a A_\mu^m A_\nu^n}(k_1, k_2) = [q^2 D^{aa'}(q)] \left\{ \Gamma_{c^{a'} A_\nu^n A_d^{*\gamma}}(k_2, k_1) \Gamma_{A_\gamma^d A_\mu^m}(k_1) + \Gamma_{c^{a'} A_\mu^m A_d^{*\gamma}}(k_1, k_2) \Gamma_{A_\gamma^d A_\nu^n}(k_2) \right\}. \quad (\text{D.9})$$

Notice that since we are working with the minimal action (see subsection III C), one has

$$\Gamma_{A_\alpha^a A_\beta^b}^{(0)}(q) = iq^2 \delta^{ab} P_{\alpha\beta}(q), \quad (\text{D.10})$$

and therefore

$$\begin{aligned} \Gamma_{A_\alpha^a A_\beta^b}(q) &= (\Delta^{-1})_{\alpha\beta}^{ab}(q) - i\delta^{ab} q_\alpha q_\beta \\ &= i\delta^{ab} P_{\alpha\beta}(q) \Delta^{-1}(q^2). \end{aligned} \quad (\text{D.11})$$

As an overall consistency check of our definitions and conventions, notice that Eq.s (2.7) and (D.11) imply that $-\Gamma_{A_\alpha^a A_\beta^b}(q) = \delta^{ab} \Pi_{\alpha\beta}(q)$, in full agreement with Eq. (3.18). Using the above relation, we can now check the identity at tree-level; we get

$$\begin{aligned} q^\alpha \Gamma_{A_\alpha^a A_\mu^m A_\nu^n}^{(0)}(k_1, k_2) &= [q^2 D^{aa'}(q)]^{(0)} \left\{ \Gamma_{c^{a'} A_\nu^n A_d^{*\gamma}}^{(0)}(k_2, k_1) \Gamma_{A_\gamma^d A_\mu^m}^{(0)}(k_1) \right. \\ &\quad \left. + \Gamma_{c^{a'} A_\mu^m A_d^{*\gamma}}^{(0)}(k_1, k_2) \Gamma_{A_\gamma^d A_\nu^n}^{(0)}(k_2) \right\} \\ &= igf^{amn} [(g_{\mu\nu} k_1^2 - k_{1\mu} k_{1\nu}) - (g_{\mu\nu} k_2^2 - k_{2\mu} k_{2\nu})]. \end{aligned} \quad (\text{D.12})$$

Notice also that Eq. (D.11) allows us to compare the STI of Eq. (D.9) with that of Eq. (2.10), which is written in the conventional formalism; in this way we get the identity (factoring out the color structure)

$$H_{\mu\gamma}(k_1, k_2) = \Gamma_{c A_\mu A_\gamma^*}(k_1, k_2). \quad (\text{D.13})$$

We pause here to show what would have happened had we worked with the complete generating functional. In this case, due to the extra term appearing in the master equation (3.27) satisfied by the complete action, the differentiation carried out in Eq. (D.8) would generate two more terms with respect to the ones already appearing in Eq. (D.9), namely

$$\delta^{dn} k_{2\nu} \Gamma_{c^a A_\mu^m \bar{c}^d}(k_1, k_2) + \delta^{dm} k_{2\mu} \Gamma_{c^a A_\nu^n \bar{c}^d}(k_2, k_1). \quad (\text{D.14})$$

To get to the terms above we have used the equation of motion of the Nakanishi-Lautrup multiplier B eliminating the latter in favor of the corresponding gauge-fixing function \mathcal{F} . Then, making use of the FPE (C.5), we get

$$-i\delta^{dn} k_{2\nu} k_{2\gamma} \Gamma_{c^a A_\mu^m A_d^{*\gamma}}(k_1, k_2) - i\delta^{dm} k_{1\mu} k_{1\gamma} \Gamma_{c^a A_\nu^n A_d^{*\gamma}}(k_2, k_1), \quad (\text{D.15})$$

so that we finally would get the STI

$$\begin{aligned} q^\alpha \Gamma_{A_\alpha^a A_\mu^m A_\nu^n}(k_1, k_2) &= [q^2 D^{aa'}(q)] \left\{ \Gamma_{c^{a'} A_\nu^n A_d^{*\gamma}}(k_2, k_1) \left[\Gamma_{A_\gamma^d A_\mu^m}^C(k_1) - i\delta^{dm} k_{1\mu} k_{1\gamma} \right] \right. \\ &\quad \left. + \Gamma_{c^{a'} A_\mu^m A_d^{*\gamma}}(k_1, k_2) \left[\Gamma_{A_\gamma^d A_\nu^n}^C(k_2) - i\delta^{dn} k_{2\gamma} k_{2\nu} \right] \right\}, \end{aligned} \quad (\text{D.16})$$

where we have indicated explicitly that the two-point functions are to be evaluated from the completed functional (for the three point functions appearing in the STI above there is no difference). We then see that the difference amounts to a tree-level piece appearing in the two-point function, as has been anticipated in our general discussion of subsection III C (recall that we are using the Feynman gauge $\xi = 1$). In particular notice that we correctly find the relation $\Gamma_{A_\alpha^a A_\beta^b}^C(q) = (\Delta^{-1})_{\alpha\beta}^{ab}(q)$.

Another STI that will be needed in the PT construction is the one involving the quadri-linear gluon vertex; carrying out the functional differentiation

$$\left. \frac{\delta^4 \mathcal{S}(\Gamma)}{\delta c^{m'}(k_1) \delta A_\nu^n(k_2) \delta A_\rho^r(p_2) \delta A_\sigma^s(-p_1)} \right|_{\Phi, \Phi^* = 0} = 0 \quad k_1 + k_2 + p_2 = p_1, \quad (\text{D.17})$$

and using Eq. (C.4), we arrive at the result

$$\begin{aligned} k_1^\mu \Gamma_{A_\mu^m A_\nu^n A_\rho^r A_\sigma^s}(k_2, p_2, -p_1) &= [k_1^2 D^{mm'}(k_1)] \left\{ \Gamma_{c^{m'} A_\sigma^s A_d^{*\gamma}}(-p_1, k_2 + p_2) \Gamma_{A_\gamma^d A_\nu^n A_\rho^r}(k_2, p_2) \right. \\ &+ \Gamma_{c^{m'} A_\rho^r A_d^{*\gamma}}(p_2, k_2 - p_1) \Gamma_{A_\gamma^d A_\nu^n A_\sigma^s}(k_2, -p_1) + \Gamma_{c^{m'} A_\nu^n A_d^{*\gamma}}(k_2, p_2 - p_1) \Gamma_{A_\gamma^d A_\rho^r A_\sigma^s}(p_2, -p_1) \\ &+ \Gamma_{c^{m'} A_\rho^r A_\sigma^s A_d^{*\gamma}}(p_2, -p_1, k_2) \Gamma_{A_\gamma^d A_\nu^n}(k_2) + \Gamma_{c^{m'} A_\nu^n A_\sigma^s A_d^{*\gamma}}(k_2, -p_1, p_2) \Gamma_{A_\gamma^d A_\rho^r}(p_2) \\ &\left. + \Gamma_{c^{m'} A_\nu^n A_\rho^r A_d^{*\gamma}}(k_2, p_2, -p_1) \Gamma_{A_\gamma^d A_\sigma^s}(p_1) \right\}. \end{aligned} \quad (\text{D.18})$$

At tree-level, notice that only the first two lines of this identity are different from zero; then, using the Jacobi identity, we obtain

$$\begin{aligned} k_1^\mu \Gamma_{A_\mu^m A_\nu^n A_\rho^r A_\sigma^s}^{(0)}(k_2, p_2, -p_1) &= [k_1^2 D^{mm'}(k_1)]^{(0)} \left\{ \Gamma_{c^{m'} A_\sigma^s A_d^{*\gamma}}^{(0)}(-p_1, k_2 + p_2) \Gamma_{A_\gamma^d A_\nu^n A_\rho^r}^{(0)}(k_2, p_2) \right. \\ &+ \Gamma_{c^{m'} A_\rho^r A_d^{*\gamma}}^{(0)}(p_2, k_2 - p_1) \Gamma_{A_\gamma^d A_\nu^n A_\sigma^s}^{(0)}(k_2, -p_1) \\ &\left. + \Gamma_{c^{m'} A_\nu^n A_d^{*\gamma}}^{(0)}(k_2, p_2 - p_1) \Gamma_{A_\gamma^d A_\rho^r A_\sigma^s}^{(0)}(p_2, -p_1) \right\} \\ &= -i g^2 \left\{ f^{mse} f^{ern} (g_{\nu\sigma} k_{1\rho} - g_{\rho\sigma} k_{1\nu}) + f^{mre} f^{esn} (g_{\nu\rho} k_{1\sigma} - g_{\rho\sigma} k_{1\nu}) \right. \\ &\left. + f^{mne} f^{esr} (g_{\nu\rho} k_{1\sigma} - g_{\nu\sigma} k_{1\rho}) \right\}. \end{aligned} \quad (\text{D.19})$$

3. STIs for mixed quantum/background Green's functions

Let us consider a Green's function involving background as well as quantum fields. Clearly, when contracting such a function with the momentum corresponding to a background leg it will satisfy a linear WI [see, *e.g.*, Eq.s (2.37) – (2.40)], whereas when contracting it with the momentum corresponding to a quantum leg it will satisfy a non-linear STI.

Let us then study the particularly interesting case of the STI satisfied by the vertex $\Gamma_{\widehat{AA}}$ when contracted with the momentum of one of the quantum fields. Taking the functional differentiation

$$\left. \frac{\delta^3 \mathcal{S}'(\Gamma')}{\delta c^m(k_1) \delta \widehat{A}_\alpha^a(q) \delta A_\nu^n(k_2)} \right|_{\Phi, \Phi^*, \Omega=0} = 0 \quad q + k_1 + k_2 = 0, \quad (\text{D.20})$$

we get

$$k_1^\mu \Gamma_{\widehat{A}_\alpha^a A_\mu^m A_\nu^n}(k_1, k_2) = [k_1^2 D^{mm'}(k_1)] \left\{ \Gamma_{c^{m'} A_\nu^n A_\epsilon^{*e}}(k_2, q) \Gamma_{\widehat{A}_\alpha^a A_\epsilon^e}(q) + \Gamma_{c^{m'} \widehat{A}_\alpha^a A_\epsilon^{*e}}(q, k_2) \Gamma_{A_\epsilon^e A_\nu^n}(k_2) \right\}. \quad (\text{D.21})$$

Notice that the same result can be achieved by contracting directly the BQI of Eq. (E.24) with the momentum of one of the quantum fields and then using the STI of Eq. (D.9) together with the BQIs of Eq.s(E.2) and (E.26) to bring the result in the above form.

It is particularly important to correctly identify in the above identity the missing tree-level contributions (due to the use of the reduced functional, see also the discussion in Section E2). In order to do that, one can either work with the complete functional and use the FPE (C.8), or add them by hand using Eq. (E.24), obtaining in either cases the STI

$$k_1^\mu \Gamma_{\widehat{A}_\alpha^a A_\mu^m A_\nu^n}(k_1, k_2) = [k_1^2 D^{mm'}(k_1)] \left\{ \Gamma_{c^{m'} A_\nu^n A_\epsilon^{*e}}(k_2, q) \Gamma_{\widehat{A}_\alpha^a A_\epsilon^e}(q) + \Gamma_{c^{m'} \widehat{A}_\alpha^a A_\epsilon^{*e}}(q, k_2) \Gamma_{A_\epsilon^e A_\nu^n}(k_2) \right\} - ig f^{amn} (k_1^2 g_{\alpha\nu} - k_{1\alpha} k_{2\nu}). \quad (\text{D.22})$$

This STI can be further manipulate by using Eq. (D.11) and the FPE (C.8) for rewriting the term proportional to $\Gamma_{AA}(k_2)$ as

$$\begin{aligned} \Gamma_{c^{m'} \widehat{A}_\alpha^a A_\epsilon^{*e}}(q, k_2) \Gamma_{A_\epsilon^e A_\nu^n}(k_2) &= \Gamma_{c^{m'} \widehat{A}_\alpha^a A_\epsilon^{*e}}(q, k_2) (\Delta^{-1})_{c\nu}^{en}(k_2) + k_{2\nu} \Gamma_{c^{m'} \widehat{A}_\alpha^a \bar{c}^n}(q, k_2) \\ &+ ig f^{aen} k_{2\nu} \Gamma_{c^{m'} A_\alpha^{*e}}(-k_1). \end{aligned} \quad (\text{D.23})$$

On the other hand, employing Eq. (C.4) we find

$$[k_1^2 D^{mm'}(k_1)] (ig f^{nae} k_{2\nu}) \Gamma_{c^{m'} A_\alpha^{*e}}(-k_1) = -ig f^{amn} k_{1\alpha} k_{2\nu}; \quad (\text{D.24})$$

so, inserting Eq. (D.23) back into Eq. (D.22) we see that the term above partially cancels the tree level contribution, thus leaving us with the STI

$$k_1^\mu \Gamma_{\widehat{A}_\alpha^a A_\mu^m A_\nu^n}(k_1, k_2) = [k_1^2 D^{mm'}(k_1)] \left\{ \Gamma_{c^{m'} A_\nu^n A_\epsilon^{*e}}(k_2, q) \Gamma_{\widehat{A}_\alpha^a A_\epsilon^e}(q) + \Gamma_{c^{m'} \widehat{A}_\alpha^a A_\epsilon^{*e}}(q, k_2) (\Delta^{-1})_{c\nu}^{en}(k_2) + k_{2\nu} \Gamma_{c^{m'} \widehat{A}_\alpha^a \bar{c}^n}(q, k_2) \right\} - ig f^{amn} k_1^2 g_{\alpha\nu}. \quad (\text{D.25})$$

4. STIs for the quark SD kernel

In addition to the STIs for 1PI (proper) vertices, the PT construction for SDEs requires the additional knowledge of the result of the action of longitudinal momenta on connected kernels. The first one of these kernels is encountered in the construction of the PT gluon-quark-quark vertex, and can be written as follows (see Fig. 11)

$$\begin{aligned}\mathcal{K}_{A_\mu^m A_\nu^n \psi \bar{\psi}}(k_2, p_2, -p_1) &= \Gamma_{A_\mu^m A_\nu^n \psi \bar{\psi}}(k_2, p_2, -p_1) \\ &+ i\Gamma_{A_\mu^m \psi \bar{\psi}}(\ell, -p_1) iS(\ell) i\Gamma_{A_\nu^n \psi \bar{\psi}}(p_2, -\ell) \\ &+ i\Gamma_{A_\nu^n \psi \bar{\psi}}(\ell', -p_1) iS(\ell') i\Gamma_{A_\mu^m \psi \bar{\psi}}(p_2, -\ell').\end{aligned}\quad (\text{D.26})$$

where $\ell = k_2 + p_2 = p_1 - k_1$ and $\ell' = k_1 + p_2 = p_1 - k_2$. Then, using the STI of Eq. (D.4) and the relation (D.3), one gets the results

$$\begin{aligned}k_1^\mu i\Gamma_{A_\mu^m \psi \bar{\psi}}(\ell, -p_1) iS(\ell) i\Gamma_{A_\nu^n \psi \bar{\psi}}(p_2, -\ell) &= -[k_1^2 D^{mm'}(k_1)] \{ \Gamma_{\psi^* \bar{\psi} c^{m'}}(-p_1, k_1) \\ &+ i\Gamma_{\psi \bar{\psi}}(p_1) \Gamma_{\psi c^{m'} \bar{\psi}^*}(k_1, -p_1) S(\ell) \} \Gamma_{A_\nu^n \psi \bar{\psi}}(p_2, -\ell),\end{aligned}\quad (\text{D.27})$$

$$\begin{aligned}k_1^\mu i\Gamma_{A_\nu^n \psi \bar{\psi}}(\ell', -p_1) iS(\ell') i\Gamma_{A_\mu^m \psi \bar{\psi}}(p_2, -\ell') &= -\Gamma_{A_\nu^n \psi \bar{\psi}}(\ell', -p_1) [k_1^2 D^{mm'}(k_1)] \{ \Gamma_{\psi c^{m'} \bar{\psi}^*}(k_1, -\ell') \\ &+ iS(\ell') \Gamma_{\psi^* \bar{\psi} c^{m'}}(-\ell', k_1) \Gamma_{\psi \bar{\psi}}(p_2) \}.\end{aligned}\quad (\text{D.28})$$

We then see that the first term in Eq.s (D.27) and (D.28) will cancel the first two terms of the STI of the 1PI vertex of Eq. (D.7), and we finally arrive at the STI

$$\begin{aligned}k_1^\mu \mathcal{K}_{A_\mu^m A_\nu^n \psi \bar{\psi}}(k_2, p_2, -p_1) &= [k_1^2 D^{mm'}(k_1)] \left\{ \Gamma_{c^{m'} A_\nu^n A_d^{*\gamma}}(k_2, -k_1 - k_2) \Gamma_{A_\nu^n \psi \bar{\psi}}(p_2, -p_1) \right. \\ &+ \Gamma_{\psi \bar{\psi}}(p_1) \mathcal{K}_{A_\nu^n \psi c^{m'} \bar{\psi}^*}(p_2, k_1, -p_1) + \mathcal{K}_{A_\nu^n \psi^* \bar{\psi} c^{m'}}(p_2, -p_1, k_1) \Gamma_{\psi \bar{\psi}}(p_2) \\ &\left. + \Gamma_{c^{m'} A_d^{*\gamma} \psi \bar{\psi}}(k_2, p_2, -p_1) \Gamma_{A_\nu^n A_\nu^n}(k_2) \right\},\end{aligned}\quad (\text{D.29})$$

where we have defined the auxiliary kernels

$$\begin{aligned}\mathcal{K}_{A_\nu^n \psi c^{m'} \bar{\psi}^*}(p_2, k_1, -p_1) &= \Gamma_{A_\nu^n \psi c^{m'} \bar{\psi}^*}(p_2, k_1, -p_1) \\ &+ i\Gamma_{\psi c^{m'} \bar{\psi}^*}(k_1, -p_1) iS(\ell) i\Gamma_{A_\nu^n \psi \bar{\psi}}(p_2, -\ell),\end{aligned}\quad (\text{D.30})$$

$$\begin{aligned}\mathcal{K}_{A_\nu^n \psi^* \bar{\psi} c^{m'}}(p_2, -p_1, k_1) &= \Gamma_{A_\nu^n \psi^* \bar{\psi} c^{m'}}(p_2, -p_1, k_1) \\ &+ i\Gamma_{A_\nu^n \psi \bar{\psi}}(\ell, -p_1) iS(\ell) i\Gamma_{\psi^* \bar{\psi} c^{m'}}(-\ell, k_1).\end{aligned}\quad (\text{D.31})$$

5. STIs for the gluon SD kernel

In the construction of the SDEs for the gluon self-energy and three-gluon vertex, one needs the knowledge of the STI satisfied by the kernel (see Fig. 15)

$$\begin{aligned}
\mathcal{K}_{A_\mu^m A_\nu^p A_\rho^r A_\sigma^s}(k_2, p_2, -p_1) &= \Gamma_{A_\mu^m A_\nu^p A_\rho^r A_\sigma^s}(k_2, p_2, -p_1) \\
&+ i\Gamma_{A_\sigma^s A_\mu^m A_\epsilon^e}(k_1, \ell) i\Delta_{e\epsilon'}^{\epsilon\epsilon'}(\ell) i\Gamma_{A_{\epsilon'}^{e'} A_\nu^p A_\rho^r}(k_2, p_2) \\
&+ i\Gamma_{A_\sigma^s A_\nu^p A_\epsilon^e}(k_2, \ell') i\Delta_{e\epsilon'}^{\epsilon\epsilon'}(\ell') i\Gamma_{A_{\epsilon'}^{e'} A_\mu^m A_\rho^r}(k_1, p_2). \quad (\text{D.32})
\end{aligned}$$

Using the above relation, together with STI of Eq. (D.9), we find the following result

$$\begin{aligned}
k_1^\mu i\Gamma_{A_\sigma^s A_\mu^m A_\epsilon^e}(k_1, \ell) i\Delta_{e\epsilon'}^{\epsilon\epsilon'}(\ell) i\Gamma_{A_{\epsilon'}^{e'} A_\nu^p A_\rho^r}(k_2, p_2) &= -[k_1^2 D^{mm'}(k_1)] \times \\
&\times \left\{ \Gamma_{c^{m'} A_\sigma^s A_\epsilon^{*e'}}(-p_1, \ell) P^{\epsilon\epsilon'}(\ell) + i\Gamma_{c^{m'} A_\epsilon^e A_d^{*\gamma}}(\ell, -p_1) \Gamma_{A_\gamma^d A_\sigma^s}(p_1) \Delta_{e\epsilon'}^{\epsilon\epsilon'}(\ell) \right\} \Gamma_{A_{\epsilon'}^{e'} A_\nu^p A_\rho^r}(k_2, p_2). \quad (\text{D.33})
\end{aligned}$$

In this case this is, however, not the end of the story, since the first term in the equation above still contains (virtual) longitudinal momenta, which will trigger the STI of Eq. (D.9) together with the FPE (C.5). After taking this into account, we obtain

$$\begin{aligned}
k_1^\mu i\Gamma_{A_\sigma^s A_\mu^m A_\epsilon^e}(k_1, \ell) i\Delta_{e\epsilon'}^{\epsilon\epsilon'}(\ell) i\Gamma_{A_{\epsilon'}^{e'} A_\nu^p A_\rho^r}(k_2, p_2) &= -[k_1^2 D^{mm'}(k_1)] \times \\
&\times \left\{ \left[\Gamma_{c^{m'} A_\sigma^s A_\epsilon^{*e'}}(-p_1, \ell) + i\Gamma_{c^{m'} A_\epsilon^e A_d^{*\gamma}}(\ell, -p_1) \Gamma_{A_\gamma^d A_\sigma^s}(p_1) \Delta_{e\epsilon'}^{\epsilon\epsilon'}(\ell) \right] \Gamma_{A_{\epsilon'}^{e'} A_\nu^p A_\rho^r}(k_2, p_2) \right. \\
&\left. + i\Gamma_{c^{m'} A_\sigma^s \bar{c}^e}(-p_1, \ell) D^{e\epsilon'}(\ell) \left[\Gamma_{c^{e'} A_\rho^r A_d^{*\gamma}}(p_2, k_2) \Gamma_{A_\gamma^d A_\nu^p}(k_2) + \Gamma_{c^{e'} A_\nu^p A_d^{*\gamma}}(k_2, p_2) \Gamma_{A_\gamma^d A_\rho^r}(p_2) \right] \right\}. \quad (\text{D.34})
\end{aligned}$$

Similarly we find

$$\begin{aligned}
k_1^\mu i\Gamma_{A_\sigma^s A_\nu^p A_\epsilon^e}(k_2, \ell') i\Delta_{e\epsilon'}^{\epsilon\epsilon'}(\ell') i\Gamma_{A_{\epsilon'}^{e'} A_\mu^m A_\rho^r}(k_1, p_2) &= -[k_1^2 D^{mm'}(k_1)] \times \\
&\times \left\{ \Gamma_{A_\sigma^s A_\nu^p A_\epsilon^e}(k_2, \ell') \left[\Gamma_{c^{m'} A_\rho^r A_\epsilon^{*e}}(p_2, -\ell') + i\Delta_{e\epsilon'}^{\epsilon\epsilon'}(\ell') \Gamma_{c^{m'} A_{\epsilon'}^{e'} A_d^{*\gamma}}(-\ell', p_2) \Gamma_{A_\gamma^d A_\rho^r}(p_2) \right] \right. \\
&+ iD^{e\epsilon'}(\ell') \left[\Gamma_{c^e A_\nu^p A_d^{*\gamma}}(k_2, -p_1) \Gamma_{A_\gamma^d A_\sigma^s}(p_1) + \Gamma_{c^e A_\sigma^s A_d^{*\gamma}}(-p_1, k_2) \Gamma_{A_\gamma^d A_\nu^p}(k_2) \right] \\
&\left. \times \Gamma_{c^{m'} A_\rho^r \bar{c}^{e'}}(p_2, -\ell') \right\}. \quad (\text{D.35})
\end{aligned}$$

As before, after combining these results with the four-gluon 1PI vertex STI of Eq. (D.18) we arrive at the needed STI for the four-gluon SD kernel, namely

$$k_1^\mu \mathcal{K}_{A_\mu^m A_\nu^p A_\rho^r A_\sigma^s}(k_2, p_2, -p_1) = [k_1^2 D^{mm'}(k_1)] \left\{ \Gamma_{c^{m'} A_\nu^p A_d^{*\gamma}}(k_2, -k_1 - k_2) \Gamma_{A_\gamma^d A_\rho^r A_\sigma^s}(p_2, -p_1) \right.$$

$$\begin{aligned}
& + \mathcal{K}_{c^{m'} A_\nu^r A_\sigma^s A_d^{*\gamma}}(k_2, -p_1, p_2) \Gamma_{A_\gamma^d A_\rho^r}(p_2) \\
& + \mathcal{K}_{c^{m'} A_\nu^r A_\rho^r A_d^{*\gamma}}(k_2, p_2, -p_1) \Gamma_{A_\gamma^d A_\sigma^s}(p_1) \\
& + \mathcal{K}_{c^{m'} A_\rho^r A_\sigma^s A_d^{*\gamma}}(p_2, -p_1, k_2) \Gamma_{A_\gamma^d A_\nu^r}(k_2) \Big\}, \tag{D.36}
\end{aligned}$$

where the following auxiliary kernels have been defined

$$\begin{aligned}
\mathcal{K}_{c^{m'} A_\nu^r A_\sigma^s A_d^{*\gamma}}(k_2, -p_1, p_2) &= \Gamma_{c^{m'} A_\nu^r A_\sigma^s A_d^{*\gamma}}(k_2, -p_1, p_2) \\
&+ i \Gamma_{A_\sigma^s A_\nu^r A_\epsilon^e}(k_2, \ell') i \Delta_{e\epsilon'}^{\epsilon\epsilon'}(\ell') i \Gamma_{c^{m'} A_{\epsilon'}^e A_d^{*\gamma}}(-\ell', p_2) \\
&+ i \Gamma_{c^{m'} A_\sigma^s \bar{c}^e}(-p_1, \ell) i D^{e\epsilon'}(\ell) i \Gamma_{c^{e'} A_\nu^r A_d^{*\gamma}}(k_2, p_2), \tag{D.37}
\end{aligned}$$

$$\begin{aligned}
\mathcal{K}_{c^{m'} A_\nu^r A_\rho^r A_d^{*\gamma}}(k_2, p_2, -p_1) &= \Gamma_{c^{m'} A_\nu^r A_\rho^r A_d^{*\gamma}}(k_2, p_2, -p_1) \\
&+ i \Gamma_{c^{m'} A_\epsilon^e A_d^{*\gamma}}(\ell, -p_1) i \Delta_{e\epsilon'}^{\epsilon\epsilon'}(\ell) i \Gamma_{A_{\epsilon'}^e A_\rho^r A_\nu^r}(k_2, p_2) \\
&+ i \Gamma_{c^e A_\nu^r A_d^{*\gamma}}(k_2, -p_1) i D^{e\epsilon'}(\ell') i \Gamma_{c^{m'} A_\rho^r \bar{c}^{e'}}(p_2, -\ell'), \tag{D.38}
\end{aligned}$$

$$\begin{aligned}
\mathcal{K}_{c^{m'} A_\rho^r A_\sigma^s A_d^{*\gamma}}(p_2, -p_1, k_2) &= \Gamma_{c^{m'} A_\rho^r A_\sigma^s A_d^{*\gamma}}(p_2, -p_1, k_2) \\
&+ i \Gamma_{c^{m'} A_\sigma^s \bar{c}^{e'}}(-p_1, \ell) i D^{e\epsilon'}(\ell) i \Gamma_{c^{e'} A_\rho^r A_d^{*\gamma}}(p_2, k_2) \\
&+ i \Gamma_{c^e A_\sigma^s A_d^{*\gamma}}(-p_1, k_2) i D^{e\epsilon'}(\ell') i \Gamma_{c^{m'} A_\rho^r \bar{c}^{e'}}(p_2, -\ell'). \tag{D.39}
\end{aligned}$$

Appendix E: Background-Quantum Identities

BQIs are obtained by functional differentiation of the STI functional of Eq. (3.32) with respect to combinations of background fields, quantum fields and background sources.

1. BQIs for two-point functions

The first BQI we can construct is the one relating the conventional with the BFM gluon self-energies. To this end, consider the following functional differentiation

$$\begin{aligned}
\left. \frac{\delta^2 \mathcal{S}'(\Gamma')}{\delta \Omega_\alpha^a(p) \delta A_\beta^b(q)} \right|_{\Phi, \Phi^*, \Omega=0} &= 0 \quad q + p = 0, \\
\left. \frac{\delta^2 \mathcal{S}'(\Gamma')}{\delta \Omega_\alpha^a(p) \delta \widehat{A}_\beta^b(q)} \right|_{\Phi, \Phi^*, \Omega=0} &= 0 \quad q + p = 0, \tag{E.1}
\end{aligned}$$

which will give the relations

$$i \Gamma_{\widehat{A}_\alpha^a A_\beta^b}(q) = \left[i g_\alpha^\gamma \delta^{ad} + \Gamma_{\Omega_\alpha^a A_d^{*\gamma}}(q) \right] \Gamma_{A_\gamma^d A_\beta^b}(q), \tag{E.2}$$

$$i \Gamma_{\widehat{A}_\alpha^a \widehat{A}_\beta^b}(q) = \left[i g_\alpha^\gamma \delta^{ad} + \Gamma_{\Omega_\alpha^a A_d^{*\gamma}}(q) \right] \Gamma_{A_\gamma^d \widehat{A}_\beta^b}(q). \tag{E.3}$$

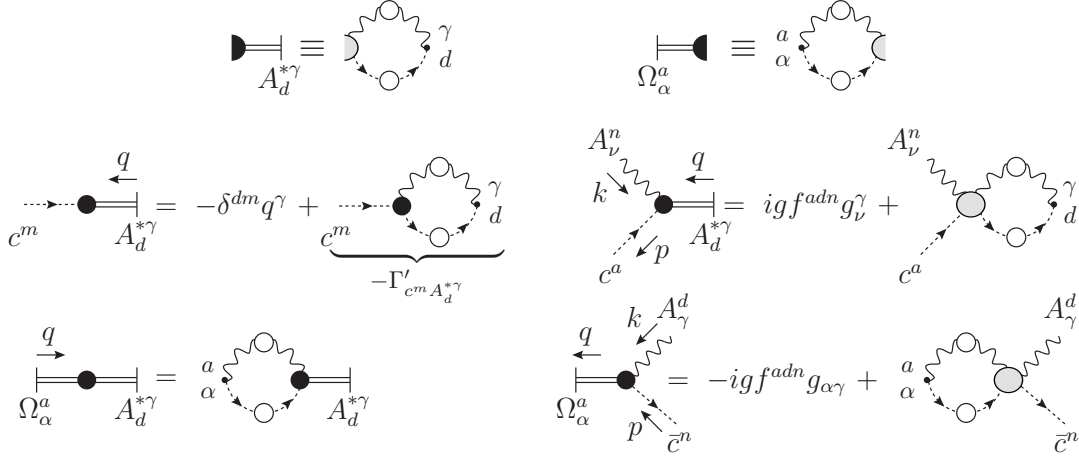


FIG. 24: Expansions of the gluon anti-field and BFM source in terms of the corresponding composite operators. Notice that if the anti-field or the BFM sources are attached to a 1PI vertex, as shown in the first line, such an expansion will in general convert the 1PI vertex into a (connected) SD kernel. The equivalence shown is therefore not valid at tree-level (*e.g.*, in the case of three-point functions such an equivalence would imply that the kernels shown on the rhs of the corresponding expansions would be disconnected); when present, the tree-level needs to be added by hand, as explicitly shown in the two expansions of the second line and the last one of the third line. This type of expansion allows one to express the terms appearing in the BQIs in a form that reveals kernels appearing in the STIs [see, *e.g.*, Eq.s (E.14), (E.15), (E.18) and (E.19)]

We can now combine Eq.s (E.2) and (E.3) such that the two-point function mixing background and quantum fields drops out, to get the BQI

$$\begin{aligned}
i\Gamma_{\widehat{A}_\alpha^a \widehat{A}_\beta^b}(q) &= i\Gamma_{A_\alpha^a A_\beta^b}(q) + \Gamma_{\Omega_\alpha^a A_d^{*\gamma}}(q)\Gamma_{A_\gamma^d A_\beta^b}(q) + \Gamma_{\Omega_\beta^b A_d^{*\gamma}}(q)\Gamma_{A_\alpha^a A_\gamma^d}(q) \\
&\quad - i\Gamma_{\Omega_\alpha^a A_d^{*\gamma}}(q)\Gamma_{A_\gamma^d A_\epsilon^e}(q)\Gamma_{\Omega_\beta^b A_\epsilon^e}(q) \\
&= i\Gamma_{A_\alpha^a A_\beta^b}(q) + 2\Gamma_{\Omega_\alpha^a A_d^{*\gamma}}(q)\Gamma_{A_\gamma^d A_\beta^b}(q) - i\Gamma_{\Omega_\alpha^a A_d^{*\gamma}}(q)\Gamma_{A_\gamma^d A_\epsilon^e}(q)\Gamma_{\Omega_\beta^b A_\epsilon^e}(q), \quad (\text{E.4})
\end{aligned}$$

where the last identity is due to the transversality of the Γ_{AA} two-point function.

In order for our PT procedure to be self-contained, it is important to express the 1PI auxiliary Green's function involved in the various STIs and the BQIs in terms of kernels that also appear in the relevant STIs. The key observation that makes this possible is that one may always replace an anti-field or BFM source with its corresponding BRST composite

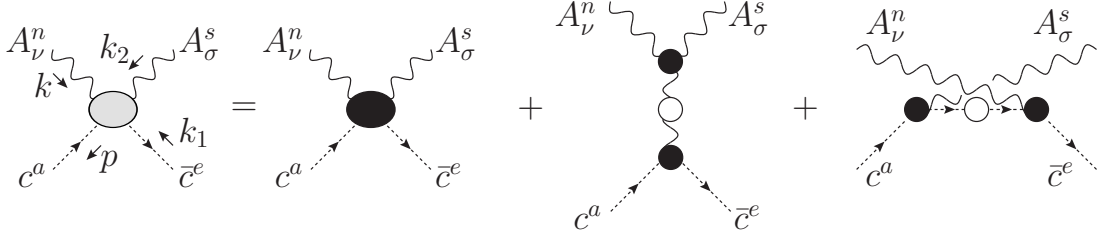


FIG. 25: Skeleton expansion of the kernel appearing in the SDE for the auxiliary function Γ_{cAA^*} .

operator. Thus, for example, one has (see Fig. 24)

$$A_d^{*\gamma}(q) \rightarrow i\Gamma_{c^e A_\nu^n A_d^{*\gamma}}^{(0)} \int_{k_1} i\Delta_{n'n}^{\nu'\nu}(k_2) iD^{e'e}(k_1), \quad (\text{E.5})$$

$$\Omega_\alpha^a(q) \rightarrow i\Gamma_{\Omega_\alpha^a A_\nu^n \bar{c}^e}^{(0)} \int_{k_1} i\Delta_{n'n}^{\nu'\nu}(k_2) iD^{e'e}(k_1), \quad (\text{E.6})$$

where k_1 and k_2 are related through $k_2 = q - k_1$. In this way we get the following SDEs (see again Fig. 24)

$$\begin{aligned} -\Gamma_{c^m A_d^{*\gamma}}(q) &= -\delta^{dm} q_\gamma - \Gamma'_{c^m A_d^{*\gamma}}(q) \\ &= -\delta^{dm} q_\gamma + g f^{dn'e'} g_\nu^\gamma \int_{k_1} D^{e'e}(k_1) \Delta_{\nu'\nu}^{nn'}(k_2) \Gamma_{c^m A_\nu^n \bar{c}^e}(k_2, k_1), \end{aligned} \quad (\text{E.7})$$

$$i\Gamma_{c^a A_\nu^n A_d^{*\gamma}}(k, q) = ig f^{adn} g_\nu^\gamma - ig f^{e'ds'} g_{\sigma'}^\gamma \int_{k_1} D^{e'e}(k_1) \Delta_{ss'}^{\sigma\sigma'}(k_2) \mathcal{K}_{c^a A_\nu^n A_\sigma^s \bar{c}^e}(k, k_2, k_1), \quad (\text{E.8})$$

$$-\Gamma_{\Omega_\alpha^a A_d^{*\gamma}}(q) = g f^{ae'n'} g_{\alpha\nu'} \int_{k_1} D^{e'e}(k_1) \Delta_{n'n}^{\nu'\nu}(k_2) \Gamma_{c^e A_\nu^n A_d^{*\gamma}}(k_2, -q), \quad (\text{E.9})$$

$$i\Gamma_{\Omega_\alpha^a A_\nu^n \bar{c}^e}(k, p) = -ig f^{adn} g_{\alpha\gamma} - ig f^{ae'n'} g_{\alpha\nu'} \int_{k_1} D^{e'e}(k_1) \Delta_{n'n}^{\nu'\nu}(k_2) \mathcal{K}_{c^e A_\nu^n A_\sigma^s \bar{c}^e}(k_2, k, p). \quad (\text{E.10})$$

The kernel $\mathcal{K}_{cAA\bar{c}}$ appearing in the SDEs (E.8) and (E.10) is shown in Fig. 25 and reads

$$\begin{aligned} \mathcal{K}_{c^a A_\nu^n A_\sigma^s \bar{c}^e}(k, k_2, k_1) &= \Gamma_{c^a A_\nu^n A_\sigma^s \bar{c}^e}(k, k_2, k_1) \\ &+ i\Gamma_{A_\nu^n A_\sigma^s A_\rho^r}(k_2, -k - k_2) i\Delta_{rr'}^{\rho\rho'}(k + k_2) i\Gamma_{c^m A_{\rho'}^r \bar{c}^e}(k + k_2, k_1) \\ &+ i\Gamma_{c^a A_\sigma^s \bar{c}^e}(k_2, -k_1 - k_2) iD^{rr'}(k_1 + k_2) i\Gamma_{c^{r'} A_\nu^n \bar{c}^e}(k, k_1). \end{aligned} \quad (\text{E.11})$$

Finally notice that the auxiliary function $\Gamma_{\Omega_\alpha A_\beta^*}$ corresponds precisely to the auxiliary function $\Lambda_{\alpha\beta}$ introduced in Eq. (2.33), and therefore its part proportional to $g_{\alpha\beta}$ corresponds to the scalar function $G(q^2)$.

2. BQIs for three-point functions

The relation between the trilinear quantum gluon-quark vertex and the trilinear background gluon-quark vertex, can be obtained by considering the following functional differentiation

$$\left. \frac{\delta^3 \mathcal{S}'(\Gamma')}{\delta \Omega_\alpha^a(q) \delta \psi(p_2) \delta \bar{\psi}(-p_1)} \right|_{\Phi, \Phi^*, \Omega=0} = 0 \quad q + p_2 = p_1. \quad (\text{E.12})$$

We then get

$$\begin{aligned} i\Gamma_{\widehat{A}_\alpha^a \psi \bar{\psi}}(p_2, -p_1) &= [ig_\alpha^\gamma \delta^{ad} + \Gamma_{\Omega_\alpha^a A_d^{*\gamma}}(-q)] \Gamma_{A_\gamma^d \psi \bar{\psi}}(p_2, -p_1) \\ &+ \Gamma_{\psi^* \bar{\psi} \Omega_\alpha^a}(-p_1, q) \Gamma_{\psi \bar{\psi}}(p_2) + \Gamma_{\psi \bar{\psi}}(p_1) \Gamma_{\psi \Omega_\alpha^a \bar{\psi}^*}(q, -p_1). \end{aligned} \quad (\text{E.13})$$

In order to explore further the all-order structure of these two auxiliary Green's functions, replace the BFM source with the corresponding composite operator using Eq. (E.6), thus obtaining

$$i\Gamma_{\psi \Omega_\alpha^a \bar{\psi}^*}(q, -p_1) = i\Gamma_{\Omega_\alpha^a A_{\nu'}^{\prime} \bar{c}^{m'}}^{(0)} \int_{k_1} iD^{m'm}(k_1) i\Delta_{n'n}^{\nu'\nu}(k_2) \mathcal{K}_{A_{\nu'}^{\prime} \psi c^m \bar{\psi}^*}(p_2, k_1, -p_1), \quad (\text{E.14})$$

$$i\Gamma_{\psi^* \bar{\psi} \Omega_\alpha^a}(-p_1, q) = i\Gamma_{\Omega_\alpha^a A_{\nu'}^{\prime} \bar{c}^{m'}}^{(0)} \int_{k_1} iD^{m'm}(k_1) i\Delta_{n'n}^{\nu'\nu}(k_2) \mathcal{K}_{A_{\nu'}^{\prime} \psi^* \bar{\psi} c^m}(p_2, -p_1, k_1). \quad (\text{E.15})$$

where the kernels $\mathcal{K}_{A_{\nu'}^{\prime} \psi c^m \bar{\psi}^*}$ and $\mathcal{K}_{A_{\nu'}^{\prime} \psi^* \bar{\psi} c^m}$ have been defined in Eq. (D.30) and (D.31). As it is clear from the two equations above, while the (auxiliary) functions appearing in the STIs and BQIs ought to be 1PI (lhs of the equations), that is not true for the kernels appearing after using the substitutions of Eq. (E.5) or (E.6), which, in fact, consist of both 1PI and 1PR diagrams (rhs of the equations).

For the BQI involving the three-gluon vertex a similar result can be obtained; choosing

$$\left. \frac{\delta^3 \mathcal{S}'(\Gamma')}{\delta \Omega_\alpha^a(q) \delta A_\rho^r(p_2) \delta A_\sigma^s(-p_1)} \right|_{\Phi, \Phi^*, \Omega=0} = 0 \quad q + p_2 = p_1, \quad (\text{E.16})$$

we will get

$$\begin{aligned} i\Gamma_{\widehat{A}_\alpha^a A_\rho^r A_\sigma^s}(p_2, -p_1) &= [ig_\alpha^\gamma \delta^{ad} + \Gamma_{\Omega_\alpha^a A_d^{*\gamma}}(-q)] \Gamma_{A_\gamma^d A_\rho^r A_\sigma^s}(p_2, -p_1) \\ &+ \Gamma_{\Omega_\alpha^a A_\sigma^s A_d^{*\gamma}}(-p_1, p_2) \Gamma_{A_\gamma^d A_\rho^r}(p_2) + \Gamma_{\Omega_\alpha^a A_\rho^r A_d^{*\gamma}}(p_2, -p_1) \Gamma_{A_\gamma^d A_\sigma^s}(p_1). \end{aligned} \quad (\text{E.17})$$

Again we can write

$$i\Gamma_{\Omega_\alpha^a A_\sigma^s A_d^{*\gamma}}(-p_1, p_2) = i\Gamma_{\Omega_\alpha^a A_{\nu'}^{\prime} \bar{c}^{m'}}^{(0)} \int_{k_1} iD^{m'm}(k_1) i\Delta_{n'n}^{\nu'\nu}(k_2) \mathcal{K}_{c^m A_{\nu'}^{\prime} A_\sigma^s A_d^{*\gamma}}(k_2, -p_1, p_2), \quad (\text{E.18})$$

$$i\Gamma_{\Omega_\alpha^a A_\rho^r A_d^{*\gamma}}(p_2, -p_1) = i\Gamma_{\Omega_\alpha^a A_{\nu'}^{\prime} \bar{c}^{m'}}^{(0)} \int_{k_1} iD^{m'm}(k_1) i\Delta_{n'n}^{\nu'\nu}(k_2) \mathcal{K}_{c^m A_{\nu'}^{\prime} A_\rho^r A_d^{*\gamma}}(k_2, p_2, -p_1), \quad (\text{E.19})$$

where the kernels appearing in the above equations have been defined in Eq.s (D.37) and (D.38). Notice the emergence of the pattern exploited in the application of the PT to the SDEs of QCD: namely that the auxiliary functions appearing in the BQI satisfied by a particular Green's function can be written in terms of kernels appearing in the STIs triggered when the PT procedure is applied to that same Green's function. The BQI of Eq. (E.17) gives at tree-level the result

$$\Gamma_{\widehat{A}_\alpha^a A_\rho^r A_\sigma^s}(p_2, -p_1) = \Gamma_{A_\alpha^a A_\rho^r A_\sigma^s}(p_2, -p_1). \quad (\text{E.20})$$

This is once again due to the use of the reduced functional: in fact in such case the two (tree-level) vertices need to coincide, since the difference between them is proportional to the inverse of the gauge fixing parameter (see Appendix F) and therefore entirely due to the gauge fixing Lagrangian. To restore the correct tree-level terms one would have to use the complete functional; in that case the differentiation of Eq. (E.16) shows the two additional terms

$$- \delta^{ds} p_{1\sigma} \Gamma_{\Omega_\alpha^a A_\rho^r \bar{c}^d}(p_2, -p_1) + \delta^{dr} p_{2\rho} \Gamma_{\Omega_\alpha^a A_\sigma^s \bar{c}^d}(-p_1, p_2), \quad (\text{E.21})$$

which, with the help of Eq. (C.7) become

$$-i\delta^{ds} p_{1\sigma} p_{1\gamma} \Gamma_{\Omega_\alpha^a A_\rho^r A_d^{*\gamma}}(p_2, -p_1) - i\delta^{dr} p_{2\rho} p_{2\gamma} \Gamma_{\Omega_\alpha^a A_\sigma^s A_d^{*\gamma}}(-p_1, p_2) + g f^{ars} (q_{\alpha\rho} p_{1\sigma} + g_{\alpha\sigma} p_{2\rho}). \quad (\text{E.22})$$

Therefore we get the final identity

$$\begin{aligned} i\Gamma_{\widehat{A}_\alpha^a A_\rho^r A_\sigma^s}^{\text{C}}(p_2, -p_1) &= [i g_\alpha^\gamma \delta^{ad} + \Gamma_{\Omega_\alpha^a A_d^{*\gamma}}(-q)] \Gamma_{A_\gamma^d A_\rho^r A_\sigma^s}(p_2, -p_1) + g f^{ars} (q_{\alpha\rho} p_{1\sigma} + g_{\alpha\sigma} p_{2\rho}) \\ &+ \Gamma_{\Omega_\alpha^a A_\sigma^s A_d^{*\gamma}}(-p_1, p_2) \left[\Gamma_{A_\gamma^d A_\rho^r}^{\text{C}}(p_2) - i\delta^{dr} p_{2\rho} p_{2\gamma} \right] \\ &+ \Gamma_{\Omega_\alpha^a A_\rho^r A_d^{*\gamma}}(p_2, -p_1) \left[\Gamma_{A_\gamma^d A_\sigma^s}^{\text{C}}(p_1) - i\delta^{ds} p_{1\sigma} p_{1\gamma} \right], \end{aligned} \quad (\text{E.23})$$

which gives the expected tree-level result. Once again we see that the difference between working with the reduced and complete functional lies in some constant (tree-level) terms that one recovers after applying the FPE for writing the STI/BQI at hand in the same form using Γ or Γ_{C} . Thus, opting for the fast way of deriving the STI/BQI with the reduced functional and adding the correct tree-level term, we write the BQI in its final form

$$\begin{aligned} i\Gamma_{\widehat{A}_\alpha^a A_\rho^r A_\sigma^s}(p_2, -p_1) &= [i g_\alpha^\gamma \delta^{ad} + \Gamma_{\Omega_\alpha^a A_d^{*\gamma}}(-q)] \Gamma_{A_\gamma^d A_\rho^r A_\sigma^s}(p_2, -p_1) \\ &+ \Gamma_{\Omega_\alpha^a A_\sigma^s A_d^{*\gamma}}(-p_1, p_2) \Gamma_{A_\gamma^d A_\rho^r}(p_2) + \Gamma_{\Omega_\alpha^a A_\rho^r A_d^{*\gamma}}(p_2, -p_1) \Gamma_{A_\gamma^d A_\sigma^s}(p_1) \\ &+ g f^{ars} (p_{2\rho} g_{\alpha\sigma} + p_{1\sigma} g_{\alpha\rho}). \end{aligned} \quad (\text{E.24})$$

3. BQI for the ghost-gluon trilinear vertex

In this section we are going to derive the BQIs relating the R_ξ ghost sector with the BFM ones. We start from the trilinear ghost-gluon coupling, for which we choose the following functional differentiation

$$\left. \frac{\delta^3 \mathcal{S}'(\Gamma')}{\delta \Omega_\alpha^a(-q) \delta c^m(k_1) \delta \bar{c}^n(k_2)} \right|_{\Phi, \Phi^*, \Omega=0} = 0 \quad k_1 + k_2 = q, \quad (\text{E.25})$$

thus getting the result

$$\begin{aligned} i\Gamma_{c^m \hat{A}_\alpha^a \bar{c}^n}(-q, k_2) &= [i\delta^{da} g_\alpha^\gamma + \Gamma_{\Omega_\alpha^a A_d^{*\gamma}}(q)] \Gamma_{c^m A_\gamma^d \bar{c}^n}(-q, k_2) \\ &\quad - \Gamma_{c^m A_d^{*\gamma}}(-k_1) \Gamma_{\Omega_\alpha^a A_\gamma^d \bar{c}^n}(k_1, k_2) - \Gamma_{\Omega_\alpha^a c^m c^{*d}}(k_1, k_2) \Gamma_{c^d \bar{c}^n}(k_2). \end{aligned} \quad (\text{E.26})$$

At tree-level we then correctly recover the result

$$\begin{aligned} i\Gamma_{c^m \hat{A}_\alpha^a \bar{c}^n}^{(0)}(-q, k_2) &= i\Gamma_{c^m A_\alpha^a \bar{c}^n}^{(0)}(-q, k_2) - g f^{amn} k_{1\alpha} \\ &= -g f^{amn} (k_1 - k_2)_\alpha, \end{aligned} \quad (\text{E.27})$$

(in this case there is no difference between using the complete or reduced functional).

Appendix F: Feynman rules

1. R_ξ and BFM gauges

The Feynman rules for QCD in R_ξ gauges are given in Fig. 26. In the case of the BFM gauge, since the gauge fixing Lagrangian is quadratic in the quantum fields, apart from vertices involving ghost fields only vertices containing exactly two quantum fields might differ from the conventional ones. Thus, the vertices $\Gamma_{\hat{A}\psi\bar{\psi}}$ and $\Gamma_{\hat{A}AAA}$ have to lowest order the same expression as the corresponding R_ξ ones $\Gamma_{A\psi\bar{\psi}}$ and Γ_{AAAA} (to higher order their relation is described by the corresponding BQIs).

2. Anti-fields

The couplings of anti-fields with fields is entirely encoded in the BRST Lagrangian of Eq. (3.20). When choosing the BFM gauge the additional coupling $g f^{amn} A_\mu^{*m} \hat{A}_\nu^n c^a$ will arise in the BRST Lagrangian $\mathcal{L}_{\text{BRST}}$ as a consequence of the BFM splitting $A \rightarrow \hat{A} + A$. One then gets the Feynman rules given in Fig. 28.

$m, \mu \rightsquigarrow n, \nu$	$-i \frac{\delta^{mn}}{k^2} \left[g_{\mu\nu} - (1 - \xi) \frac{k_\mu k_\nu}{k^2} \right]$	$i \Delta_{\mu\nu}^{mn}(k)$
$m \dashrightarrow n$	$i \frac{\delta^{mn}}{k^2}$	$i D^{mn}(k)$
$i, f \longrightarrow j, f'$	$i \frac{\delta^{ij} \delta^{ff'}}{k^\mu \gamma_\mu - m_f}$	$i S_{ij}^{ff'}(k)$
	$g f^{amn} [g_{\mu\nu} (k_1 - k_2)_\alpha + g_{\alpha\nu} (k_2 - q)_\mu + g_{\alpha\mu} (q - k_1)_\nu]$	$i \Gamma_{A_\alpha^a A_\mu^m A_\nu^n}(k_1, k_2)$
	$g f^{amn} k_{1\alpha}$	$i \Gamma_{c^n A_\alpha^a \bar{c}^m}(q, -k_1)$
	$i g \gamma^\alpha (t^a)_{ij}$	$i \Gamma_{\psi^j A_\alpha^a \bar{\psi}^i}(q, -p_1)$
	$-i g^2 [f^{mse} f^{ern} (g_{\mu\rho} g_{\nu\sigma} - g_{\mu\nu} g_{\rho\sigma}) + f^{mne} f^{esr} (g_{\mu\sigma} g_{\nu\rho} - g_{\mu\rho} g_{\nu\sigma}) + f^{mre} f^{esn} (g_{\mu\sigma} g_{\nu\rho} - g_{\mu\nu} g_{\rho\sigma})]$	$\Gamma_{A_\mu^m A_\nu^n A_\rho^r A_\sigma^s}(k_2, k_3, k_4)$

FIG. 26: Feynman rules for QCD in the R_ξ gauges. The first two columns show the lowest order Feynman diagrams and rule respectively, while the last one shows the corresponding all-order Green's function according to the conventions of Eq. (3.18).

3. BFM sources

The couplings of BFM sources Ω_μ^m with fields can be derived from the Faddeev-Popov ghost Lagrangian, since making use of the extended BRST transformation of Eq. (3.31) we get

$$\mathcal{L}_{\text{FPG}} = -\bar{c}^a s \mathcal{F}_{\text{BFM}}^a \supset -\bar{c}^a g f^{amn} (s \hat{A}_\mu^m) A_n^\mu = -g f^{amn} \bar{c}^a \Omega_\mu^m A_n^\mu. \quad (\text{F.1})$$

The corresponding Feynman rule is finally given in Fig. 29.

	$gf^{amn} \left[g_{\mu\nu}(k_1 - k_2)_\alpha + g_{\alpha\nu}(k_2 - q + \frac{1}{\xi}k_1)_\mu + g_{\alpha\mu}(q - k_1 - \frac{1}{\xi}k_2)_\nu \right]$	$i\Gamma_{\widehat{A}_\alpha^a A_\mu^m A_\nu^n}(k_1, k_2)$
	$gf^{amn}(k_1 + k_2)_\alpha$	$i\Gamma_{c^n \widehat{A}_\alpha^a \bar{c}^m}(q, -k_1)$
	$-ig^2 \left[f^{mse} f^{ern} (g_{\mu\rho} g_{\nu\sigma} - g_{\mu\nu} g_{\rho\sigma} + \frac{1}{\xi} g_{\mu\sigma} g_{\nu\rho}) + f^{mne} f^{esr} (g_{\mu\sigma} g_{\nu\rho} - g_{\mu\rho} g_{\nu\sigma} - \frac{1}{\xi} g_{\mu\nu} g_{\rho\sigma}) + f^{mre} f^{esn} (g_{\mu\sigma} g_{\nu\rho} - g_{\mu\nu} g_{\rho\sigma}) \right]$	$\Gamma_{\widehat{A}_\mu^m A_\nu^n \widehat{A}_\rho^r A_\sigma^s}(k_2, p_2, p_1)$
	$-ig^2 g_{\alpha\rho} f^{mae} f^{ern}$	$\Gamma_{c^n \widehat{A}_\alpha^a A_\rho^r \bar{c}^m}(q, k_3, -k_1)$
	$-ig^2 g_{\alpha\rho} (f^{mae} f^{ern} + f^{mre} f^{ean})$	$\Gamma_{c^n \widehat{A}_\alpha^a \widehat{A}_\rho^r \bar{c}^m}(q, k_3, -k_1)$

FIG. 27: Feynman rules for QCD in the BFM gauge. We only include those rules which are different from the R_ξ ones to lowest order. As usual, gray circle on a gluon line indicates a background field.

-
- [1] F. J. Dyson, Phys. Rev. **75**, 1736 (1949).
[2] J. S. Schwinger, Proc. Nat. Acad. Sci. **37**, 452 (1951).
[3] J. M. Cornwall, R. Jackiw, and E. Tomboulis, Phys. Rev. **D10**, 2428 (1974).
[4] W. J. Marciano and H. Pagels, Phys. Rept. **36**, 137 (1978).
[5] D. C. Curtis and M. R. Pennington, Phys. Rev. **D42**, 4165 (1990); D. C. Curtis, M. R. Pennington, and D. A. Walsh, Phys. Lett. **B249**, 528 (1990); D. C. Curtis and M. R. Pennington, Phys. Rev. **D48**, 4933 (1993).
[6] A. Bashir and M. R. Pennington, Phys. Rev. **D50**, 7679 (1994), hep-ph/9407350; Phys. Rev.

	$-q^\mu \delta^{mn}$	$-\Gamma_{c^n A_\mu^{*m}}(q)$
	$igf^{amn} g_{\mu\nu}$	$i\Gamma_{c^a A_\nu^n A_\mu^{*m}}(k_2, q)$
	$igf^{amn} g_{\mu\nu}$	$i\Gamma_{c^a \hat{A}_\nu^n A_\mu^{*m}}(k_2, q)$
	$-g(t^a)_{ji}$	$i\Gamma_{\psi^i c^a \bar{\psi}^{*j}}(k_2, q)$
	$g(t^a)_{ji}$	$i\Gamma_{\psi^{*i} \bar{\psi}^j c^a}(-p_1, k_2)$
	$-igf^{amn}$	$i\Gamma_{c^a c^n c^{*m}}(k_2, q)$

FIG. 28: Feynman rules for QCD anti-fields.

D53, 4694 (1996), hep-ph/9510436. A. Bashir, A. Kizilersu, and M. R. Pennington, Phys. Rev. **D57**, 1242 (1998), hep-ph/9707421; A. Bashir, A. Huet, and A. Raya, Phys. Rev. **D66**,

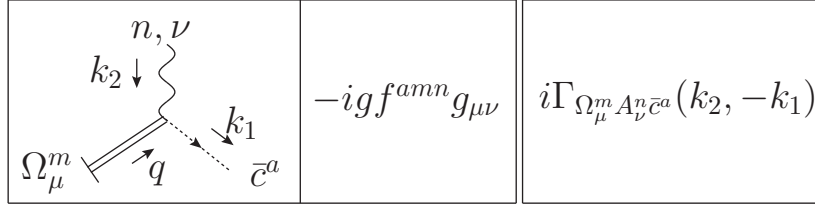


FIG. 29: Feynman rule for the BFM gluon source Ω_{μ}^m .

- 025029 (2002), hep-ph/0203016; A. Bashir and A. Raya, Nucl. Phys. **B709**, 307 (2005), hep-ph/0405142.
- [7] K.-i. Kondo, Y. Kikukawa, and H. Mino, Phys. Lett. **B220**, 270 (1989).
- [8] V. Sauli, JHEP **02**, 001 (2003), hep-ph/0209046.
- [9] S. Mandelstam, Phys. Rev. **D20**, 3223 (1979).
- [10] A. A. Slavnov, Theor. Math. Phys. **10**, 99 (1972).
- [11] J. C. Taylor, Nucl. Phys. **B33**, 436 (1971).
- [12] C. Becchi, A. Rouet, and R. Stora, Commun. Math. Phys. **42**, 127 (1975); Annals Phys. **98**, 287 (1976).
- [13] D. Binosi and J. Papavassiliou, Phys. Rev. **D77**, 061702(R) (2008), arXiv:0712.2707 [hep-ph].
- [14] J. M. Cornwall, Phys. Rev. **D26**, 1453 (1982);
- [15] J. M. Cornwall and J. Papavassiliou, Phys. Rev. **D40**, 3474 (1989).
- [16] B. S. DeWitt, Phys. Rev. **162**, 1195 (1967).
- [17] L. F. Abbott, Nucl. Phys. **B185**, 189 (1981); Acta Phys. Polon. **B13**, 33 (1982).
- [18] J. Papavassiliou, Phys. Rev. **D41**, 3179 (1990).
- [19] J. Papavassiliou, Phys. Rev. **D50**, 5958 (1994), hep-ph/9406258.
- [20] D. Binosi and J. Papavassiliou, Phys. Rev. **D65**, 085003 (2002), hep-ph/0110238.
- [21] J. Papavassiliou and A. Pilaftsis, Phys. Rev. Lett. **75**, 3060 (1995), hep-ph/9506417.
- [22] J. Papavassiliou, E. de Rafael, and N. J. Watson, Nucl. Phys. **B503**, 79 (1997), hep-ph/9612237.
- [23] J. Papavassiliou and A. Pilaftsis, Phys. Rev. **D54**, 5315 (1996), hep-ph/9605385.
- [24] J. Papavassiliou and A. Pilaftsis, Phys. Rev. Lett. **80**, 2785 (1998), hep-ph/9710380.
- [25] S. Weinberg, *The quantum theory of fields. Vol 2: Modern applications* (Cambridge, UK: Univ. Pr. (1996) 489 p, 1996).

- [26] A. Denner, G. Weiglein, and S. Dittmaier, Phys. Lett. **B333**, 420 (1994), hep-ph/9406204; S. Hashimoto, J. Kodaira, Y. Yasui, and K. Sasaki, Phys. Rev. **D50**, 7066 (1994), hep-ph/9406271;
- [27] J. Papavassiliou, Phys. Rev. **D51**, 856 (1995), hep-ph/9410385.
- [28] D. Binosi and J. Papavassiliou, Phys. Rev. **D66**, 111901(R) (2002), hep-ph/0208189; J. Phys. **G30**, 203 (2004), hep-ph/0301096.
- [29] M. Binger and S. J. Brodsky, Phys. Rev. **D74**, 054016 (2006), hep-ph/0602199.
- [30] J. Papavassiliou, Phys. Rev. Lett. **84**, 2782 (2000), hep-ph/9912336; Phys. Rev. **D62**, 045006 (2000), hep-ph/9912338.
- [31] J. S. Ball and T.-W. Chiu, Phys. Rev. **D22**, 2550 (1980).
- [32] U. Bar-Gadda, Nucl. Phys. **B163**, 312 (1980).
- [33] P. Pascual and R. Tarrach, Lect. Notes Phys. **194**, 1 (1984).
- [34] D. Binosi and J. Papavassiliou, Phys. Rev. **D66**, 025024 (2002), hep-ph/0204128.
- [35] P. A. Grassi, T. Hurth, and M. Steinhauser, Annals Phys. **288**, 197 (2001), hep-ph/9907426; Nucl. Phys. **B610**, 215 (2001), hep-ph/0102005.
- [36] D. Binosi and J. Papavassiliou, JHEP **03**, 041 (2007), hep-ph/0611354.
- [37] A. C. Aguilar and J. Papavassiliou, JHEP **12**, 012 (2006), hep-ph/0610040.
- [38] M. E. Peskin and D. V. Schroeder, *An Introduction to quantum field theory* (Reading, USA: Addison-Wesley, 842 p, 1995).
- [39] I. A. Batalin and G. A. Vilkovisky, Phys. Lett. **B69**, 309 (1977).
- [40] C. Itzykson and J. B. Zuber, *Quantum Field Theory*, International Series in Pure and Applied Physics (New York, USA: Mcgraw-Hill (1980) 705 p., 1980).
- [41] A. Pilaftsis, Nucl. Phys. **B487**, 467 (1997), hep-ph/9607451.
- [42] A. C. Aguilar, D. Binosi, and J. Papavassiliou (2008), arXiv:0802.1870 [hep-ph].
- [43] D. Binosi, J. Papavassiliou, and A. Pilaftsis, Phys. Rev. **D71**, 085007 (2005), hep-ph/0501259.
- [44] Y. A. Simonov, Phys. Atom. Nucl. **58**, 107 (1995), hep-ph/9311247, and references therein.
- [45] D. Binosi and L. Theussl, Comput. Phys. Commun. **161**, 76 (2004), hep-ph/0309015.
- [46] N. J. Watson, Phys. Lett. **B349**, 155 (1995), hep-ph/9412319.
- [47] A. Salam, Phys. Rev. **130**, 1287 (1963); A. Salam and R. Delbourgo, Phys. Rev. **135**, B1398 (1964); R. Delbourgo and P. C. West, J. Phys. **A10**, 1049 (1977).
- [48] N. K. Nielsen, Nucl. Phys. **B101**, 173 (1975).